Master equations for hybrid quantum systems

Dissertation
zur Erlangung des Grades
des Doktors der Naturwissenschaften
der Naturwissenschaftlich-Technischen Fakultät
der Universität des Saarlandes

von

Ralf Betzholz

Saarbrücken

2016

Tag des Kolloquiums: 07.10.2016

m.d.W.d.G.b. Dekan: Univ.-Prof. Dr. Christoph Becher

Mitglieder des   Univ.-Prof. Dr. Rolf Pelster
Prüfungsausschusses: Univ.-Prof. Dr. Giovanna Morigi
                       Univ.-Prof. Dr. Frank Wilhelm-Mauch
                       Dr. Adam Miroslaw Wysocki

题献给我女儿倪琰

距离虽大心里很近

iii

Eidesstattliche Versicherung

Hiermit versichere ich an Eides statt, dass ich die vorliegende Arbeit selbstständig und ohne Benutzung anderer als der angegebenen Hilfsmittel angefertigt habe. Die aus anderen Quellen oder indirekt übernommenen Daten und Konzepte sind unter Angabe der Quelle gekennzeichnet. Die Arbeit wurde bisher weder im In- noch im Ausland in gleicher oder ähnlicher Form in einem Verfahren zur Erlangung eines akademischen Grades vorgelegt.

Ort, Datum

Saarbrücken, 11.10.2016

Unterschrift

Zusammenfassung

In dieser Arbeit erweitern wir die Werkzeuge zur Lösung der Born-Markovschen Mastergleichung für spezifische Systeme. Im Hauptteil präsentieren wir die Beschreibung eines Festkörperquantenemitters, gegeben durch eine Mastergleichung, welche die Eigenschaften der Kristallgitterumgebung beinhaltet. Wir leiten die Lösung dieser Gleichung in der Form der spektralen Zerlegung des Liouville-Operators her und geben Beispiele für ihre Anwendung.

Im zweiten Teil dieser Arbeit analysieren wir die Dynamik eines optomechanischen Hybridsystems, das aus einem Zwei-Niveau-Atom in einem optomechanischen Resonator befindet. Hier präsentieren wir einen Effekt, bei dem die Dipol-Resonator-Wechselwirkung durch die Bewegung des Spiegels unterdrückt wird. Zusätzlich zeigen wir die spektrale Zerlegung des Liouville-Operators eines dissipativen optomechanischen Systems.

Der Fokus des letzten Teils liegt auf einzelnen durch Laser gekühlten Atomen, die in nicht harmonischen Fallenpotentialen gefangen sind. Im Lamb-Dicke-Regime zeigen wir die Eigenschaften der Laserkühlung und beschreiben die Signaturen der atomaren Schwerpunktsbewegung im Spektrum der Resonanzfluoreszenz. Anhand zweier Beispiele zeigen wir die Abweichungen von den bekannten Ergebnissen für harmonische Fallenpotentiale.

Abstract

In this thesis we extend the toolbox for solving the Born-Markov master equation for specific systems. In the main part we present a description of a solid-state quantum emitter, in the form of a master equation which takes the properties of the phonon environment into account. We present the solution of this equation in the form of the spectral decomposition of the Liouville operator and exemplify its application.

In the second part of this work we analyze the dynamics of a hybrid optomechanical system consisting of a two-level atom in an optomechanical cavity. Here, we present an effect where the dipole-cavity interaction is suppressed due to the mirror motion. In addition we derive the spectral decomposition of the Liouville operator of a dissipative optomechanical system.

The last part focuses on the a single laser-cooled atom trapped in a non-harmonic potential. In the Lamb-Dicke regime we present the laser-cooling performance and the signatures of the atomic center-of-mass motion in the spectrum of resonance fluorescence. For two exemplary potentials we show the deviations from the known results for a harmonic potential.

x

Contents

List of Figures

Introduction

The recent progress in quantum physics focuses increasingly on its technological applications. Such applications range from quantum information processing [Nie03] over protocols for secure communication [Gis02] to simulation of complex systems [Bul09, Blo12, Geo14] and high-precision sensing [Gio11]. This progress draws from the control of the quantum dynamics of a wide variety of quantum systems, *e.g.* single photons [Har13], nuclear spins [Pla13], and atoms [Lei03] up to mesoscopic system such as superconducting circuits [Bla04] and nanomechanical oscillators [Poo12].

However, most of these quantum systems are only suitable for a specific task. For instance, information is best transmitted using photons while spins are more useful for its storage. This shortcoming of the individual systems call for the development of *hybrid quantum systems* that combine the advantages of its constituents and are thus able to perform several task simultaneously. Examples for such hybrid systems are circuit electromechanical setups [Lec15, Pir15], ultracold atoms coupled to membranes [Cam11], or superconducting resonator-spin ensemble interfaces [Kub10], to mention only a very few, for more examples we point out Refs. [Xia13, Kur14, Rog14] and references therein.

In many solid-state based setups, which are among the candidates for hybrid quantum systems, environmental noise plays a crucial role in the dynamics. In a perturbative treatment of this noise, in the framework of master equations, special care has to be taken about the validity of the Born-Markov approximation, since the coupling to the environment can be relatively large *and* the Markovian assumption may not be warranted [Wei12].

In the main part of this work we present a description of a solid-state quantum emitter in which a part of the environment is included into the system, thereby accounting for possibly strong coupling and environmental memory effects. The resulting dynamical equation is nevertheless given by a Born-Markov master equation, however, for the density operator of the system including an environmental degree of freedom. For this equation we present the solution in terms of the spectral decomposition of the associated Liouville operator, called the *damping basis* [Bri93, Bar00], allowing a straightforward derivation of analytical expressions for the dynamics and light scattering properties. We thereby also provide a general tool for the theoretical analysis of systems governed by similar equations of motion, such as dissipative optomechanical systems for whose master equation we also derive the solution in the form of the damping basis.

This thesis is divided into four parts and we give a brief outline of their general structure: Part I introduces the basic theoretical tools and comprises two chapters. In Chapter 1 we present a derivation of the Born-Markov master equation and familiarize the reader with the damping basis. Chapter 2 contains the explicit calculation of the

damping basis of a damped harmonic oscillator, which is an essential tool for the following treatments.

The focus of Part II lies on the description of the interaction of solid-state emitters with their surrounding crystal environment and consists of two chapters. Here, Chapter 3 reviews an earlier model from the literature for the light-scattering properties of two-level defects in crystals which serves as a reference for the following work. In Chapter 4 we present our model formulated as a single Born-Markov master equation, derive the solution of this equation and show some examples for its application. Our results are then compared to the ones from the previously reviewed model.

Part III is dedicated to cavity optomechanics and involves three chapters. Chapter 5 recapitulates the description of generic optomechanical systems in order to lay the foundation for what follows. In Chapter 6 we then analyze, in the spirit of hybrid quantum systems, the dynamics of a hybrid optomechanical system, consisting of a two-level atom placed inside an optomechanical cavity. In this system we identify a distinct effect where the cavity-dipole interaction is suppressed due to the optomechanical coupling and analyze the influence of dissipation on this feature. In Chapter 7 we transfer the methods we used in our description of solid-state quantum emitters to optomechanical systems and derive the damping basis of dissipative optomechanics.

Finally, in Part IV of this work we investigate, in its single Chapter 8, the cooling of a single laser-driven two-level atom trapped in a non-harmonic potential and the signatures of its center-of-mass motion in the spectrum of resonance fluorescence. This work was motivated by recent cavity-cooling experiments in which the atom is trapped in the standing wave of an optical optical resonator and the spectrum of scattered photons shows distinct features of the anharmonicity of the optical lattice potential. Giving two explicit examples, the infinite square well and the Morse potential, we show the deviations from the known results for a harmonic trap [Lin86, Cir92, Cir93].

PART I

Basics

Born-Markov master equations

Conventionally the term *master equation* refers to a first-order differential equation describing the time evolution of probabilities. In the case of a quantum master equation the dynamical equation does not only cover the diagonal elements of a density operator, which constitute probabilities, but also its off-diagonal elements, called *coherences*. Although it might not always be possible, the master equations we will deal with here can be derived from underlying microscopic models.

In general the dynamics of a non-relativistic quantum system is fully described by the *Schrödinger equation*. Here, the term *system* usually stands for a limited number of degrees of freedom, such as a single electronic system. However, when describing such a such system one often has to take into account the fact that it is not isolated: it is in constant contact with its environment. Since this environment is generally given by a vast number of degrees of freedom, it is, similar to the case of classical mechanics, an insurmountable task to determine the initial conditions or solve the equations of motion. To cope with this problem one has to rely on techniques known from statistical mechanics and consider the environment to be a *reservoir* with which the system exchanges energy, or both energy and particles. One can then characterize this reservoir by only a small number of quantities, such as the nature of its constituents, its temperature and its density of states.

This is what is called the *system plus reservoir* approach [Sar74, Lou90]: from the dynamics of the full density operator, covering both the system and the environment, an equation of motion for the system's reduced density operator is derived which depends only parametrically on the properties of the reservoir. Generally, an equation for the time evolution of the system's reduced density operator can be obtained using a projection operator technique leading to the so-called *Nakajima-Zwanzig equation* [Nak58, Zwa60, Haa73]. However, in some cases suitable approximations, summarized under the name *Born-Markov approximation*, can be performed in the derivation of the dynamical equation. These approximations include a weak interaction of the system with the external degrees of freedom, thermal equilibrium of the reservoir and assumptions on the timescales of the system and the reservoir. The resulting equation is then called a *Born-Markov master equation*, accordingly, and is the type of master equation we will focus on. In the derivation care has to be taken and the validity of the approximations has to be examined critically for every physical situation. For example, a timescale separation between the reservoir relaxation and the system evo-

lution is valid in most quantum optical situations while it is not necessarily valid in solid-state systems [Wei12].

Two prominent examples for the successful application of the Born-Markov approximation in quantum optics are the description it delivers for an atom interacting with the free electromagnetic field and the description of a damped quantum harmonic oscillator such as the mode of a cavity field. We will hark back to both of these cases at a later instance.

In general, solving Born-Markov master equations is a challenging task due to their operator-valued character. Among many methods to solve a master equation is a way, proposed by *Briegel and Englert* [Bri93], that is analogous to the standard method of solving the Schrödinger equation, in which the Hamiltonian is diagonalized. Translated to a master equation this means one has to find a basis of operators in which the generator of the dynamics, termed the *Liouvillian*, is diagonal. Unfortunately, the fact that the restriction to the reduced dynamics of the system's density operator results in a non-unitary time evolution is reflected in the property of this Liouvillian that it is not self-adjoint. This in turn implies that the diagonalization requires the eigenoperators of the Liouvillian as well as the ones of its adjoint, or in different words its right and left eigenoperators.

This chapter is organized as follows: After briefly outlining the derivation of the Born-Markov master equation in Sec. 1.1 we also present in Sec. 1.2 a useful result that can be extracted from the master equation with little effort, the so-called quantum regression theorem. In Sec. 1.3 we then formally introduce the basis of eigenoperators of the Liouvillian and summarize some of its properties and give a first example of its application, the damped two-level atom.

There exists a host of literature in which the derivation of quantum master equations is treated in general as well as for specific physical systems, we refer to Refs. [Lou90, Car02] to mention only two. Here, we assume the system to couple weakly to a large reservoir. We denote by $\mathcal{H}_S$ and $\mathcal{H}_R$ the Hilbert spaces of the system and the reservoir, respectively, and by χ the full density operator, that describes the system *and* the reservoir. Our aim is to derive an equation of motion for the reduced density operator of the system

$$\varrho = \mathrm{Tr}_R\{\chi\}\,, \tag{1.1}$$

which is obtained by the partial trace of χ over the reservoir degrees of freedom, where the partial trace is defined as $\mathrm{Tr}_R\{\,\cdot\,\} = \sum_n {}_R\langle n|\,\cdot\,|n\rangle_R$, with some basis $\{|n\rangle_R\}$ of the Hilbert space $\mathcal{H}_R$. The starting point of this derivation is the time evolution of χ, given by the *von Neumann equation*

$$\frac{\partial}{\partial t}\chi(t) = \frac{1}{i\hbar}[H, \chi(t)]\,. \tag{1.2}$$

The Hamiltonian that governs the time evolution can be split into different parts as

$$H = H_0 + V = H_{\mathrm{S}} + H_{\mathrm{R}} + V \,, \tag{1.3}$$

where H_{S} and H_{R} denote the system and reservoir Hamiltonians, respectively, and the operator V describes the mutual coupling.

The operators χ and V are now transformed into the interaction picture with respect to $H_0 = H_{\mathrm{S}} + H_{\mathrm{R}}$ according to

$$\tilde{\chi}(t) = e^{iH_0 t/\hbar} \chi(t) e^{-iH_0 t/\hbar} \,, \tag{1.4}$$

$$\tilde{V}(t) = e^{iH_0 t/\hbar} V e^{-iH_0 t/\hbar} \,. \tag{1.5}$$

For the density operator the equation of motion in the interaction picture now has the form

$$\frac{\partial}{\partial t} \tilde{\chi}(t) = \frac{1}{i\hbar} [\tilde{V}(t), \tilde{\chi}(t)] \,. \tag{1.6}$$

It is convenient to formally integrate Eq. (1.6) in the time interval $[0, t]$ resulting in

$$\tilde{\chi}(t) = \tilde{\chi}(0) + \frac{1}{i\hbar} \int_0^t \mathrm{d}\tau \, [\tilde{V}(\tau), \tilde{\chi}(\tau)] \,. \tag{1.7}$$

This expression can be substituted back into the right-hand side of Eq. (1.6) for $\tilde{\chi}(t)$ obtaining

$$\frac{\partial}{\partial t} \tilde{\chi}(t) = \frac{1}{i\hbar} [\tilde{V}(t), \tilde{\chi}(0)] - \frac{1}{\hbar^2} \int_0^t \mathrm{d}\tau \, [\tilde{V}(t), [\tilde{V}(\tau), \tilde{\chi}(\tau)]] \,. \tag{1.8}$$

Up to this point we have merely cast the original equation into a different form, it is still exact. Now a major assumption is made that is sometimes called the *Born approximation*: we assume that the density operator is separable, meaning that it can be written as a tensor product of a density operator on $\mathcal{H}_{\mathrm{S}}$ and a density operator on $\mathcal{H}_{\mathrm{R}}$ according to

$$\tilde{\chi}(t) = \tilde{\varrho}(t) \varrho_{\mathrm{R}} \,, \tag{1.9}$$

with the system's reduced density operator $\tilde{\varrho}(t)$ and the reservoir density operator ϱ_{R}. The essence of this approximation is twofold: *(i)* We take the system-reservoir interaction only into account up to second order. Correlations arising during the time evolution that lead to non-separability, *i.e.* the impossibility to write the density operator as a tensor product of the form (1.9), are neglected because they are at least of order one in the interaction. *(ii)* The reservoir state is assumed to be in thermal equilibrium with an inverse temperature $\beta = 1/k_{\mathrm{B}}T$, *viz.*

$$\varrho_{\mathrm{R}} = \frac{e^{-\beta H_{\mathrm{R}}}}{\mathrm{Tr}\{e^{-\beta H_{\mathrm{R}}}\}} \,, \tag{1.10}$$

and remains unchanged during the dynamics. This includes the additional requirement that the reservoir is large enough, compared to the system, that it is not affected by the interaction.

Under these assumptions taking the partial trace of Eq. (1.8) leads to

$$\frac{\partial}{\partial t}\tilde{\varrho}(t) = \frac{1}{i\hbar}\mathrm{Tr}_{\mathrm{R}}\big\{[\tilde{V}(t),\tilde{\varrho}(0)\varrho_{\mathrm{R}}]\big\} - \frac{1}{\hbar^2}\int_0^t \mathrm{d}\tau\,\mathrm{Tr}_{\mathrm{R}}\big\{[\tilde{V}(t),[\tilde{V}(\tau),\tilde{\varrho}(\tau)\varrho_{\mathrm{R}}]]\big\} \quad (1.11)$$

which is the time evolution of the system's reduced density operator in the interaction picture under the Born approximation. For many concrete models the first term in this equation vanishes, *i.e.* $\mathrm{Tr}_{\mathrm{R}}\{[\tilde{V}(t),\tilde{\varrho}(0)\varrho_{\mathrm{R}}]\} = 0$. If this is not the case it is always possible to incorporate an additional (ϱ_{R}-dependent) term in the Hamiltonians, in the manner

$$V \to V - \mathrm{Tr}_{\mathrm{R}}\{V\varrho_{\mathrm{R}}\}, \quad H_{\mathrm{S}} \to H_{\mathrm{S}} + \mathrm{Tr}_{\mathrm{R}}\{V\varrho_{\mathrm{R}}\}, \quad (1.12)$$

such that it vanishes nonetheless [Riv12]. Going back to the original picture yields the equation:

$$\frac{\partial}{\partial t}\varrho(t) = \frac{1}{i\hbar}\left[H_{\mathrm{S}},\varrho(t)\right] + \int_0^t \mathrm{d}\tau\,\mathcal{K}(\tau)\varrho(t-\tau) \quad (1.13)$$

with the memory Kernel $\mathcal{K}(t)$ whose action on an arbitrary system operator X is given by

$$\mathcal{K}(t)X(t') = -\frac{1}{\hbar^2}\mathrm{Tr}_{\mathrm{R}}\left\{\left[V,e^{-iH_0 t/\hbar}[V,X(t')\varrho_{\mathrm{R}}]e^{iH_0 t/\hbar}\right]\right\}. \quad (1.14)$$

The system itself, the reservoir and the system-reservoir interaction are still not specified. By choosing a microscopic model for the interaction one can identify the operator V accordingly, leading to an explicit form of the Kernel $\mathcal{K}$ and thereby the master equation itself. Since Eq. (1.13) contains a convolution of the memory kernel and the density operator, the future evolution depends on the history of the density operator. This is the reason why Eq. (1.13) is still a *non-Markovian* equation [Gar04] and the solution remains a difficult task. We therefore seek another approximation to further reduce the complexity.

In some physical systems there exist two widely separated time scales: the time scale on which reservoir correlations decay and the time scale on which the system evolves. If the system's time scale, given by the inverse of the frequencies in the Hamiltonian, is small compared to the characteristic time scale of the memory kernel (1.14), which is given by the thermal time $\hbar\beta$ of the reservoir [Wei12], it is justified to use the *Markov approximation* in Eq. (1.13), *i.e.* to approximate $\varrho(t-\tau)$ by $\varrho(t)$. This enables us to carry out the τ-integration in Eq. (1.13) to arrive at an equation of the form

$$\frac{\partial}{\partial t}\varrho(t) = \mathcal{L}\varrho(t) \quad (1.15)$$

with a superoperator $\mathcal{L}$, which is referred to as the Liouville operator. This is the type of master equations we will deal with in the subsequent text, *e.g.* in the master-equation description of spontaneous emission or the damped harmonic oscillator. It can be shown, see for example [Lin76, Riv12], that if after performing the approximations introduced above the master equation is still physically admissible, meaning that it preserves the properties of density operators, it can be written in terms of a Liouville operator of the form

$$\mathcal{L}\varrho = \frac{1}{i\hbar}[H_\mathrm{S}, \varrho] + \sum_k \frac{\gamma_k}{2}\mathcal{D}[X_k]\varrho \tag{1.16}$$

with a set of bounded operators X_k and real numbers $\gamma_k \geq 0$. Here, we defined superoperators of the *Lindblad form* by the expression

$$\mathcal{D}[X]\varrho = 2X\varrho X^\dagger - X^\dagger X \varrho - \varrho X^\dagger X \,. \tag{1.17}$$

For a time-independent Liouville operator and the initial condition $\varrho(0)$ the formal solution of the master equation (1.15) is given by

$$\varrho(t) = e^{\mathcal{L}t}\varrho(0)\,. \tag{1.18}$$

For a detailed evaluation of the Liouville operator for a two-level atom undergoing spontaneous emission or pure dephasing and a damped harmonic oscillator we refer to [Car02].

In the previous section we derived an equation of motion for the reduced density operator of the system. However, in many situations we will encounter two-time correlation functions of two system operators X and Y, defined on $\mathcal{H}_\mathrm{S}$, of the form

$$\langle X(t+\tau)Y(t)\rangle = \mathrm{Tr}\{X(t+\tau)Y(t)\chi(0)\}\,, \tag{1.19}$$

$$\langle X(t)Y(t+\tau)\rangle = \mathrm{Tr}\{X(t)Y(t+\tau)\chi(0)\}\,, \tag{1.20}$$

where the trace extends over the Hilbert space $\mathcal{H}_\mathrm{S} \otimes \mathcal{H}_\mathrm{R}$ and the time evolution is generated by the same system plus reservoir Hamiltonian H as in the previous section, given by Eq. (1.3). The two operators X and Y obey the *Heisenberg equations* whose formal solutions read

$$X(t) = e^{iHt/\hbar}X(0)e^{-iHt/\hbar}\,, \tag{1.21}$$

$$Y(t) = e^{iHt/\hbar}Y(0)e^{-iHt/\hbar}\,. \tag{1.22}$$

Let us focus on the first of the two correlation functions, Eq. (1.19), and assume $\tau > 0$. Given the time evolution from Eqs. (1.21) and (1.22) and the formal solution of the

von Neumann equation (1.2) we can use the cyclic property of the trace and write

$$\mathrm{Tr}\{X(t+\tau)Y(t)\chi(0)\} = \mathrm{Tr}\{X(0)e^{-iH\tau/\hbar}Y(0)\chi(t)e^{iH\tau/\hbar}\}. \tag{1.23}$$

Since X is a pure system operator the trace can be split into a trace over the system and a trace over the reservoir according to

$$\mathrm{Tr}\{X(t+\tau)Y(t)\chi(0)\} = \mathrm{Tr}_{\mathrm{S}}\{X(0)\mathrm{Tr}_{\mathrm{R}}\{e^{-iH\tau/\hbar}Y(0)\chi(t)e^{iH\tau/\hbar}\}\}. \tag{1.24}$$

In the reservoir trace we now define the time-dependent operator

$$\bar{Y}(\tau) = e^{-iH\tau/\hbar}Y(0)\chi(t)e^{iH\tau/\hbar} \tag{1.25}$$

which is now defined on the system plus reservoir Hilbert space $\mathcal{H}_{\mathrm{S}} \otimes \mathcal{H}_{\mathrm{R}}$. With the initial condition $\bar{Y}(0) = Y(0)\chi(t)$ it satisfies the differential equation

$$\frac{\partial}{\partial\tau}\bar{Y}(\tau) = \frac{1}{i\hbar}[H, \bar{Y}(\tau)] \tag{1.26}$$

in the time variable τ, of whose solution we need to evaluate the reservoir trace. By using the same arguments as in the derivation of the Born-Markov master equation (1.16) one obtains

$$\frac{\partial}{\partial\tau}\mathrm{Tr}_{\mathrm{R}}\{\bar{Y}(\tau)\} = \mathcal{L}\mathrm{Tr}_{\mathrm{R}}\{\bar{Y}(\tau)\} \tag{1.27}$$

and the formal solution of this differential equation is given by

$$\mathrm{Tr}_{\mathrm{R}}\{\bar{Y}(\tau)\} = e^{\mathcal{L}\tau}\mathrm{Tr}_{\mathrm{R}}\{\bar{Y}(0)\} = e^{\mathcal{L}\tau}[Y(0)\varrho(t)] \tag{1.28}$$

with the same reduced system density operator ϱ that is the solution of Eq. (1.16). This finally results in

$$\mathrm{Tr}\{X(t+\tau)Y(t)\chi(0)\} = \mathrm{Tr}\{X(0)e^{\mathcal{L}\tau}Y(0)\varrho(t)\}, \tag{1.29}$$

where one has to be careful that the superoperator exponential acts on all operators inside the trace that are to its right. The procedure for the second correlation function (1.20) is analogous and the two results can be summarized as

$$\langle X(t+\tau)Y(t)\rangle = \mathrm{Tr}\{X(0)e^{\mathcal{L}\tau}Y(0)\varrho(t)\}, \tag{1.30}$$

$$\langle X(t)Y(t+\tau)\rangle = \mathrm{Tr}\{Y(0)e^{\mathcal{L}\tau}\varrho(t)X(0)\}. \tag{1.31}$$

This result is called the *quantum regression theorem* and was derived in Refs. [Lax63, Lax67]. Of special interest are correlation functions evaluated after the system has settled in its steady state, if such a state exists, namely the limit $t \to \infty$, for which we find

$$\lim_{t\to\infty}\langle X(t+\tau)Y(t)\rangle = \langle X(\tau)Y(0)\rangle_{\mathrm{st}} = \mathrm{Tr}\{X(0)e^{\mathcal{L}\tau}Y(0)\varrho_{\mathrm{st}}\} \tag{1.32}$$

with the steady state ϱ_{st} of the system.

The determination of the time evolution of an arbitrary initial state under a Born-Markov master equation can be achieved by finding the eigenbasis of the associated Liouville operator $\mathcal{L}$. Following Ref. [Bri93] we will call this basis the *damping basis* and its elements *eigenelements*. The existence of such an eigenbasis is not *a priori* warranted but has to be checked case by case for every Liouville operator. The solution has been found only for very few cases.

We consider the space $L(\mathcal{H})$ of linear operators on a Hilbert space $\mathcal{H}$. In this space the set of density operators forms a convex subset. For $X, Y \in L$ a scalar product can be defined by

$$(X, Y) = \text{Tr}\{X^\dagger Y\}. \tag{1.33}$$

This definition of an inner product also induces an outer product of two elements whose action is given by

$$[X \otimes Y]Z = X(Y, Z) = \text{Tr}\{Y^\dagger Z\}X. \tag{1.34}$$

In the previous section we already referred to the Liouville operator as a superoperator. This common notation comes from the fact that it is a linear operator itself, acting on linear operators, formally expressed as $\mathcal{L} \in L(L(\mathcal{H}))$ (for a review of the properties of superoperators see for example Ref. [Tar08]). In the subsequent text we will mostly refer to superoperators simply as operators.

Our aim is to find a basis of operators in which a Liouville $\mathcal{L}$ of the form Eq. (1.16) is diagonal. Using the fact $\mathcal{L}X^\dagger = (\mathcal{L}X)^\dagger$, which is valid for all superoperators of the Lindblad form (1.16), one finds

$$(X, \mathcal{L}Y) \neq (\mathcal{L}X, Y), \tag{1.35}$$

which shows that the Liouville operator is *not* self-adjoint. This implies that it is not sufficient to find the set of *right eigenelements*, but one has to additionally find the set of *left eigenelements*. They, respectively, have to fulfill the eigenvalue equations

$$\mathcal{L}\hat{\varrho}_\lambda = \lambda\hat{\varrho}_\lambda, \tag{1.36}$$

$$\check{\varrho}_\lambda^\dagger \mathcal{L} = \lambda\check{\varrho}_\lambda^\dagger. \tag{1.37}$$

Here, we denoted the left eigenelements by $\check{\varrho}_\lambda^\dagger$ and the right ones by $\hat{\varrho}_\lambda$, for a common eigenvalue λ. In some references they are denoted by $\langle\!\langle \varrho_\lambda|$ and $|\varrho_\lambda\rangle\!\rangle$, respectively, in analogy to the bra-ket notation for state vectors [Bar87, Jak03, Sch12]. The action to the left is defined via the scalar product

$$(X, \mathcal{L}Y) = (X\mathcal{L}, Y) \tag{1.38}$$

and for superoperators of the Lindblad form, defined in Eq. (1.17), the action to the left is derived using the cyclic property of the trace explicitly given by $\check{\mathcal{D}}[X]\varrho := \varrho\mathcal{D}[X]$ with

$$\check{\mathcal{D}}[X]\varrho = 2X^\dagger\varrho X - X^\dagger X\varrho - \varrho X^\dagger X \,. \tag{1.39}$$

We will restrict ourselves to the case of a non-degenerate spectrum of eigenvalues λ. In this case one can write

$$0 = \text{Tr}\{\check{\varrho}_\lambda^\dagger \mathcal{L}\hat{\varrho}_{\lambda'}\} - \text{Tr}\{\check{\varrho}_\lambda^\dagger \mathcal{L}\hat{\varrho}_{\lambda'}\} = (\lambda - \lambda')\text{Tr}\{\check{\varrho}_\lambda^\dagger \hat{\varrho}_{\lambda'}\} \tag{1.40}$$

which directly shows that the right and left eigenelements can be normalized to fulfill the *orthogonality relation*

$$\text{Tr}\{\check{\varrho}_\lambda^\dagger \hat{\varrho}_{\lambda'}\} = \delta_{\lambda,\lambda'} \,. \tag{1.41}$$

In general the question whether the set of left and right eigenelements forms a complete basis has to be checked for every specific Liouville operator, which is not always possible. If they do form a complete set the *closure relation* reads

$$\sum_\lambda \hat{\varrho}_\lambda \otimes \check{\varrho}_\lambda = \mathbb{1} \,. \tag{1.42}$$

We will see that for the damped two-level system this can be shown straightforwardly. For the damped harmonic oscillator the completeness was shown in Ref. [Eng02].

Employing again the relation $(\mathcal{L}X)^\dagger = \mathcal{L}X^\dagger$ to the eigenvalue equation (1.36) yields

$$\mathcal{L}\hat{\varrho}_\lambda^\dagger = \lambda^* \hat{\varrho}_\lambda^\dagger \,, \tag{1.43}$$

which shows that the eigenvalues of $\mathcal{L}$ appear in complex conjugate pairs and the corresponding eigenelement to the eigenvalue λ^* is given by the Hermitian conjugate of the eigenelement for λ.

For a non-degenerate spectrum with $\text{Re}\,\lambda \leq 0$ the unique steady state of the dynamics fulfills $\mathcal{L}\varrho_{\text{st}} = 0$, meaning that it is the right eigenelement of the Liouville operator with the eigenvalue $\lambda = 0$, *i.e.* $\varrho_{\text{st}} = \hat{\varrho}_0$. It is the single eigenelement that is an actual physical state. The trace condition $\text{Tr}\{\varrho_{\text{st}}\} = 1$ combined with the

orthogonality relation (1.41) leads to

$$1 = \text{Tr}\{\varrho_{\text{st}}\} = \text{Tr}\{\hat{\varrho}_0\} = \text{Tr}\{1\hat{\varrho}_0\} = \text{Tr}\{\check{\varrho}_0^\dagger \hat{\varrho}_0\} \tag{1.44}$$

which means that, in the case of a unique steady state, the corresponding left eigenelement is always the *unity operator*. This also implies that all eigenelements except the steady state are *traceless*.

With the damping basis of a given Liouville operator at hand the master equation is formally solved. The calculation of the time evolution of a given initial state can then be carry out after an established procedure. We saw in Eq. (1.18) that the formal solution of a Markovian master equation is given by the exponential of the Liouville operator applied to the initial state. Using the spectral resolution and the completeness relation (1.42) allows us to write

$$\varrho(t) = e^{\mathcal{L}t} \sum_\lambda \left[\hat{\varrho}_\lambda \otimes \check{\varrho}_\lambda\right] \varrho(0) = \sum_\lambda c_\lambda e^{\lambda t} \hat{\varrho}_\lambda \tag{1.45}$$

with the expansion coefficients

$$c_\lambda = \text{Tr}\{\check{\varrho}_\lambda^\dagger \varrho(0)\} . \tag{1.46}$$

Analogous to a time evolution given by a Schrödinger equation one has to calculate the overlap, given by the scalar product (1.46), of the initial state with the elements of the basis. Since we established that for a non-degenerate eigenvalue $\lambda = 0$ the right eigenelement is $\check{\varrho}_0^\dagger = 1$ we find that the overlap of any initial state with the steady state is unity, $c_0 = 1$. The negative real part of the remaining eigenvalues ensures that the dynamics converges towards this steady state. Furthermore, the fact that Hermitian conjugates of eigenelements are also eigenelements to complex conjugate eigenvalues ensures the Hermiticity of $\varrho(t)$ for all times.

As a simple example for a damping basis we consider a two-level atom with ground state $|g\rangle$ and excited state $|e\rangle$ whose density operator we denote by ρ.

Undriven case

If the transition frequency between the two states is given by ω and we set the ground-state energy to zero the Hamiltonian has the simple form

$$H = \hbar\omega|e\rangle\langle e| . \tag{1.47}$$

The time evolution of such an atom undergoing spontaneous emission at rate Γ and pure dephasing at rate Γ^* can be described by a Born-Markov master equation with

the Liouville operator

$$\mathcal{L}\rho = -i\omega[|e\rangle\langle e|, \rho] + \frac{\Gamma}{2}\mathcal{D}[\sigma_-]\rho + \frac{\Gamma^*}{2}\mathcal{D}[|e\rangle\langle e|]\rho \qquad (1.48)$$

with the atomic lowering operator $\sigma_- = |g\rangle\langle e|$ whose Hermitian conjugate, the raising operator, we denote by $\sigma_+ = |e\rangle\langle g|$. One can verify that the values and the corresponding elements summarized in Tab. 1.1 fulfill the eigenvalue equation of $\mathcal{L}$ [Bri93, Jak03].

λ	$\hat{\rho}_\lambda$	$\check{\rho}_\lambda^\dagger$
$\lambda_0 = 0$	$\hat{\rho}_0 = |g\rangle\langle g|$	$\check{\rho}_0^\dagger = 1$
$\lambda_\pm = \mp i\omega - \bar{\Gamma}/2$	$\hat{\rho}_\pm = \sigma_\pm$	$\check{\rho}_\pm^\dagger = \sigma_\mp$
$\lambda_\rightsquigarrow = -\Gamma$	$\hat{\rho}_\rightsquigarrow = |e\rangle\langle e| - |g\rangle\langle g|$	$\check{\rho}_\rightsquigarrow^\dagger = |e\rangle\langle e|$

Table 1.1: *Eigenvalues λ and the corresponding eigenelements $\hat{\rho}_\lambda$ and $\check{\rho}_\lambda^\dagger$ of the Liouvillian describing a two-level atom undergoing spontaneous emission and pure dephasing.*

Here, we defined the total rate $\bar{\Gamma} = \Gamma + \Gamma^*$ at which the coherence is lost.

Spectra

In Sec. 1.2 we saw that the quantum regression theorem allows to express two-time correlation functions in terms of the Liouville operator. Correlation functions of the negative and positive electric field components at a fixed position, $E^{(-)}(t)$ and $E^{(+)}(t)$, are of special interest for the theory of the ideal photon detector [Gla63, Gla07]. In the steady state ρ_{st} of a radiating system the spectral signal $\mathcal{S}(\omega)$ at such a detector is given by the Fourier transform [Mol69]

$$\mathcal{S}(\omega) = \text{Re}\int_0^\infty \text{d}t\, \langle E^{(-)}(t)E^{(+)}(0)\rangle_{st}\, e^{-i\omega t}\,, \qquad (1.49)$$

where the correlation function is evaluated according to $\langle\,\cdot\,\rangle_{st} = \text{Tr}\{\,\cdot\,\rho_{st}\}$. For a dipole-allowed transition between $|g\rangle$ and $|e\rangle$ the electric field components in the far-field are related to the atomic raising and lowering operators by $E^{(\pm)} \propto \sigma_\mp$ [Bre07]. Making use of the quantum regression theorem (1.30) transform the expression (1.49) into

$$\mathcal{S}(\omega) = \text{Re}\int_0^\infty \text{d}t\, \text{Tr}\{\sigma_+(0)e^{(\mathcal{L}-i\omega)t}\sigma_-(0)\rho_{st}\}\,, \qquad (1.50)$$

where we disregarded the proportionality factor between the field components and the atomic operators. Inserting a completeness relation Eq. (1.42) next to the super-operator exponential leads an eigenvalue decomposition of the spectral signal of the

form [Lin86]

$$\mathcal{S}(\omega) = \mathrm{Re} \sum_\lambda \mathrm{Tr}\{\sigma_+(0)\hat{\rho}_\lambda\}\mathrm{Tr}\{\check{\rho}_\lambda^\dagger \sigma_-(0)\rho_{\mathrm{st}}\} \int_0^\infty \mathrm{d}t\, e^{(\lambda - i\omega)t}\,. \tag{1.51}$$

Since $\mathrm{Re}\,\lambda \geq 0$ the integrals are readily carried out yielding

$$\mathcal{S}(\omega) = \sum_\lambda \mathrm{Re}\,\frac{w_\lambda}{i\omega - \lambda} \tag{1.52}$$

with the definition of the *weight factors*

$$w_\lambda = \mathrm{Tr}\{\sigma_+(0)\hat{\varrho}_\lambda\}\mathrm{Tr}\{\check{\varrho}_\lambda^\dagger \sigma_-(0)\rho_{\mathrm{st}}\}\,. \tag{1.53}$$

This results shows that, if a complete eigenbasis of the Liouville operator exists, the spectrum can be decomposed into contributions from the eigenvalues λ weighted with w_λ. Depending on the real and imaginary part of these weight factors the eigenvalue components in the spectrum have a *Lorentzian* or a *Fano* profile. For the zero eigenvalue the proper limit results in a delta peak $\delta(\omega)$ weighted with the factor $w_0 = \pi|\mathrm{Tr}\{\sigma_+\rho_{\mathrm{st}}\}|^2$, proportional to the squared modulus of the steady-state coherence. The decomposition (1.52) will be used later to calculate the power spectrum of the light emitted by a dipole source.

Since the two-level atom is not driven the steady state is the ground state such that the emission spectrum Eq. (1.50) is zero, which follows directly from $\sigma_-\rho_{\mathrm{st}} = 0$. Similarly to the emission one can calculate the response $\mathcal{A}(\omega_{\mathrm{L}})$ of the two-level system to a weak probe field of frequency ω_{L}, which is given by [Mol72, CT77]

$$\mathcal{A}(\omega_{\mathrm{L}}) = \mathrm{Re} \int_0^\infty \mathrm{d}t\, \langle [\sigma_-(0), \sigma_+(t)] \rangle_{\mathrm{st}}\, e^{-i\omega_{\mathrm{L}}t}\,. \tag{1.54}$$

In the same fashion as for the power spectrum of the emitted radiation, given by Eq. (1.50), we can use the quantum regression theorem (1.30)-(1.31) and formal integration to write the absorption spectrum as

$$\mathcal{A}(\omega_{\mathrm{L}}) = \mathrm{Re} \sum_\lambda \frac{1}{i\omega_{\mathrm{L}} - \lambda}\mathrm{Tr}\{\sigma_+\hat{\rho}_\lambda\}\mathrm{Tr}\{\check{\rho}_\lambda^\dagger \rho_{\mathrm{st}}\sigma_-\}\,. \tag{1.55}$$

where the second term of the commutator vanished for the same reason that the emission spectrum vanished. Checking the first trace $\mathrm{Tr}\{\sigma_+\hat{\rho}_\lambda\}$ already suffices to show that only the eigenvalue $\lambda = \lambda_-$ contributes with

$$\mathcal{A}(\omega_{\mathrm{L}}) = \mathrm{Re}\,\frac{1}{i\omega_{\mathrm{L}} - \lambda_-} = \frac{\bar{\Gamma}/2}{(\omega_{\mathrm{L}} - \omega)^2 + \bar{\Gamma}^2/4} \tag{1.56}$$

giving the expected Lorentzian absorption lineshape centered around the transition frequency ω with a full width at half maximum $\bar{\Gamma}$.

Driven case

Including a laser which is detuned from the atomic resonance by Δ and drives the dipole transition with a Rabi frequency Ω leads to an additional term in Hamiltonian which can then be written, in the frame rotating with the laser frequency, as

$$H = -\hbar\Delta|e\rangle\langle e| + \hbar\frac{\Omega}{2}\left(|e\rangle\langle g| + |g\rangle\langle e|\right) . \tag{1.57}$$

In the basis $\{|g\rangle\langle g|, |e\rangle\langle g|, |g\rangle\langle e|, |e\rangle\langle e|\}$ the corresponding Liouville operator can be written in its matrix representation

$$\mathcal{L} = \begin{bmatrix} 0 & -i\Omega/2 & i\Omega/2 & \Gamma \\ -i\Omega/2 & i\Delta - \bar{\Gamma}/2 & 0 & i\Omega/2 \\ i\Omega/2 & 0 & -i\Delta - \bar{\Gamma}/2 & -i\Omega/2 \\ 0 & i\Omega/2 & -i\Omega/2 & -\Gamma \end{bmatrix} \tag{1.58}$$

from which it is straightforward to derive the actual form of the eigenelements, being the left and right eigenvectors of the matrix (1.58). For instance, the steady state ρ_{st}, fulfilling $\mathcal{L}\rho_{\text{st}} = 0$, is given by

$$\rho_{\text{st}} = \frac{1}{N} \begin{pmatrix} \bar{\Gamma}^2/4 + \Delta^2 + \bar{\Gamma}\Omega^2/4\Gamma & \left[\Delta + i\bar{\Gamma}/2\right]\Omega/2 \\ \left[\Delta - i\bar{\Gamma}/2\right]\Omega/2 & \bar{\Gamma}\Omega^2/4\Gamma \end{pmatrix} \tag{1.59}$$

in the basis $\{|g\rangle, |e\rangle\}$, with the normalization constant $N = \bar{\Gamma}^2/4 + \Delta^2 + \bar{\Gamma}\Omega^2/2\Gamma$. The shape of the remaining three right eigenelements is more complicated and is not reported here but can be found in Ref. [Jak03].

Damped harmonic oscillator

After introducing the damping basis as a convenient tool for the solution of master equations and a first example of its application to the damped two-level atom we present in this chapter the derivation of the eigenbasis of a harmonic oscillator which is damped by a reservoir of thermal oscillators. Since the damped harmonic oscillator plays a central role in many physical systems, for example a lossy cavity or a mechanical resonator in contact with a thermal reservoir, and some of our later treatments of more complex systems rely on the solution of its eigenvalue problem, we present the derivation of its damping basis in more detail. For further reading on the subject we refer to Refs. [Bri93, Bar00, Eng02].

We begin in Sec. 2.1 by presenting the master equation and the eigenvalue problem. One possible way to a solution is the use of phase-space distributions, which we will briefly introduce in Sec. 2.2. In Sec. 2.3 we transform the master equation of the damped harmonic oscillator into its phase-space equivalent, the *Fokker-Planck equation*, and derive its eigensolutions which in turn lead to the eigenelements. Finally, in Sec. 2.4 we apply the solution to the time evolution of a particular initial state.

We consider a harmonic oscillator of mass M and frequency ν and denote the *annihilation* and *creation operators* by b and $b^\dagger$, respectively. Their commutator is given by $[b, b^\dagger] = 1$ and their relation to the *position* and *momentum operators*, x and p, reads

$$x = \xi(b + b^\dagger)\,, \tag{2.1}$$

$$p = -\frac{i\hbar}{2\xi}(b - b^\dagger)\,, \tag{2.2}$$

with the ground-state wavepacket width $\xi = \sqrt{\hbar/2M\nu}$. In terms of these two operators the harmonic oscillator Hamiltonian has the form

$$H = \hbar\nu b^\dagger b\,, \tag{2.3}$$

where we neglected the constant zero-point energy $\hbar\nu/2$. The *number states* $|n\rangle$, also called *Fock states*, which fulfill $b^\dagger b|n\rangle = n|n\rangle$, for $n = 0, 1, 2...$, are the eigenstates of

this Hamiltonian and the annihilation and creation operators act on them according to

$$b|n\rangle = \sqrt{n}|n-1\rangle\,, \tag{2.4}$$

$$b^\dagger|n\rangle = \sqrt{n+1}|n+1\rangle\,. \tag{2.5}$$

The coupling of this harmonic oscillator to a reservoir with the *inverse temperature* $\beta = 1/k_\mathrm{B}T$, resulting in a *mean thermal occupation* $\bar{m} = (\exp[\beta\hbar\nu] - 1)^{-1}$, leads to a master equation

$$\frac{\partial}{\partial t}\mu = \mathcal{L}\mu \tag{2.6}$$

for the density operator μ with the Liouville operator [Car02, Bre07]

$$\mathcal{L}\mu = -i\nu[b^\dagger b, \mu] + \frac{\gamma}{2}(\bar{m}+1)\mathcal{D}[b]\mu + \frac{\gamma}{2}\bar{m}\mathcal{D}[b^\dagger]\mu\,, \tag{2.7}$$

where γ denotes the decay rate. The damping basis is given by the spectral decomposition of $\mathcal{L}$, *i.e.* the solutions of the eigenvalue equations

$$\mathcal{L}\hat{\mu}_\lambda = \lambda\hat{\mu}_\lambda\,, \tag{2.8}$$

$$\check{\mu}_\lambda^\dagger \mathcal{L} = \lambda\check{\mu}_\lambda^\dagger\,. \tag{2.9}$$

The adjoint equation in the second line can be found by the action to the left of $\mathcal{L}$ according to Eq. (1.39) and is explicitly given by

$$\check{\mu}_\lambda^\dagger \mathcal{L} = i\nu[b^\dagger b, \check{\mu}_\lambda^\dagger] + \frac{\gamma}{2}(\bar{m}+1)\check{\mathcal{D}}[b]\check{\mu}_\lambda^\dagger + \frac{\gamma}{2}\bar{m}\check{\mathcal{D}}[b^\dagger]\check{\mu}_\lambda^\dagger\,. \tag{2.10}$$

Before we proceed we briefly comment that for zero temperature, *i.e.* for $\bar{m} = 0$, the Liouville operator without the so-called *jump operator* $\mathcal{J}$, whose action is given by $\mathcal{J}\mu = \gamma b\mu b^\dagger$, fulfills the eigenvalue equation

$$\left[\mathcal{L} - \mathcal{J}\right]|n+|l|\rangle\langle n| = \left[-il\nu - \left(n + \frac{|l|}{2}\right)\gamma\right]|n+|l|\rangle\langle n|\,, \tag{2.11}$$

for $l \geq 0$, and the Hermitian conjugate equation for $l < 0$. Later we will find that the spectrum of eigenvalues $\lambda_{n,l} = -il\nu - [n+|l|/2]\gamma$ is not changed by including the jump operator $\mathcal{J}$. We will encounter this fact, that the operators $\mathcal{L} - \mathcal{J}$ and $\mathcal{L}$ have the same spectrum, again in a subsequent chapter.

Since our derivation of the damping basis relies on the transformation the eigenvalue equations (2.8) and (2.9) into differential equations for phase-space distributions, we briefly review some properties of *quasiprobability distributions*.

We begin by defining the s-ordered exponential operator as

$$D(\beta, s) = e^{\beta b^\dagger - \beta^* b + \frac{s}{2}|\beta|^2} \tag{2.12}$$

which coincides with the well-known *displacement operator* $D(\alpha) = \exp[\alpha b^\dagger - \alpha^* b]$ in the case $s = 0$. On the basis of these exponential operators one can define a whole class of quasiprobability distributions [Gla07, Cah69a]. This is achieved by defining the s-parametrized *characteristic function* of an operator μ as

$$\chi(\beta, s, \mu) = \mathrm{Tr}\{D(\beta, s)\mu\} \tag{2.13}$$

which is useful to calculate expectation values of s-ordered products of creation and annihilation operators [Cah69b]. A Fourier transform of this characteristic function then yields the s-parametrized quasiprobability distribution

$$W(\alpha, s, \mu) = \frac{1}{\pi^2} \int \mathrm{d}^2\beta \, \chi(\beta, s, \mu) e^{\alpha\beta^* - \alpha^*\beta} \,. \tag{2.14}$$

This class of distributions includes the most widely used phase-space distributions: the Wigner function, the Glauber-Sudarshan P-distribution and the Husimi Q-function. On the other hand, the characteristic function can obviously be obtained from the quasiprobability distribution by the inverse Fourier transform

$$\chi(\beta, s, \mu) = \int \mathrm{d}^2\alpha \, W(\alpha, s, \mu) e^{\beta\alpha^* - \beta^*\alpha} \,. \tag{2.15}$$

The quasiprobability distributions introduced here will be useful on many occasions in the text below and we therefore summarize a collection of their properties.

The density operator of a harmonic oscillator in *thermal equilibrium*, which is the steady state solution of Eq. (2.6), fulfilling $\mathcal{L}\mu = 0$, is given by

$$\mu_{\mathrm{th}} = \frac{e^{-\beta H}}{\mathrm{Tr}\{e^{-\beta H}\}} = \frac{1}{\bar{m} + 1} \left[\frac{\bar{m}}{\bar{m} + 1}\right]^{b^\dagger b} \,. \tag{2.16}$$

Writing this density operator in the number state basis $|n\rangle$ we arrive at an expression that contains the diagonal elements of the exponential operator, which can be found in [Cah69a], and has the form

$$\chi(\beta, s, \mu_{\mathrm{th}}) = \frac{e^{\frac{1}{2}(s-1)|\beta|^2}}{\bar{m} + 1} \sum_{n=0}^{\infty} \left[\frac{\bar{m}}{\bar{m} + 1}\right]^n L_n^{(0)}(|\beta|^2) \tag{2.17}$$

with the generalized Laguerre polynomials $L_n^{(\alpha)}(z)$ [Abr65]. A closer look reveals that the sum in Eq. (2.17) is nothing but the generating function [Mag67]

$$\sum_{n=0}^{\infty} z^n L_n^{(l)}(x) = \frac{1}{[1-z]^{l+1}} e^{-\frac{zx}{1-z}} , \qquad (2.18)$$

where we identify $z = \bar{m}/(\bar{m} + 1)$ and $x = |\beta|^2$, leading to

$$\chi(\beta, s, \mu_{\text{th}}) = e^{-\frac{1}{2}[2\bar{m}+1-s]|\beta|^2} \qquad (2.19)$$

which is the characteristic function of a thermal state. Since we now have the characteristic function (2.19) at hand we can perform the Fourier transform (2.15) using the integral

$$\int \mathrm{d}^2\zeta \, e^{-c|\zeta|^2} e^{\varphi\zeta^* + \bar{\varphi}\zeta} = \frac{\pi}{c} e^{\frac{\varphi\bar{\varphi}}{c}} \qquad (2.20)$$

to arrive at the s-parametrized quasiprobability distribution

$$W(\alpha, s, \mu_{\text{th}}) = \frac{2}{\pi[2\bar{m} + 1 - s]} e^{-\frac{2|\alpha|^2}{2\bar{m}+1-s}} . \qquad (2.21)$$

These distributions have the same Gaussian shape as the distributions for a coherent state with the only difference that the thermal occupation $\bar{m}$ adds an additional width. The form also suggests that for high thermal occupations the value of s becomes more and more irrelevant.

There are three prominent examples for phase-space distributions. They correspond to the s-parametrized distributions for the values $s = -1, 0, 1$. For $s = -1$ the distribution is given by the so-called Q-function introduced by *Husimi* [Hus40]

$$Q(\alpha) = W(\alpha, -1, \mu) = \frac{1}{\pi} \langle \alpha | \mu | \alpha \rangle , \qquad (2.22)$$

which turns out to be the expectation value of μ in a coherent state $|\alpha\rangle$ and is thereby strictly positive.

The next example is especially useful to illustrate quantum states. It was introduced by *Wigner* [Wig32] and is given by the $s = 0$ distribution

$$W(x, p) = \frac{1}{2\hbar} W(\alpha = x/2\xi + \mathrm{i}\xi p/\hbar, 0, \mu) . \qquad (2.23)$$

An equivalent definition is given by the Fourier transform

$$W(x, p) = \frac{1}{2\pi\hbar} \int \mathrm{d}y \, \langle x + y/2 | \mu | x - y/2 \rangle e^{-ipy/\hbar} . \qquad (2.24)$$

This distribution is particularly interesting because its marginals are the position and momentum probability distributions. On the contrary to the Q-function the Wigner function can assume negative values, which is generally accepted to be an indicator for the non-classicality of quantum states [Sch01]. We will later make use of this distribution to illustrate the states of an oscillator in order to discuss properties such as the above mentioned non-classicality or its spread in phase space.

The last candidate is the $s = 1$ case, called the *Glauber-Sudarshan P-distribution*:

$$W(\alpha, 1, \mu) = P(\alpha) \,, \tag{2.25}$$

which can be rewritten as the diagonal representation of a density operator in the coherent state basis [Sud63, Meh65, Gla07], *viz.*

$$\mu = \int \mathrm{d}^2\alpha\, P(\alpha)|\alpha\rangle\langle\alpha| \,. \tag{2.26}$$

Opposed to the Wigner- and Q-function this distribution can have a highly pathological behavior [Cah69b].

With the Q- and P-distributions at hand the scalar product of two operators X and Y can be expressed as

$$\mathrm{Tr}\{X^\dagger Y\} = \int \mathrm{d}^2\alpha\, P(\alpha)\mathrm{Tr}\{|\alpha\rangle\langle\alpha|Y\} = \pi \int \mathrm{d}^2\alpha\, P(\alpha)Q(\alpha) \tag{2.27}$$

which is a phase space integral over the product of the P-function of $X^\dagger$ and the Q-function of Y. This relation can be useful to turn the problem of calculating involved traces of operator products into mere c-number integrals.

The term Fokker-Planck equation refers is a certain type of differential equation for a probability density function [Ris96]. The procedure to find the eigenbasis of the damped harmonic oscillator is the following: *(i)* Starting from the Liouville operator (2.6) and its adjoint there is a straightforward way to obtain the corresponding differential operators for the phase-space distribution. *(ii)* The resulting eigenvalue equations for these differential operators can be cast into the form of differential equations with well-known solutions. *(iii)* From these solutions the inverse transformation to operators leads to the eigenelements.

On the basis of the equation of motion for μ we can write down the dynamical equation of the associated characteristic function as

$$\chi\left(\beta, s, \frac{\partial}{\partial t}\mu\right) = \chi(\beta, s, \mathcal{L}\mu) \,. \tag{2.28}$$

This means we have to find the phase-space equivalent of the terms occurring in $\mathcal{L}\mu$. It is sufficient to derive $\chi(\beta, s, bX)$, $\chi(\beta, s, Xb)$, $\chi(\beta, s, b^\dagger X)$ and $\chi(\beta, s, Xb^\dagger)$ for an arbitrary operator X. As an example we inspect the term $\chi(\beta, s, bX)$ which leads to

$$\chi(\beta, s, bX) = \text{Tr}\{D(\beta, s)bX\}. \tag{2.29}$$

At this point we can use the Baker-Haussdorf formula to write the derivative of $D(\beta, s)$ with respect to β^* as

$$\frac{\partial D(\beta, s)}{\partial \beta^*} = \left[-b + \frac{\beta}{2}(s+1)\right] D(\beta, s) = D(\beta, s)\left[-b + \frac{\beta}{2}(s-1)\right] \tag{2.30}$$

which on the other hand means we can write for example

$$\chi(\beta, s, bX) = \left[-\frac{\partial}{\partial \beta^*} + \frac{s+1}{2}\beta\right] \chi(\beta, s, X). \tag{2.31}$$

When going from the characteristic function to the quasiprobability distribution the properties of the Fourier transform then relate multiplications with derivatives, and *vice versa*. The resulting expressions are summarized in Tab. 2.1.

X	$W(\alpha, s, X)$	X	$W(\alpha, s, X)$
$b\mu$	$\left[\alpha - \frac{s-1}{2}\frac{\partial}{\partial \alpha^*}\right] W(\alpha, s, \mu)$	$b^\dagger \mu$	$\left[\alpha^* - \frac{s+1}{2}\frac{\partial}{\partial \alpha}\right] W(\alpha, s, \mu)$
μb	$\left[\alpha - \frac{s+1}{2}\frac{\partial}{\partial \alpha^*}\right] W(\alpha, s, \mu)$	$\mu b^\dagger$	$\left[\alpha^* - \frac{s-1}{2}\frac{\partial}{\partial \alpha}\right] W(\alpha, s, \mu)$

Table 2.1: *Relations between multiplication with b (left panel) and $b^\dagger$ (right panel) from both sides and operations on the quasi probability distributions.*

With this table one can then construct the Fokker-Planck equation for the desired s-parametrized phase space function by transforming the different terms in the master equation (2.6) individually, yielding

$$\frac{\partial}{\partial t}W(\alpha, s, \mu) = \hat{L}_s W(\alpha, s, \mu) \tag{2.32}$$

where the differential operator $\hat{L}_s$ is given by

$$\hat{L}_s = i\nu\left[\frac{\partial}{\partial \alpha}\alpha - \frac{\partial}{\partial \alpha^*}\alpha^*\right] + \frac{\gamma}{2}\left[\frac{\partial}{\partial \alpha}\alpha + \frac{\partial}{\partial \alpha^*}\alpha^*\right] + \frac{\gamma}{2}[2\bar{m}+1-s]\frac{\partial^2}{\partial \alpha \partial \alpha^*}. \tag{2.33}$$

Likewise one can define the differential operator $\check{L}_s$ that corresponds to the adjoint Liouville operator as

$$\check{L}_s = \left[-i\nu - \frac{\gamma}{2}\right]\alpha\frac{\partial}{\partial \alpha} + \left[i\nu - \frac{\gamma}{2}\right]\alpha^*\frac{\partial}{\partial \alpha^*} + \frac{\gamma}{2}[2\bar{m}+1+s]\frac{\partial^2}{\partial \alpha \partial \alpha^*}. \tag{2.34}$$

In the next subsections we will take a specific value of s and find the eigenfunctions

of the differential operators $\hat{L}_s$ and $\check{L}_s$.

In the remaining derivation we will restrict ourselves to the Q-function and denote the differential operators $\hat{L}_s$ and $\check{L}_s$ for $s = -1$ simply by $\hat{L}$ and $\check{L}$. Since we eventually want to solve the eigenvalue equations (2.8) and (2.9) we introduce a new notation to label the Q-functions of $\hat{\mu}_\lambda$ and $\check{\mu}_\lambda^\dagger$, namely

$$\hat{Q}_\lambda(\alpha) = \frac{1}{\pi}\langle\alpha|\hat{\mu}_\lambda|\alpha\rangle\,, \quad \check{Q}_\lambda(\alpha) = \frac{1}{\pi}\langle\alpha|\check{\mu}_\lambda^\dagger|\alpha\rangle\,. \tag{2.35}$$

With this new notation the phase-space eigenvalue equations read

$$\left[\hat{L} - \lambda\right]\hat{Q}_\lambda(\alpha) = 0\,, \tag{2.36}$$

$$\left[\check{L} - \lambda\right]\check{Q}_\lambda(\alpha) = 0\,. \tag{2.37}$$

Eigenfunctions associated to the right eigenelements

For the right eigenfunctions the differential equation explicitly reads

$$\left\{\left[\mathrm{i}\nu + \frac{\gamma}{2}\right]\frac{\partial}{\partial\alpha}\alpha + \left[-\mathrm{i}\nu + \frac{\gamma}{2}\right]\frac{\partial}{\partial\alpha^*}\alpha^* + \gamma[\bar{m} + 1]\frac{\partial^2}{\partial\alpha\partial\alpha^*} - \lambda\right\}\hat{Q}_\lambda(\alpha) = 0\,. \tag{2.38}$$

In the number state representation the Liouville operators only couples entries of the density operator that are on the same diagonal, which suggests the ansatz

$$\hat{Q}_\lambda(\alpha) = \alpha^{*(|k|+k)/2}\alpha^{(|k|-k)/2}f_k(|\alpha|^2) \tag{2.39}$$

with an integer k. Substituting this ansatz in Eq. (2.38) leads to

$$\gamma(\bar{m}+1)|\alpha|^2 f_k''(|\alpha|^2) + \gamma\left[(\bar{m}+1)(|k|+1) + |\alpha|^2\right]f_k'(|\alpha|^2)$$
$$+ \left[\mathrm{i}\nu|k| + \frac{\gamma}{2}(|k|+2) - \lambda\right]f_k(|\alpha|^2) = 0\,. \tag{2.40}$$

The change of variables $z = -|\alpha|^2/(\bar{m}+1)$ finally gives the so-called *Kummer's differential equation* [Abr65]

$$zf_k''(z) + [B_k - z]f_k'(z) - A_k f_k(z) = 0 \tag{2.41}$$

with the constants

$$A_k = \frac{-\mathrm{i}\nu k - \lambda}{\gamma} + \frac{|k|+2}{2}\,, \quad B_k = |k| + 1\,. \tag{2.42}$$

Since Kummer's equation is an ordinary differential equation of second order there exist two independent solutions, of which the one that remains finite at $z = 0$ is given

by the *hypergeometric function* $_1F_1(A_k; B_k; z)$ [Mag67]. They obey

$$_1F_1(A_k; B_k; z) = \, _1F_1(B_k - A_k; B_k; z)e^z \tag{2.43}$$

In order to have a finite series in Eq. (2.43) the condition $B_k - A_k = -m$ has to be fulfilled with a positive integer m, which is independent of k. This fact combined with Eq. (2.42) immediately reveals the form of the eigenvalues, which are given by

$$\lambda_{m,k} = -\mathrm{i}\nu k - \gamma \left[m + \frac{|k|}{2} \right] . \tag{2.44}$$

Here, we already gave the eigenvalues a double index, because they depend on the two integers $m \geq 0$ and k. This also means we have already found the functions $f_{m,k}$ which we will now also index with the two integers. It is proportional to the generalized hypergeometric series

$$f_{m,k}(z) \propto \, _1F_1(-m; |k| + 1; z)e^z = \binom{m + |k|}{m}^{-1} L_m^{(|k|)}(-z)e^z \tag{2.45}$$

which turns out to be related to the mth generalized Laguerre polynomial [Mag67]. The solutions of Eq. (2.36) can then be written

$$\hat{Q}_{m,k}(\alpha) \propto \alpha^{*(|k|+k)/2}\alpha^{(|k|-k)/2} L_m^{(k)} \left(\frac{|\alpha|^2}{\bar{m}+1} \right) e^{-\frac{|\alpha|^2}{\bar{m}+1}} , \tag{2.46}$$

where we have not yet fixed the normalization constant.

Eigenfunctions associated to the left eigenelements

We will use the same procedure to obtain the solutions of Eq. (2.37). The differential equation for left eigenfunctions is

$$\left\{ \left[-\mathrm{i}\nu - \frac{\gamma}{2} \right] \alpha \frac{\partial}{\partial \alpha} + \left[\mathrm{i}\nu - \frac{\gamma}{2} \right] \alpha^* \frac{\partial}{\partial \alpha^*} + \gamma\bar{m}\frac{\partial^2}{\partial \alpha \partial \alpha^*} - \lambda_{m,k} \right\} \check{Q}_{m,k}(\alpha) = 0 . \tag{2.47}$$

We choose an ansatz similar to Eq. (2.39), but in this case

$$\check{Q}_{m,k}(\alpha) = \alpha^{(|k|+k)/2}\alpha^{*(|k|-k)/2} g_{m,k}(|\alpha|^2) . \tag{2.48}$$

Inserting this in Eq. (2.47) yields

$$\gamma\bar{m}|\alpha|^2 g''_{m,k}(|\alpha|^2) + \gamma \left[\bar{m}(|k| + 1) - |\alpha|^2 \right] g'_{m,k}(|\alpha|^2)$$
$$- \left[\left(\mathrm{i}\nu + \frac{\gamma}{2} \right) |k| + \lambda_{m,k} \right] g_{m,k}(|\alpha|^2) = 0 \tag{2.49}$$

which can also be transformed into Kummer's differential equation using the change of variables $z = |\alpha|^2/\bar{m}$ and the eigenvalues $\lambda_{m,k}$ of Eq. (2.44). This results in

$$zg''_{m,k}(z) + [(|k| + 1) - z]g'_{m,k}(z) + mg_{m,k}(z) = 0 \tag{2.50}$$

which has the normalizable solutions

$$g_{m,k}(z) \propto {}_1F_1(-m, |k| + 1, z) = \binom{m + |k|}{m}^{-1} L_m^{(|k|)}(z). \tag{2.51}$$

By substituting this into the ansatz (2.48) we can write the eigensolutions associated with the left eigenelements as

$$\check{Q}_{m,k}(\alpha) \propto \alpha^{(|k|+k)/2} \alpha^{*(|k|-k)/2} L_m^{(k)}\left(\frac{|\alpha|^2}{\bar{m}}\right). \tag{2.52}$$

The last step is now to perform the back transform from the phase-space functions to operators.

From the eigenfunctions to the eigenelements

A product of annihilation and creation operators is said to be *normally ordered* if all creation operators stand to the left of the annihilation operators and the normal ordering is denoted by colons, for example $: bb^\dagger := b^\dagger b$. If we keep the definition (2.22) of the Q-function in mind the eigenfunctions in Eqs. (2.46) and (2.52) immediately become

$$\hat{\mu}_{m,k} = \frac{(-1)^m}{(\bar{m} + 1)^{|k|+1}} b^{\dagger(|k|+k)/2} : L_m^{(|k|)}\left(\frac{b^\dagger b}{\bar{m} + 1}\right) e^{-\frac{b^\dagger b}{\bar{m}+1}} : b^{(|k|-k)/2}, \tag{2.53}$$

$$\check{\mu}_{m,k}^\dagger = \frac{m!}{(m + |k|)!} \left[\frac{-\bar{m}}{\bar{m} + 1}\right]^m b^{\dagger(|k|-k)/2} : L_m^{(|k|)}\left(\frac{b^\dagger b}{\bar{m}}\right) : b^{(|k|+k)/2}, \tag{2.54}$$

where we substituted α by b and α^* by $b^\dagger$ and applied the normal ordering. Here, we followed Ref. [Bri93] in the choice of the normalization constants, which can in general be chosen otherwise as long as the orthogonality relation (1.41) between the left and right eigenelements is fulfilled. This is indeed the case for the normalization we employ here and it was furthermore shown in Ref. [Bri93, Bar00] that the basis is complete in the sense

$$\sum_{m=0}^{\infty} \sum_{k=-\infty}^{\infty} \hat{\mu}_{m,k} \otimes \check{\mu}_{m,k} = 1. \tag{2.55}$$

From the Q-function one can also obtain the P-distribution using the methods reported in App. A.1. A brief summary of the necessary steps and the resulting P-functions are reported in App. A.2. From the P-distributions it is then straightforward to obtain the *antinormally ordered* form of the eigenelements.

As an example for the use of the damping basis we will calculate the time evolution of a simple initial state, a number state. Let us consider the oscillator to be initially in the state $|N\rangle$. The expansion coefficients (1.46) are then given by

$$c_{m,k} = \mathrm{Tr}\{\check{\mu}_{m,k}^\dagger |N\rangle\langle N|\} = \left[\frac{-\bar{m}}{\bar{m}+1}\right]^m \langle N| b^{\dagger \frac{|k|-k}{2}} : L_m^{(|k|)}\left(\frac{b^\dagger b}{\bar{m}}\right) : b^{\frac{|k|+k}{2}} |N\rangle, \quad (2.56)$$

where we already see that only the terms with $k = 0$ contribute, since they are the only terms containing the same number of creation and annihilation operators. This fact is also expected since in phase space number states show a radial symmetry [Sch01]. The coefficients then become $c_{m,k} = \delta_{k,0} c_{m,0}$ with

$$c_{m,0} = (-1)^m \, {}_2F_1\left(-m, N+1; 1; \frac{1}{\bar{m}+1}\right) \quad (2.57)$$

and the *hypergeometric function* ${}_2F_1(\alpha, \beta; \gamma; z)$ [Mag67]. The state at time t then takes the form

$$\mu(t) = \frac{1}{\bar{m}+1} \sum_{m=0}^\infty e^{-m\gamma t} \, {}_2F_1\left(-m, N+1; 1; \frac{1}{\bar{m}+1}\right) : L_m^{(0)}\left(\frac{b^\dagger b}{\bar{m}+1}\right) e^{-\frac{b^\dagger b}{\bar{m}+1}} : \quad (2.58)$$

from which we can deduce the Q-function using a newly found generating function that is reported in App. A.3. The resulting Q-function is given by

$$Q(\alpha, t) = \frac{e^{-\frac{|\alpha|^2}{\bar{m}(t)+1}}}{\pi[\bar{m}(t)+1]} \left[1 - \frac{e^{-\gamma t}}{\bar{m}(t)+1}\right]^N L_N^{(0)}\left(-\frac{\frac{e^{-\gamma t}}{\bar{m}(t)+1}}{1 - \frac{e^{-\gamma t}}{\bar{m}(t)+1}} \frac{|\alpha|^2}{\bar{m}(t)+1}\right) \quad (2.59)$$

with the definition of the time-dependent thermal width $\bar{m}(t) = \bar{m}(1 - \exp[-\gamma t])$. This can be translated to a normally ordered density operator of which one can evaluate the diagonal elements yielding the quantum state

$$\mu(t) = \frac{1}{\bar{m}(t)+1} \left[\frac{\bar{m}(t)}{\bar{m}(t)+1}\right]^{b^\dagger b} \left[1 - \frac{e^{-\gamma t}}{\bar{m}(t)+1}\right]^N$$
$$\times \, {}_2F_1\left(-b^\dagger b, -N; 1; \frac{1}{\bar{m}(t)} \frac{\frac{e^{-\gamma t}}{\bar{m}(t)+1}}{1 - \frac{e^{-\gamma t}}{\bar{m}(t)+1}}\right). \quad (2.60)$$

The limiting case $\bar{m} \to 0$ of this state reproduces the known result of a number state damped by a zero temperature reservoir [Bar00], given by a *binomial distribution* of the probabilities, *viz.*

$$\mu(t) = \binom{N}{b^\dagger b} \left(e^{-\gamma t}\right)^{b^\dagger b} \left(1 - e^{-\gamma t}\right)^{N - b^\dagger b}. \quad (2.61)$$
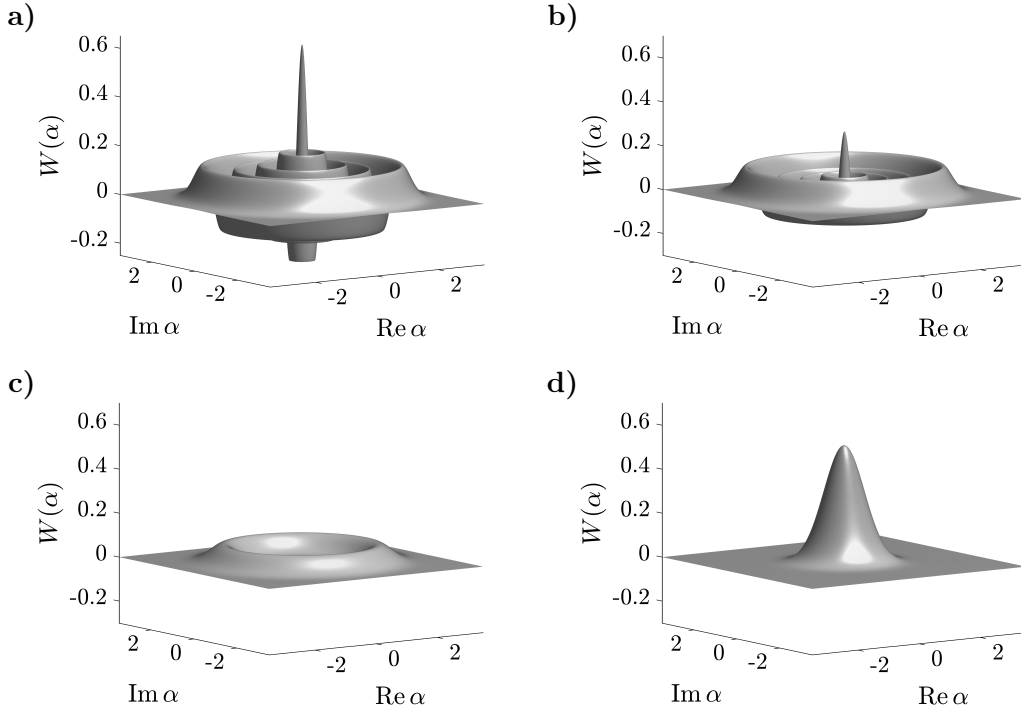
Figure 2.1: *Wigner function of a decaying Fock state N for $\gamma = \nu$ and $\bar{m} = 0.1$ at different times:* **a)** $\gamma t = 0$, **b)** $\gamma t = 1/25$, **c)** $\gamma t = \log(\bar{m} + 1) - \log(\bar{m} + 1/2)$ *and* **d)** $\gamma t = 50$.

It is also straightforward to go from the Q-function (2.59) to the corresponding Wigner function using the steps described in App. A.1 and one arrives at

$$W(\alpha, t) = \frac{e^{-\frac{|\alpha|^2}{\bar{m}(t)+1/2}}}{\pi[\bar{m}(t) + 1/2]} \left[1 - \frac{e^{-\gamma t}}{\bar{m}(t) + 1/2}\right]^N L_N^{(0)}\left(\frac{\frac{e^{-\gamma t}}{\bar{m}(t)+1/2}}{1 - \frac{e^{-\gamma t}}{\bar{m}(t)+1/2}} \frac{-|\alpha|^2}{\bar{m}(t) + 1/2}\right) \quad (2.62)$$

which is shown in Fig. 2.1 for different times, illustrating the decay of the number state towards a thermal state. The time $\gamma t = \log(\bar{m}+1) - \log(\bar{m}+1/2)$, see Fig. 2.1 c), is particularly interesting because it is the threshold time after which the Laguerre polynomials in Eq. (2.62) possess no zeros anymore, making the Wigner function fully positive thereafter.

PART II

Solid-state quantum emitters

The steady growth of the field of quantum-information science over the last decades is the main motivation for today's research on *single-photon sources* [San10, Eis11], which are vital components for the realization of quantum cryptography [Eke00] or quantum computation with photonic qubits [Kok07]. The resulting demand for sources of non-classical light for these quantum technological applications has triggered a wide search for alternatives to single-photon sources based on single trapped atoms [Die87] or molecules in several fields of physics. Hereby, solid-state platforms, such as semi-conductor quantum dots [Kir04] and crystal defect centers [Kur00], turned out to be attractive candidates.

Compared to atoms, solid-state quantum emitters demand a much lower experimental overhead and offer several advantages. For example, they show relatively high rates of single-photon emission [Hoa16], they can be employed at ambient conditions [Miz12, Alb14] and they do not need to be trapped, since they are embedded in their solid-state matrix. However, the latter advantage also comes at a high price: the embedding in the crystal environment leads to a strong coupling of the electronic degrees of freedom to lattice vibrations, while single atoms ideally only couple to the free electromagnetic field. It is this coupling to lattice vibrations that gives rise to the broad spectrum of the absorbed and spontaneously emitted single photons, the so-called *phonon sideband*.

In the case of atomic single-photon sources, the spectral properties of the scattered photons can be conveniently obtained from the Born-Markov master equation (1.48) describing the spontaneous emission. Their solid-state counterparts, on the other hand, lack such a theoretical description based on a simplified physical picture that reproduces the phonon sideband. With the work presented in this part we shall contribute to filling this gap by proposing a model for the description of solid-state emitters and their coupling to lattice phonons in terms of a Born-Markov master equation in which the continuum of phonons is replaced by a single *damped* vibrational mode. This model thereby provides the means for the analysis of the emitter's dynamics as well as its light scattering properties based on a single dynamical equation.

Among the variety of solid-state emitters, color centers in diamond, primarily the *negatively charged nitrogen-vacancy* (NV^-) *centers*, have experienced an impressively successful development [Jel06, Doh13, Sch16] in their application to quantum technologies during the last two decades. In the following we will therefore comment on the applicability of our model to NV^- centers at several points. These defect centers provide optically addressable electronic transitions between discrete quantum states energetically situated between the valence and conduction band. For example, anti-bunching of the light emitted on this transition was shown [Kur00], Wheeler's delayed-choice experiment was realized [Jac07] and the coupling to optical micro- or nano-cavities [Alb13, Li15] as well as photonic crystal cavities [RM14, RM15] was performed, to mention only a very few of the experimental breakthroughs. Moreover, applicability of the centers for quantum information technology using coupled electronic and nuclear spins has been shown [Dut07, Tog10, Wal14], high precision magnetic sensing using the states of the ground state triplet has been reported [Deg08, Bal08, Maz08, Tri16] and coupling to mechanical oscillators was achieved [Tei14].

This part is arranged as follows: To lay the basis for our model to describe the emitter-phonon interaction, in Chapter 3 we review a model from the literature that is used to describe, among other properties, the light-absorption spectra of solid-state defect centers. In Chapter 4 we introduce our model for two-level quantum emitters coupling to localized vibration modes in form of a Born-Markov master equation. A full solution of this master equation is then derived, followed by some applications of the model before we finally compare the obtained results to the previously introduced model from the literature.

Huang-Rhys model for color centers in crystals

A color center in a crystal, or what we refer to as a solid-state quantum emitter, is a point defect in the crystal lattice that absorbs and emits light in a spectral region where the crystal itself does not absorb or emit. They were first investigated in alkali-halide crystals [Poh37] and were originally termed *Farbzentren* (German for color centers) or *F*-centers [Sch62]. Usually they are formed by a single or multiple electrons confined to a lattice vacancy which is sometimes accompanied by a neighboring impurity atom.

One of the first, most elementary and quantitative models for color centers was developed by *Huang and Rhys* [Hua50]. The basis of their model is the *Franck-Condon principle* applied to color centers in crystals, in their case specifically to *F*-centers. In order to model the shape of the absorption band it takes the strength of the interaction between the electron and the lattice into account with the so-called Huang-Rhys parameter. The vibrational modes of the crystal in this model are assumed to be all of the same frequency in a continuum approximation, hence being essentially a model with a single vibrational degree of freedom. This assumption is a textbook example for the description of crystals referred to as the *Einstein model* [Kit04, Mah00]. Later developments generalized this approach to an arbitrary spectrum of the vibrational frequencies [Lax52, Mar66, Mar67] and afterwards these ideas were applied to color centers in diamond [Dav74], *e.g.* the NV^- center, especially for the calculation of their absorption and emission spectra.

More recent models include pragmatic approaches [Su08], using somehow artificially but successfully a certain number of vibrational levels, also called *vibronic sublevels*, associated with the electronic ground state with each transition to the excited state damped by an individual Markovian reservoir, thereby lacking a clear underlying physical picture. A more sophisticated description is based on a non-Markovian master equation, *i.e.* a master equation where the Markov approximation discussed in Sec. 1.1 is not performed, for the emitter's reduced density operator with general phononic spectral functions [Wei12]. This method was later applied to quantum dots in Ref. [WR02].

To gain first insight into the physics of defect centers and for a later comparison we review the main features of the Huang-Rhys model in this chapter. In Sec. 3.1 we introduce the linearized interaction of an electronic two-level system with the phonons of the surrounding crystal. From the Hamiltonian describing this interaction we derive in Sec. 3.2 the electronic correlation function from which the absorption spectrum is

derived. Finally in Sec. 3.3 we make the single frequency approximation and explicitly derive the form of the absorption lines.

We consider a single two-level defect, with the electronic ground state $|g\rangle$, the excited state $|e\rangle$, and a transition frequency ω, embedded in a crystal lattice. An electronic excitation to the state $|e\rangle$ is accompanied with a change in the electronic charge distribution thereby altering the electrostatic potential that the surrounding lattice experiences. A schematic picture of this *deformation potential* interaction is depicted in Fig. 3.1. The annihilation and creation operator of the kth phonon mode of the
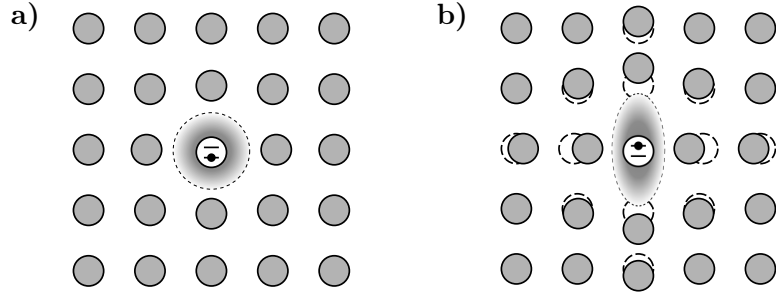
Figure 3.1:   **a)** *The Coulomb interaction of the ground state electronic orbital (shaded gray) of a two-level defect center lets the surrounding atoms take on a certain equilibrium lattice position.* **b)** *The excited electronic orbital displaces the adjacent crystal atoms into an altered equilibrium configuration.*

lattice with frequency ν_k will be denoted b_k and $b_k^\dagger$, respectively. In first order of the displacement of the atoms from their former equilibrium position the Hamiltonian describing this system has the form [Zim60, Mah00]

$$H = \hbar\omega|e\rangle\langle e| + \sum_k \hbar\nu_k b_k^\dagger b_k - \hbar|e\rangle\langle e| \sum_k \lambda_k(b_k + b_k^\dagger)\,, \qquad (3.1)$$

where λ_k is the strength of the interaction between the kth phonon mode with the defect. This Hamiltonian is also called the *independent boson model* [Mah00] and can be diagonalized exactly using the so-called *polaron transform*, given by the unitary operator [Bra05]

$$P = \exp\left\{ -|e\rangle\langle e| \sum_k \beta_k(b_k^\dagger - b_k) \right\}\,, \qquad (3.2)$$

with the dimensionless relative interaction strengths $\beta_k = \lambda_k/\nu_k$. The transformation leads to a Hamiltonian $\bar{H} = PHP^\dagger$ of the form

$$\bar{H} = \hbar(\omega - \Delta)|e\rangle\langle e| + \sum_k \hbar\nu_k b_k^\dagger b_k\,. \tag{3.3}$$

where the bosons are fully decoupled. The frequency shift of the defect center's transition due to the electron-phonon interaction is given by

$$\Delta = \sum_k \nu_k \beta_k^2 \tag{3.4}$$

and is referred to as the *polaron shift.*

The absorption lineshape (1.54) of a weak probe laser of frequency ω_L coupling the two electronic states under stationary conditions, *i.e.* assuming that the phonon modes are in thermal equilibrium and the two-level system has relaxed to its ground state, is given by the Fourier transform

$$\mathcal{A}(\omega_\mathrm{L}) = \mathrm{Re}\int_0^\infty \mathrm{d}t\, e^{-i\omega_\mathrm{L}t}\Sigma(t)\,. \tag{3.5}$$

with the correlation function $\Sigma(t)$

$$\Sigma(t) = \langle\sigma_-(0)\sigma_+(t)\rangle_\mathrm{st} = \mathrm{Tr}\left\{\sigma_-(0)\sigma_+(t)|g\rangle\langle g|\prod_k \mu_\mathrm{th}^{(k)}\right\}\,. \tag{3.6}$$

Here, we defined the raising and lowering operators $\sigma_+ = |e\rangle\langle g|$ and $\sigma_- = |g\rangle\langle e|$ and used the steady state $\varrho_\mathrm{st} = |g\rangle\langle g|\prod_k \mu_\mathrm{th}^{(k)}$ of the system with the thermal equilibrium density operator $\mu_\mathrm{th}^{(k)}$ of the kth phonon mode. Inserting $1 = P^\dagger P$ between all operators and taking into account that ϱ_st remains unchanged by the polaron transform the correlation function can be rewritten as

$$\Sigma(t) = \mathrm{Tr}\left\{\sigma_- B\, e^{i\bar{H}t/\hbar}\sigma_+ B^\dagger\, e^{-i\bar{H}t/\hbar}|g\rangle\langle g|\prod_k \mu_\mathrm{th}^{(k)}\right\}\,. \tag{3.7}$$

In order to obtain this we have used the fact that the raising operator transforms according to $P\sigma_+ P^\dagger = \sigma_+ B^\dagger$, with

$$B = \prod_k \exp\{\beta_k(a_k^\dagger - a_k)\} = \prod_k D_k(\beta_k) \tag{3.8}$$

which is a product of displacement operators D_k of the kth phonon mode. In the polaron picture, *i.e.* under the Hamiltonian $\bar{H}$, the operator σ_+ rotates with the

frequency $\omega - \Delta$ and the correlation function becomes

$$\Sigma(t) = e^{i(\omega-\Delta)t} \prod_k \mathrm{Tr}\Big\{ D_k(\beta_k) e^{i\nu_k a_k^\dagger a_k t} D_k(-\beta_k) e^{-i\nu_k a_k^\dagger a_k t} \mu_{\mathrm{th}}^{(k)} \Big\}. \qquad (3.9)$$

This can be simplified using $\exp[i\nu a^\dagger a t] D(\alpha) \exp[-i\nu a^\dagger a t] = D(\alpha \exp[i\nu t])$ and the product rule for displacement operators yielding

$$\Sigma(t) = e^{i(\omega-\Delta)t} \prod_k \mathrm{Tr}\Big\{ D_k(\beta_k(t)) \mu_{\mathrm{th}}^{(k)} \Big\} e^{i\beta_k^2 \sin(\nu_k t)} \qquad (3.10)$$

with the definition $\beta_k(t) = \beta_k(1 - \exp[i\nu_k t])$. The remaining trace is the characteristic function of a thermal state which we derived in Eq. (2.19) and have to employ here for $s = 0$. With the kth thermal occupation $\bar{m}(\nu_k) = (\exp[\beta\hbar\nu_k] - 1)^{-1}$ this then leads to the final form

$$\Sigma(t) = e^{i(\omega-\Delta)t} e^{-\Phi(t)} \qquad (3.11)$$

with the function

$$\Phi(t) = \sum_k \beta_k^2 \Big[(\bar{m}(\nu_k) + 1)(1 - e^{i\nu_k t}) + \bar{m}(\nu_k)(1 - e^{-i\nu_k t}) \Big]. \qquad (3.12)$$

When going over to a continuum description one introduces the spectral function $J(\nu) = \sum_k \lambda_k^2 \delta(\nu - \nu_k)$ to represent the distribution of the interaction strength. The sum over all modes is then rewritten as an integral over the whole frequency range. The resulting integrals in $\Phi(t)$ can be solved analytically only in some cases, *e.g.* for an ohmic spectral density [Wei12, Sch12].

Including electronic relaxation in the form of spontaneous emission, similar to Eq. (1.48), leads to a master equation in the polaron picture that includes the term $\mathcal{D}[\sigma_- B]$ which is not purely atomic but also includes the phonon operators.

As originally suggested by Huang and Rhys we now assume all phonon modes to have the same frequency ν. The relative strength of the interaction to the defect is then given by the *Huang-Rhys parameter*

$$S = \sum_k \beta_k^2 \qquad (3.13)$$

leading to a polaron shift $\Delta = S\nu$. Under this assumption we can derive analytical results for the absorption spectrum from which we can obtain some physical insight into the influence of the electron-phonon coupling on the light-scattering properties of the defect.

We begin by examining the case of a zero temperature crystal. This implies a vanish thermal occupation $\bar{m}(\nu) = 0$, resulting in the correlation function

$$\Sigma(t) = e^{-S(1-\exp[i\nu t])}\,. \tag{3.14}$$

When evaluating the Fourier transform of this function it is helpful to write the exponential in its power-series expansion, leading to an absorption spectrum (3.5) of the form

$$\mathcal{A}(\omega_\mathrm{L}) = \sum_{l=0}^{\infty} e^{-S}\frac{S^l}{l!}\mathrm{Re}\int_0^\infty \mathrm{d}t\, e^{-i(\omega_\mathrm{L}-\omega+\Delta-l\nu)t}\,, \tag{3.15}$$

where the integration naturally results in a series of *Dirac-delta peaks*

$$\mathcal{A}(\omega_\mathrm{L}) = \pi\sum_{l=0}^{\infty} e^{-S}\frac{S^l}{l!}\delta(\omega_\mathrm{L}-\omega+\Delta-l\nu)\,. \tag{3.16}$$

The spectral weight of these peaks is given by a Poissonian distribution in terms of the Huang-Rhys parameter S. The peak position is displaced from the renormalized transition frequency $\omega - \Delta$ by multiples of the phonon frequency ν. In Fig. 3.2 we show the weight of the peaks for two values of S, namely $S = 0.5$ and $S = 5$. The lth line in the spectrum corresponds to an absorption process where in addition to an electronic transition from $|g\rangle$ to $|e\rangle$ the creation of l phonons occurs. The Poissonian distribution implies that the largest weight is not necessarily given for $l = 0$, whose corresponding line is called the *zero-phonon line*. On the contrary: when the coupling strength exceeds $S = 1$ the maximum of the absorption is at frequencies higher than the pure electronic transition, as seen in Fig. 3.2 b).

Figure 3.2: *Absorption spectrum* (3.16) *of the Huang-Rhys model for a two-level defect as a function of the probe frequency ω_L, in units of the oscillator frequency ν, at zero temperature for different values of the Huang-Rhys parameter:* **a)** $S = 0.5$ *and* **b)** $S = 5$. *The gray vertical line represent the zero-phonon line at $\omega_\mathrm{L} = \omega - \Delta$.*

Finite temperatures are completely characterized by $\bar{m} = \bar{m}(\nu)$ in Eq. (3.12). In this case one can cast the function $\Phi(t)$, given by Eq. (3.12), in the alternative form

$$\Phi(t) = S\left[2\bar{m} + 1 - \sqrt{\bar{m}(\bar{m}+1)}\left(e^{i\nu t + \beta\hbar\nu/2} + e^{-i\nu t - \beta\hbar\nu/2}\right)\right] \qquad (3.17)$$

and later on the time-independent term can be taken out of the Fourier transform in the absorption spectrum. For the time-dependent term it is useful to remember the generating function of the modified Bessel functions $I_n(z)$ which reads [Abr65]

$$e^{y(z+z^{-1})/2} = \sum_{n=-\infty}^{\infty} I_n(y)z^n \,. \qquad (3.18)$$

The identifications $y = 2S\sqrt{\bar{m}(\bar{m}+1)}$ and $z = \exp[i\nu t + \beta\hbar\nu/2]$ result in

$$\Sigma(t) = e^{i(\omega-\Delta)t}e^{-S(2\bar{m}+1)}\sum_{l=-\infty}^{\infty} I_l\left(2S\sqrt{\bar{m}(\bar{m}+1)}\right)e^{l\beta\hbar\nu/2}e^{il\nu t} \qquad (3.19)$$

and the corresponding absorption spectrum

$$\mathcal{A}(\omega_{\mathrm{L}}) = \pi\sum_{l=-\infty}^{\infty} e^{-S(2\bar{m}+1)}\sqrt{\frac{\bar{m}+1}{\bar{m}}}^{\,l} I_l\left(2S\sqrt{\bar{m}(\bar{m}+1)}\right)\delta(\omega_{\mathrm{L}} - \omega + \Delta - l\nu). \quad (3.20)$$

The spectral weight of the lth absorption line is given by a modified Bessel function of order l and the summation is not restricted to positive values anymore: negative values of l are associated with absorption events where an electronic excitation occurs under annihilation of $|l|$ thermal lattice phonons. Figure 3.3 shows the spectral weights for $S = 1$ and two different values of the thermal occupation, namely $\bar{m} = 1$ and $\bar{m} = 10$.
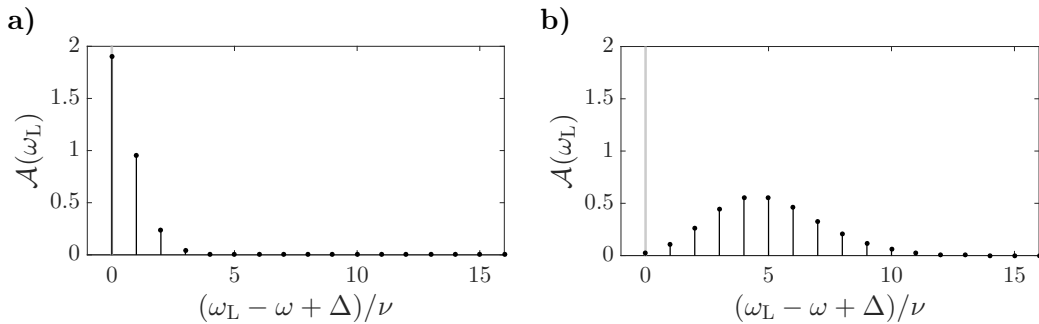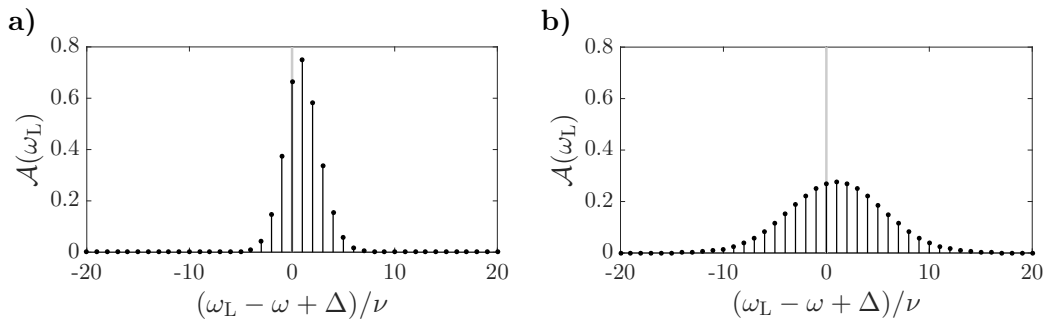

Figure 3.3: *Absorption spectrum (3.20) of the Huang-Rhys model for a two-level defect as a function of the probe frequency ω_{L}, in units of the oscillator frequency ν, at finite temperature for different values of the mean occupation:* **a)** *$\bar{m} = 1$ and* **b)** *$\bar{m} = 10$. The gray vertical line represent the zero-phonon line at $\omega_{\mathrm{L}} = \omega - \Delta$. The Huang-Rhys parameter is $S = 1$*

Master equation for solid-state quantum emitters

The numerous solid-state based applications in quantum photonics call for a tractable theoretical description of the dipole-phonon interaction which renders the basics of the photon's spectral properties and is based on a clear physical picture of the underlying mechanism. In this chapter we will present such a model by combining the *Franck-Condon principle* with a Born-Markov master-equation formalism.

The basic idea is to describe the coupling to the vibrational modes by a single harmonic oscillator, similar to the Huang-Rhys model. This single-mode assumption is reasonable since many lattice defects are accompanied by the presence of *localized modes* that strongly couple to the defect center. In our model these modes are represented by the single oscillator while the delocalized phononic modes, in contrast, play the role of a reservoir for the oscillator. This approach can also be seen in the spirit of *pseudomodes* [Dal01, Maz09] that were introduced to describe the dynamics of a system in a structured environment.

We bring this idea into the form of a Born-Markov master equation and provide its full solution in terms of the damping basis, *i.e.* the spectral decomposition of the Liouville operator that was introduced in the Chapters 1 and 2. In terms of this biorthogonal basis, we show how the absorption and emission spectra of a single defect center can be easily represented and analyzed. In such a way the basic features in the spectrum of light of solid-state quantum emitters can be reproduced by a simple dynamical equation for the system's density operator.

This chapter has the following structure: In Sec. 4.1 we present the model and set up the master equation. Sec. 4.2 is devoted to the damping basis as a solution of the dynamical equation. We derive the left- and right eigenelements of the Liouville operator together with its eigenvalues. In Sec. 4.3 we use the damping basis to describe the time evolution of both the defect's and the oscillator's reduced density operators and calculate the absorption spectrum of a single defect center. We discuss the features of the model in Sec. 4.4, and put it into context with the description of Huang and Rhys. Finally, in Sec. 4.5 we draw the conclusions.

The main results of this chapter have been published in

The presence of lattice defects alters the phononic spectrum of the crystal that contains them in such a way that special vibrational modes, called *localized modes*, emerge which have an exponentially decaying amplitude [Mar66, Mar67] away from the defect. This confinement of their vibration amplitude leads to a coupling to the defect center that is much stronger than the coupling of phonon modes whose oscillation amplitude is spread over the whole crystal. These modes are represented by the single oscillator in our model. An extension to multiple modes is straightforward but we restrict ourselves to a single one for the sake of clarity. For diamond, local vibration mode calculations [Gal11] have shown the existence of eight localized modes around an NV$^-$ center, with four almost degenerate frequencies (given by {11.4, 14.4, 15.4, 18.6} THz).

In this section we develop a simplified theoretical description of the strong electron-phonon coupling of an individual color center to such a single localized mode. The delocalized phononic modes are considered here to form a thermal reservoir, causing the singled out localized mode to thermally relax. This relaxation can have its origin in normal mode coupling arising from crystal anharmonicities.

In analogy to the previous chapter we consider two electronic states with transition frequency ω, a stable state $|g\rangle$ and an energetically higher state $|e\rangle$. For an NV$^-$ center these states can be identified with the ^{3}A$_2$ and ^{3}E levels [Doh11], respectively. The common understanding of the defect-vibration interaction assumes electronic-state dependent equilibrium positions of the atoms around the defect [Mar66, Mar67], as depicted in Fig. 3.1. Within the Franck-Condon assumption [Fra26, Con26], atoms on the lattice sites around the defect experience a modified potential due to the reconfigured electronic orbitals, see Fig. 4.1, leading to an interaction term

$$V(x) = |g\rangle\langle g|V_g(x) + |e\rangle\langle e|V_e(x) \tag{4.1}$$

in the total Hamiltonian H when only a single vibrational mode with coordinate x is taken into account. In the harmonic approximation $V_g(x) = M\nu^2 x^2/2$, with the frequency ν and effective mass M associated with the local vibrational mode, we can expand the modified potential up to first order in x and find

$$\begin{aligned} V_e(x) &= V_g(x) - Fx \\ &= V_g(x - x_0) - \hbar\omega_{\mathrm{R}} , \end{aligned} \tag{4.2}$$

with the new equilibrium position $x_0 = F/M\nu^2$ and the energy shift $\hbar\omega_{\mathrm{R}} = F^2/2M\nu^2$ that comes from completing the square. The total Hamiltonian then takes the form

$$\begin{aligned} H &= |g\rangle\langle g|H_{\mathrm{osc}} + |e\rangle\langle e|[\hbar\omega + H_{\mathrm{osc}} - Fx] \\ &= H_{\mathrm{osc}} + H_{\mathrm{tls}} + W , \end{aligned} \tag{4.3}$$
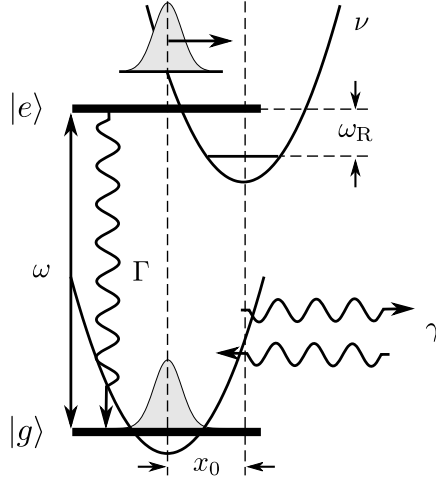
Figure 4.1: *Model of the Franck-Condon like lattice-defect center interaction in single mode and harmonic approximation including damping: In the excited state $|e\rangle$, the wavepacket of the vibrational mode experiences a potential displaced by x_0 compared to the potential in the ground state $|g\rangle$. The interaction causes a renormalized transition frequency between the states $|e\rangle$ and $|g\rangle$, shifted by the relaxation frequency ω_{R}. The single vibrational mode is coupled to a thermal reservoir modeling the phononic modes of the crystal and thermally relaxes with rate γ. The electronic two-level system decays with rate Γ due to spontaneous emission.*

where we defined the harmonic oscillator Hamiltonian

$$H_{\mathrm{osc}} = \frac{p^2}{2M} + \frac{1}{2}M\nu^2 x^2 = \hbar\nu b^\dagger b\,, \tag{4.4}$$

where we again abstain from writing the zero-point energy. The annihilation and creation operators b and $b^\dagger$ are connected to the normal coordinate x and momentum operator p by

$$x = \xi(b + b^\dagger)\,, \tag{4.5}$$

$$p = -\frac{i\hbar}{2\xi}(b - b^\dagger) \tag{4.6}$$

with the ground-state length scale $\xi = \sqrt{\hbar/2M\nu}$. In the second line of Eq. (4.3), we furthermore introduced the Hamiltonian representing the energy of the uncoupled two-level system

$$H_{\mathrm{tls}} = \hbar\omega|e\rangle\langle e| \tag{4.7}$$

and the interaction between the electronic and the vibrational degree of freedom

$$W = -\hbar\eta|e\rangle\langle e|(b + b^\dagger) \tag{4.8}$$

with a coupling constant $\eta = F\xi/\hbar$. Note that the coupling leads to an energy relaxation of $\hbar\omega_{\mathrm{R}} = \hbar\eta^2/\nu$ that corresponds to the polaron shift (3.4). Up to this point, the model corresponds basically to the description of Huang and Rhys [Hua50, Doh13] that was summarized in the previous chapter and the strength of the vibronic interaction is measured by the dimensionless Huang-Rhys factor $S = (\eta/\nu)^2$. We briefly note that the same interaction Hamiltonian also occurs in the description of different physical systems, such as a single electron spin coupled to the quantized motion of a vibrating magnetized tip [Rab10].

To complete the description we take three relaxation processes into account using a master-equation formalism: *(i)* electronic relaxation due to the coupling to the free electromagnetic field, *(ii)* additional pure dephasing of the defect and *(iii)* vibrational damping of the harmonic oscillator by a thermal reservoir. In the Born-Markov approximation the time evolution of the system's density operator ϱ, covering the electronic and vibrational degree of freedom, reads $\partial_t \varrho = \mathcal{L}\varrho$ with the Liouville operator

$$\mathcal{L}\varrho = \frac{1}{i\hbar}[H, \varrho] + \mathcal{L}_\Gamma \varrho + \mathcal{L}_\gamma \varrho. \tag{4.9}$$

The first term on the right-hand side corresponds to the coherent evolution governed by the Hamiltonian H, Eq. (4.3). Spontaneous decay with the rate Γ and pure dephasing with the rate Γ^* is taken into account by the superoperator

$$\mathcal{L}_\Gamma \varrho = \frac{\Gamma}{2}\,\mathcal{D}[\sigma_-]\varrho + \frac{\Gamma^*}{2}\mathcal{D}[|e\rangle\langle e|]\,, \tag{4.10}$$

where we defined the atomic lowering operator $\sigma_- = |g\rangle\langle e|$, with the corresponding raising operator $\sigma_+ = |e\rangle\langle g|$, and used the previously introduced abbreviation $\mathcal{D}[X]\varrho = 2X\varrho X^\dagger - X^\dagger X \varrho - \varrho X^\dagger X$ to represent a Lindblad-form term. We further assume a finite lifetime of the vibrational excitation. Imperfections in the lattice structure or non-harmonic corrections may lead to a coupling between the vibrational modes and let the mode b interact with a reservoir of delocalized phononic modes with temperature T. In a Markovian approximation, such a coupling is described by

$$\mathcal{L}_\gamma \varrho = \frac{\gamma}{2}(\bar{m} + 1)\,\mathcal{D}[b]\varrho + \frac{\gamma}{2}\bar{m}\,\mathcal{D}[b^\dagger]\varrho \tag{4.11}$$

and damps the localized mode irreversibly towards its stationary thermal state with mean vibrational occupation number $\bar{m} = (\exp[\hbar\nu/k_{\mathrm{B}}T] - 1)^{-1}$ on a time scale given by the inverse decay rate $1/\gamma$. Such a picture should be suitable for materials with few localized modes coupled strongly to the defect center, compared to the delocalized modes forming the reservoir. The model also allows for a temperature dependent decay rate $\gamma(T)$, typical for many solid-state systems [Mar62, Fre95, Pou10]. We furthermore remark that in the dissipation we neglected the dressing of the electronic states with the strongly interacting phonons of the oscillator, that leads to additional

terms [Hu15] in the Liouvillian, Eq. (4.9). Their influence can approximately be taken into account by an additional effective dephasing of the electronic subsystem.

An elegant form of providing a solution to the differential equation (4.9) is given in terms of the damping basis that was introduced in Sec. 1.3. To this end, we seek for the left and right eigenelements of the Liouville operator (4.9), fulfilling

$$\mathcal{L}\hat{\varrho}_\lambda = \lambda\hat{\varrho}_\lambda\,, \tag{4.12}$$

$$\check{\varrho}_\lambda^\dagger \mathcal{L} = \lambda\check{\varrho}_\lambda^\dagger\,. \tag{4.13}$$

The remainder of this section is dedicated to the derivation of the explicit form of the damping basis of the problem at hand. The reader who is not interested in this technical part may skip the rest of this section without loss of coherence. The explicit formulas are summarized at the end of this section.

For later convenience we reformulate the master equation, Eq. (4.9), by introducing the Liouville operators

$$\mathcal{L}_{\mathrm{tls}}\varrho = \frac{1}{i\hbar}\left[H_{\mathrm{tls}}, \varrho\right] + \mathcal{L}_\Gamma\varrho\,, \tag{4.14}$$

$$\mathcal{L}_{\mathrm{osc}}\varrho = \frac{1}{i\hbar}\left[H_{\mathrm{osc}}, \varrho\right] + \mathcal{L}_\gamma\varrho\,, \tag{4.15}$$

describing a two-level system underlying spontaneous decay and dephasing and a damped harmonic oscillator, as already encountered in Eqs. (1.48) and (2.7), respectively. Additionally, we introduce

$$\mathcal{L}_{\mathrm{int}}\varrho = \frac{1}{i\hbar}\left[W, \varrho\right] = i\eta\bigl[|e\rangle\langle e|(b + b^\dagger), \varrho\bigr] \tag{4.16}$$

and write the complete Liouvillian as

$$\mathcal{L} = \mathcal{L}_{\mathrm{tls}} + \mathcal{L}_{\mathrm{osc}} + \mathcal{L}_{\mathrm{int}}\,. \tag{4.17}$$

The superoperators $\mathcal{L}_{\mathrm{tls}}$ and $\mathcal{L}_{\mathrm{osc}}$ exclusively act on the electronic and vibrational subspace, respectively. In the following, we will express the eigenbasis of the coupled system in terms of the eigenelements $\hat{\mu}_{m,k}$ and $\check{\mu}_{m,k}^\dagger$ of a damped quantum harmonic oscillator whose form was explicitly derived in Chapter 2.

Inspired by the damping basis of a two-level system with spontaneous decay and pure dephasing that we presented in Tab. 1.1, the form of the Liouville operator (4.9)

suggests the ansatz

$$\hat{\varrho}_{\lambda}^{(0)} = |g\rangle\langle g|\, \hat{\mu}_{\lambda}^{(0)}, \tag{4.18}$$

$$\hat{\varrho}_{\lambda}^{(\pm)} = \sigma_{\pm}\, \hat{\mu}_{\lambda}^{(\pm)}, \tag{4.19}$$

$$\hat{\varrho}_{\lambda}^{(\rightsquigarrow)} = |e\rangle\langle e|\hat{\mu}_{\lambda}^{(e)} - |g\rangle\langle g|\hat{\mu}_{\lambda}^{(g)} \tag{4.20}$$

for the right eigenelements, where we furnished the two-level system operators with the operators μ that act on the oscillator Hilbert space only and their explicit shape will be derived in the following. Here, the eigenvalues λ depend on the two integers m, k and the superscript index of Eqs. (4.18)-(4.20).

Eigenelements connected to the atomic populations

We begin with Eq. (4.20), since it will also deliver the result for Eq. (4.18). Plugging the ansatz into Eq. (4.12) and using the action of $\mathcal{L}$ in the form (4.17) yields

$$[\mathcal{L} - \lambda]\hat{\varrho}_{\lambda}^{(\rightsquigarrow)} = |e\rangle\langle e| \left\{ [\mathcal{L}_{\mathrm{osc}}^{(\beta)} - \Gamma - \lambda]\hat{\mu}_{\lambda}^{(e)} \right\} - |g\rangle\langle g| \left\{ [\mathcal{L}_{\mathrm{osc}} - \lambda]\hat{\mu}_{\lambda}^{(g)} - \Gamma\hat{\mu}_{\lambda}^{(e)} \right\} = 0 \,, \tag{4.21}$$

where we defined the Liouvillian of a displaced harmonic oscillator

$$\mathcal{L}_{\mathrm{osc}}^{(\beta)}\mu = \mathcal{L}_{\mathrm{osc}}\mu + i\eta \left[(b + b^{\dagger}), \mu \right] = D(\beta) \left[\mathcal{L}_{\mathrm{osc}} D^{\dagger}(\beta)\mu D(\beta) \right] D^{\dagger}(\beta) \tag{4.22}$$

with the displacement operator $D(\beta) = \exp[\beta b^{\dagger} - \beta^* b]$. The quantity

$$\beta = \frac{\eta}{\nu - i\gamma/2} \tag{4.23}$$

will appear throughout the rest of our treatment of this problem and is connected to a generalization of the Huang-Rhys parameter S, as will become apparent later.

One possibility to fulfill Eq. (4.21) is to choose $\hat{\mu}_{\lambda}^{(e)} = 0$. Then only a component in the $|g\rangle\langle g|$-subspace remains, obeying

$$\mathcal{L}_{\mathrm{osc}}\hat{\mu}_{\lambda}^{(0)} = \lambda\hat{\mu}_{\lambda}^{(0)} \,. \tag{4.24}$$

This obviously is the case from Eq. (4.18), and we consequently relabeled the operator in Eq. (4.24) correspondingly. This is exactly the eigenvalue equation of the damped harmonic oscillator and the solution is given by the eigenelements $\hat{\mu}_{\lambda}^{(0)} = \hat{\mu}_{m,k}$ from Eq. (2.53) and the eigenvalues $\lambda_{m,k} = -ik\nu - [m + |k|/2]\gamma$ from Eq. (2.44).

We now turn to the case $\hat{\mu}_{\lambda}^{(e)} \neq 0$. From Eqs. (4.21) and (4.22) we immediately find that

$$\hat{\mu}_{\lambda}^{(e)} = D(\beta)\hat{\mu}_{m,k}D^{\dagger}(\beta) \tag{4.25}$$

fulfills the equation in the $|e\rangle\langle e|$-subspace which leads to

$$\hat{\mu}_\lambda^{(g)} = \frac{\Gamma}{\mathcal{L}_{\mathrm{osc}} - \lambda_{m,k} + \Gamma} \hat{\mu}_\lambda^{(e)} \tag{4.26}$$

in the $|g\rangle\langle g|$-subspace. The corresponding the eigenvalues are $\lambda = \lambda_{m,k} - \Gamma$.

Eigenelements connected to the atomic coherences

It remains to deal with the eigenelements associated with the electronic coherences, Eqs. (4.19). The action of $\mathcal{L}$ yields

$$[\mathcal{L} - \lambda]\sigma_\pm \hat{\mu}_\lambda^{(\pm)} = \sigma_\pm \left\{ \mathcal{L}_{\mathrm{osc}} + \mathcal{L}_\pm \mp i\omega - \frac{\Gamma + \Gamma^*}{2} - \lambda \right\} \hat{\mu}_\lambda^{(\pm)} = 0. \tag{4.27}$$

Here, we introduced $\mathcal{L}_\pm \mu = i\eta([\mu, b + b^\dagger] \pm \{\mu, b + b^\dagger\})/2$, a superoperator that multiplies μ from the right *or* left depending on the sign. To handle this eigenvalue equation, it is helpful to transform the expressions according to the *lopsided displacement*

$$\hat{\mu}_\lambda^{(\pm)} = D(\alpha_\pm) e^{\pm\varsigma b} \hat{\tilde{\mu}}_\lambda^{(\pm)} e^{\mp\varsigma b} D^\dagger(\beta_\pm) \tag{4.28}$$

and choose the displacement parameters $\alpha_\pm$, $\beta_\pm$ and ς such that in the new picture the Liouville operator is of the standard damped harmonic oscillator form (2.7) at the cost of an additional constant term. This turns out to be indeed possible if one sets

$$\alpha_+ = \beta(\bar{m} + 1) - \beta^* \bar{m}, \tag{4.29}$$
$$\beta_+ = (\beta - \beta^*)(\bar{m} + 1), \tag{4.30}$$
$$\alpha_- = (\beta^* - \beta)\bar{m}, \tag{4.31}$$
$$\beta_- = \beta^*(\bar{m} + 1) - \beta\bar{m}, \tag{4.32}$$
$$\varsigma = (\beta^* - \beta)(2\bar{m} + 1). \tag{4.33}$$

The condition on the curly bracket of Eq. (4.27) then transforms into the equation

$$\mathcal{L}_{\mathrm{osc}} \hat{\tilde{\mu}}_\lambda^{(\pm)} = \left[\lambda \pm i\widetilde{\omega} + \frac{\widetilde{\Gamma}}{2} \right] \hat{\tilde{\mu}}_\lambda^{(\pm)} \tag{4.34}$$

with the renormalized atomic transition frequency and linewidth

$$\widetilde{\omega} = \omega - |\beta|^2 \nu, \tag{4.35}$$
$$\widetilde{\Gamma} = \Gamma + \Gamma^* + (2\bar{m} + 1)|\beta|^2 \gamma. \tag{4.36}$$

The solution of the original eigenvalue equation (4.27) is then naturally given by the back transform of the harmonic oscillator eigenelements

$$\hat{\mu}_\lambda^{(\pm)} = D(\alpha_\pm) e^{\pm\varsigma b} \hat{\mu}_{m,k}^\dagger e^{\mp\varsigma b} D^\dagger(\beta_\pm) \tag{4.37}$$

and the eigenvalues

$$\lambda = \lambda_{m,k} \mp i\widetilde{\omega} - \frac{\widetilde{\Gamma}}{2} \tag{4.38}$$

are composed of the harmonic oscillator part and the renormalized electronic transition frequency and linewidth.

The derivation of the left eigenelements of $\mathcal{L}$ goes along the same lines as for their right counterparts. The action to the left [Eng02] of $\mathcal{L}$ is represented by

$$\check{\varrho}_\lambda^\dagger \mathcal{L} = \frac{i}{\hbar}\left[H, \check{\varrho}_\lambda^\dagger\right] + \frac{\Gamma}{2}\check{\mathcal{D}}[\sigma_-]\check{\varrho}_\lambda^\dagger + \frac{\Gamma^*}{2}\check{\mathcal{D}}[|e\rangle\langle e|]\check{\varrho}_\lambda^\dagger + \frac{\gamma}{2}(\bar{m}+1)\check{\mathcal{D}}[b]\check{\varrho}_\lambda^\dagger + \frac{\gamma}{2}\bar{m}\check{\mathcal{D}}[b^\dagger]\check{\varrho}_\lambda^\dagger, \tag{4.39}$$

where we again use the short notation $\check{\mathcal{D}}[b]X = 2b^\dagger X b - b^\dagger b X - X b^\dagger b$. This time

$$\check{\varrho}_\lambda^{(0)\dagger} = |g\rangle\langle g|\,\check{\mu}_\lambda^{(g)\dagger} + |e\rangle\langle e|\,\check{\mu}_\lambda^{(e)\dagger}, \tag{4.40}$$

$$\check{\varrho}_\lambda^{(\pm)\dagger} = \sigma_\mp\,\check{\mu}_\lambda^{(\pm)\dagger}, \tag{4.41}$$

$$\check{\varrho}_\lambda^{(\rightsquigarrow)\dagger} = |e\rangle\langle e|\check{\mu}_\lambda^{(\rightsquigarrow)\dagger} \tag{4.42}$$

serves as an ansatz. Following an analogous treatment as in Sec. 4.2.1, we start with Eq. (4.40), as it will again deliver the solution for Eq. (4.42), too. One arrives at

$$\check{\mu}_\lambda^{(g)\dagger} = \check{\mu}_{m,k}^\dagger \tag{4.43}$$

$$\check{\mu}_\lambda^{(e)\dagger} = D(\beta)\left[D^\dagger(\beta)\check{\mu}_{m,k}^\dagger D(\beta)\frac{\Gamma}{\Gamma + \lambda_{m,k} - \mathcal{L}_{\text{osc}}}\right]D^\dagger(\beta) \tag{4.44}$$

to the eigenvalue $\lambda = \lambda_{m,k}$ and

$$\check{\mu}_\lambda^{(\rightsquigarrow)\dagger} = D(\beta)\check{\mu}_{m,k}^\dagger D^\dagger(\beta) \tag{4.45}$$

to the eigenvalue $\lambda = \lambda_{m,k} - \Gamma$. Also the electronic coherence parts can be derived similarly as before, but this time using the asymmetric displacement transformation

$$\check{\mu}_\lambda^{(\pm)\dagger} = D(\beta_\pm)e^{\pm\varsigma b}\check{\mu}_\lambda^{(\pm)\dagger}e^{\mp\varsigma b}D^\dagger(\alpha_\pm) \tag{4.46}$$

with $\alpha_\pm$, $\beta_\pm$ and ς from Eqs. (4.29)-(4.33). This transforms the problem into the eigenvalue equation of the adjoint damped harmonic oscillator Liouville operator (2.10).

We briefly summarize the results. In the previous subsections we found that the eigenelements of the model Liouvillian $\mathcal{L}$, Eq. (4.17), can be grouped into three sets of

operators associated with: *(i)* the stable electronic subspace $|g\rangle\langle g|$, *(ii)* the electronic coherences $\sigma_\pm$ and *(iii)* a subspace which is related with the population decay in the excited state at rate Γ. The right eigenelements have the form

$$\hat{\varrho}_{m,k}^{(0)} = |g\rangle\langle g|\hat{\mu}_{m,k}\,, \tag{4.47}$$

$$\hat{\varrho}_{m,k}^{(\pm)} = \sigma_\pm D(\alpha_\pm)e^{\pm\varsigma b}\hat{\mu}_{m,k}e^{\mp\varsigma b}D^\dagger(\beta_\pm)\,, \tag{4.48}$$

$$\hat{\varrho}_{m,k}^{(\leadsto)} = \left\{|e\rangle\langle e| - |g\rangle\langle g|\Gamma[\mathcal{L}_{\rm osc} - \lambda_{m,k} + \Gamma]^{-1}\right\}D(\beta)\hat{\mu}_{m,k}D^\dagger(\beta)\,. \tag{4.49}$$

They fulfill the orthogonality relation

$$\text{Tr}\{\check{\varrho}_{m,k}^{(\jmath)\dagger}\hat{\varrho}_{m',k'}^{(\jmath')}\} = \delta_{\jmath,\jmath'}\delta_{m,m'}\delta_{k,k'}\,, \tag{4.50}$$

with $\jmath,\jmath' \in \{0,\pm,\leadsto\}$, together with their left-side counterparts

$$\check{\varrho}_{m,k}^{(0)\dagger} = |g\rangle\langle g|\check{\mu}_{m,k}^\dagger + |e\rangle\langle e|\Gamma D(\beta)\left\{D^\dagger(\beta)\check{\mu}_{n,l}^\dagger D(\beta)[\Gamma + \lambda_{m,k} - \mathcal{L}_{\rm osc}]^{-1}\right\}D^\dagger(\beta)\,, \tag{4.51}$$

$$\check{\varrho}_{m,k}^{(\pm)\dagger} = \sigma_\mp e^{\pm\varsigma b}D(\beta_\pm)\check{\mu}_{m,k}^\dagger e^{\mp\varsigma b}D^\dagger(\alpha_\pm)\,, \tag{4.52}$$

$$\check{\varrho}_{m,k}^{(\leadsto)\dagger} = |e\rangle\langle e|D(\beta)\check{\mu}_{m,k}^\dagger D^\dagger(\beta)\,, \tag{4.53}$$

both having the common eigenvalues

$$\lambda_{m,k}^{(0)} = \lambda_{m,k}\,, \tag{4.54}$$

$$\lambda_{m,k}^{(\pm)} = \lambda_{m,k} \mp i\widetilde{\omega} - \frac{\widetilde{\Gamma}}{2}\,, \tag{4.55}$$

$$\lambda_{m,k}^{(\leadsto)} = \lambda_{m,k} - \Gamma \tag{4.56}$$

for non-negative integers n and arbitrary integers l. The renormalized frequency are given by $\widetilde{\omega} = \omega - |\beta|^2\nu$ and $\widetilde{\Gamma} = \Gamma + |\beta|^2(2\bar{m}+1)\gamma$, respectively, in terms of the model parameter $\beta = \eta/(\nu - i\gamma/2)$. Moreover, $\alpha_\pm$, $\beta_\pm$ and ς are defined in Eqs. (4.29)-(4.33). The stationary state $\varrho_{\rm st} = \hat{\varrho}_{00}^{(0)} = \sigma_g\mu_{\rm th}$ of the system corresponds to the eigenvalue $\lambda = 0$ and describes the atom in the ground state and the vibrational mode in thermal equilibrium, *i.e.* $\mu_{\rm th} = \hat{\mu}_{0,0}$. The corresponding left eigenelement $\check{\varrho}_{00}^{(0)} = 1$ is the identity operator. We remark that the formal representations (4.49) and (4.51) containing the superoperator $\mathcal{L}_{\rm osc}$ can be made explicit by inserting the completeness relation (2.55) together with the relation (B.19). As a final note we point out that the completeness of the harmonic oscillator damping basis, which was shown in Ref. [Eng02], directly implies the completeness of the damping basis derived here.

The dynamics of an arbitrary initial state in terms of the damping basis is given by Eq. (1.45). We focus on the case of a separable state where the oscillator is initially in thermal equilibrium and the two-level system is prepared in an arbitrary state ρ_0, viz. $\varrho(t=0) = \rho_0 \mu_{\text{th}}$.

Reduced dynamics of the two-level system

For the time evolution of the reduced density operator $\rho(t) = \text{Tr}_{\text{osc}}\{\varrho(t)\}$, describing the dynamics of the atom, one finds

$$\rho(t) = \sum_{m=0}^{\infty} \sum_{k=-\infty}^{\infty} \text{Tr}_{\text{osc}}\left\{ c_{m,k}^{(0)} \hat{\varrho}_{m,k}^{(0)} e^{\lambda_{m,k} t} + c_{m,k}^{(\rightsquigarrow)} \hat{\varrho}_{m,k}^{(\rightsquigarrow)} e^{(\lambda_{m,k} - \Gamma) t} + \sum_{j=\pm} c_{m,k}^{(j)} \hat{\varrho}_{m,k}^{(j)} e^{\lambda_{m,k}^{(j)} t} \right\}. \tag{4.57}$$

The expansion coefficients $c_{m,k}^{(j)} = \text{Tr}\{\check{\varrho}_{m,k}^{(j)\dagger} \varrho(t=0)\}$ are determined by the initial state $\varrho(t=0)$ and are calculated using the right eigenelements $\check{\varrho}_{m,k}^{(j)\dagger}$ with $j \in \{0, \pm, \rightsquigarrow\}$. The partial trace in Eq. (4.57) over the oscillator degrees of freedom yields

$$\text{Tr}_{\text{osc}}\{\hat{\varrho}_{m,k}^{(0)}\} = |g\rangle\langle g| \delta_{m,0} \delta_{k,0}, \tag{4.58}$$

$$\text{Tr}_{\text{osc}}\{\hat{\varrho}_{m,k}^{(\rightsquigarrow)}\} = \big[|e\rangle\langle e| - |g\rangle\langle g|\big] \delta_{m,0} \delta_{k,0}, \tag{4.59}$$

according to Eqs. (4.47) and (4.49). For the first line this becomes clear when recalling that the only right oscillator eigenelement with non-vanishing trace is the stationary state $\hat{\mu}_{00}$. The same argument can be used to show the second line, after inserting the completeness relation (2.55) next to the superoperator in the eigenelement (4.49). For the two coherences, one finds

$$\text{Tr}_{\text{osc}}\{\hat{\varrho}_{m,k}^{(\pm)}\} = \sigma_{\pm} A_{m,k}^{\pm}, \tag{4.60}$$

where we defined the trace over the oscillator operators in $\hat{\varrho}_{m,k}^{(\pm)}$ as

$$A_{m,k}^{\pm} = \text{Tr}\big\{ D(\alpha_{\pm}) e^{\pm \varsigma b} \hat{\mu}_{m,k} e^{\mp \varsigma b} D^{\dagger}(\beta_{\pm}) \big\}. \tag{4.61}$$

The evaluation of these traces is conveniently carried out using phase space distributions and the relation (2.27), as it is sketched in App. B.1.1. The resulting functions depend only on β and $\bar{m}$ and are presented App. B.1.1 in the formulas (B.7)-(B.8).

We now turn to the expansion coefficients in Eq. (4.57). Because of Eqs. (4.58)-

(4.59), for the first two sets of coefficients we only need the $m = k = 0$ case,

$$c_{00}^{(0)} = \text{Tr}\{[|e\rangle\langle e| + |g\rangle\langle g|]\rho_0\} = 1\,, \tag{4.62}$$

$$c_{00}^{(\rightsquigarrow)} = \text{Tr}\{|e\rangle\langle e|\rho_0\} = \rho_{ee}\,, \tag{4.63}$$

giving unity and the initial excited state population $\rho_{ee} = \langle e|\rho_0|e\rangle$. In the last term of Eq. (4.57) the coefficients for the coherences

$$c_{m,k}^{(\pm)} = \text{Tr}\{\sigma_{\mp}\rho_0\}B_{m,k}^{\pm} = \rho_{\pm}B_{m,k}^{\pm} \tag{4.64}$$

are required, where we have defined the initial values $\rho_{\pm} = \text{Tr}\{\sigma_{\mp}\rho_0\}$ of the atomic off-diagonal elements and the trace

$$B_{m,k}^{\pm} = \text{Tr}\{D(\beta_{\pm})e^{\pm\varsigma b}\check{\mu}_{m,k}^{\dagger}e^{\mp\varsigma b}D(\alpha_{\pm})^{\dagger}\mu_{\text{th}}\}\,. \tag{4.65}$$

Again we use phase space representations of the required eigenelements to evaluate the trace. The details are reported in App. B.1.2. It is clear from the form of the solution (4.57) that

$$A_{m,k}^{-}B_{m,k}^{-} = \exp\left[-\bar{m}\beta^2 - (\bar{m}+1)\beta^{*2}\right] \times$$
$$\frac{[\bar{m}(\bar{m}+1)|\beta|^4]^m}{m!(m+|k|)!}\begin{cases} [(\bar{m}+1)\beta^{*2}]^{|k|} & \text{for} \quad k < 0 \\ [\bar{m}\beta^2]^k & \text{for} \quad k \geq 0 \end{cases} \tag{4.66}$$

and $A_{m,k}^{+}B_{m,k}^{+} = [A_{m,-k}^{-}B_{m,-k}^{-}]^*$ always appear as products. The only difference between the $+$ and $-$ cases is that $\bar{m}$ and $(\bar{m}+1)$ are interchanged. As a matter of course, for $t = 0$ the initial state must be reproduced by the solution (4.57) of the master equation. Hence, if the eigensystem is complete, the remaining sum over m and k has to fulfill this requirement. For finite times, the exponentials containing the eigenvalues generate the dynamics. The form of the eigenvalues is linear in m and k, such that the time dependency can be easily incorporated into Eq. (4.66) as follows. The terms in the time evolution of the coherences become

$$\text{Tr}_{\text{osc}}\left\{c_{m,k}^{(\pm)}\hat{\varrho}_{m,k}^{(\pm)}e^{\lambda_{m,k}^{(\pm)}t}\right\} = \rho_{\pm}\sigma_{\pm}(t)e^{(-ik\nu-|k|\frac{\gamma}{2})t}e^{-m\gamma t}A_{m,k}^{\pm}B_{m,k}^{\pm} \tag{4.67}$$

with the time dependent raising and lowering operators

$$\sigma_{\pm}(t) = \sigma_{\pm}e^{\mp i\tilde{\omega}t - \tilde{\Gamma}t}\,. \tag{4.68}$$

The sum over m that has to be carried out over Eq. (4.67) can be performed with the help of the power series representation [Abr65]

$$I_l(z) = \left(\frac{z}{2}\right)^l\sum_{n=0}^{\infty}\frac{(z/2)^{2n}}{n!(n+l)!} \tag{4.69}$$

of the modified Bessel function $I_l(z)$, if one makes the identifications $l = |k|$ and

$z = 2\sqrt{\bar{m}(\bar{m}+1)}|\beta|^2 e^{-\gamma t/2}$. The remaining sum over k is then readily evaluated using the generating function from Eq. (3.18). After performing these steps one arrives at the solution

$$\rho(t) = |g\rangle\langle g| + \rho_{ee}(|e\rangle\langle e| - |g\rangle\langle g|)e^{-\Gamma t} + \rho_-\sigma_-(t)e^{-\Psi(t)} + \rho_+\sigma_+(t)e^{-\Psi^*(t)}. \quad (4.70)$$

The function

$$\Psi(t) = \beta^{*2}(\bar{m}+1)\left[1 - e^{(i\nu - \frac{\gamma}{2})t}\right] + \beta^2\bar{m}\left[1 - e^{(-i\nu - \frac{\gamma}{2})t}\right] \quad (4.71)$$

is the correspondence to $\Phi(t)$, defined in Eq. (3.12), that we encountered in the Huang-Rhys model. The expression (4.70) indeed reproduces the initial electronic state for $t = 0$, as expected. For finite times, the population in the excited state decays with the natural rate Γ of the two-level system. It is the coherence between the ground and excited state which is modified by the coupled phonon mode. This influence on the temporal behavior is twofold: *(i)* The operators $\sigma_\pm$, Eq. (4.68), rotate and decay with the renormalized frequencies from Eq. (4.55). *(ii)* The evolution is modulated by the time-dependency of $\Psi(t)$, Eq. (4.71). The oscillator hence generates an additional effective dephasing of the two-level system.

Reduced dynamics of the oscillator

In many-body systems the vibrational degree of freedom can also play a crucial role. For instance, in protein molecules, the relaxation of a high frequency mode (approximately equivalent to the two-level system considered here) interacting with a localized mode can change the dynamics of the latter [Cru05, Sil06, Pou08]. We therefore briefly delve into its dynamics in order to provide additional insight into the overall temporal behavior. We focus on the reduced density operator of the oscillator, $\mu(t) = \text{Tr}_{\text{tls}}\{\varrho(t)\}$, with the same initial state $\varrho(t = 0) = \rho_0\mu_{\text{th}}$ as above. The dynamics is described by Eq. (4.57) with the trace this time going over the electronic degrees of freedom, leaving only the first two terms, since the atomic off-diagonal elements lead to a vanishing trace. The reduced dynamics reads

$$\mu(t) = \sum_{m=0}^{\infty}\sum_{k=-\infty}^{\infty}\left[c_{m,k}^{(0)}\text{Tr}_{\text{tls}}\{\hat{\varrho}_{m,k}^{(0)}\}e^{\lambda_{m,k}t} + c_{m,k}^{(\rightsquigarrow)}\text{Tr}_{\text{tls}}\{\hat{\varrho}_{m,k}^{(\rightsquigarrow)}\}e^{(\lambda_{m,k}-\Gamma)t}\right]. \quad (4.72)$$

With the help of the completeness relation (2.55) and the representation $\int_0^\infty dt\,\exp[(\mathcal{L}-\lambda)t] = [\lambda - \mathcal{L}]^{-1}$ the terms involving the inverse of superoperators in $c_{m,k}^{(0)}$ and $\text{Tr}_{\text{tls}}\{\hat{\varrho}_{m,k}^{(\rightsquigarrow)}\}$ can be brought into a form that contains only overlaps of displaced harmonic oscillator eigenelements, calculated in App. B.1.3, and exponentials of the eigenvalues $\lambda_{m,k}$. These time-dependent exponentials can be absorbed into the overlaps according to

$$\text{Tr}\{\breve{\mu}_{m,k}^\dagger D^\dagger(\beta)\mu_{\text{th}}D(\beta)\}e^{\lambda_{m,k}t} = \text{Tr}\{\breve{\mu}_{m,k}^\dagger D^\dagger(\beta(t))\mu_{\text{th}}D(\beta(t))\}, \quad (4.73)$$

where we defined the dynamical displacement parameter

$$\beta(t) = \beta e^{-(i\nu + \frac{\gamma}{2})t} . \tag{4.74}$$

The remaining sum can be carried out using again the completeness relation (2.55) and the expression for $\mu(t)$ can then be recast into the form

$$
\begin{aligned}
\mu(t) =& \rho_{gg}\mu_{\mathrm{th}} + \rho_{ee}e^{-\Gamma t}D(\beta - \beta(t))\mu_{\mathrm{th}}D^{\dagger}(\beta - \beta(t)) \\
& + \rho_{ee}\Gamma \int\limits_{0}^{t} \mathrm{d}\tau\, e^{-\Gamma\tau}D(\beta(t-\tau) - \beta(t))\mu_{\mathrm{th}}D^{\dagger}(\beta(t-\tau) - \beta(t)) .
\end{aligned} \tag{4.75}
$$

The result consists of three contributions: *(i)* The thermal state corresponding to the $|g\rangle$-part of $\varrho(t=0)$ showing no dynamics. *(ii)* A dynamically displaced thermal state component moving in the $|e\rangle$-potential surface, whose population dies off with the electronic decay rate Γ and *(iii)* the flow of the decayed population towards the undisplaced thermal state. In the asymptotic limit $t \to \infty$ the oscillators state $\mu(t)$ ends in the thermal state μ_{th}, as expected.

In Fig. 4.2 we illustrate the reduced dynamics of both the electronic and the vibrational degree of freedom. As an initial state of the two-level system, $\rho_0 = |\psi_0\rangle\langle\psi_0|$, we choose the equal superposition $|\psi_0\rangle = (|g\rangle + |e\rangle)/\sqrt{2}$ while we assume the oscillator to be in a thermal state. Subplot a) shows the time evolution of the population in the excited state (dashed curve) which decays exponentially with rate Γ, as in the unperturbed two-level system. The time evolution of the coherences (black solid curve) is modified by the oscillator: We show the modulus of $\langle e|\rho(t)|g\rangle$ which exhibits a faster decay compared to the pure two-level case, superimposed by an oscillating modulation with frequency ν as described by Eq. (4.70). For larger temperature (gray solid curve) the coherences are damped away even faster. Fig. 4.2 b) visualizes the temporal behavior of the oscillator's quantum state, Eq. (4.75), in phase space with the help of the Wigner function which was introduced in Sec. 2.2.2. We show four snapshots of the Wigner function within one oscillation period $\tau = 2\pi/\nu$ at the times marked in subfigure a) by empty circles. Initially, at $t = 0$, the phase space distribution corresponds to a thermal state, *i.e.* a Gaussian with variance proportional to $\bar{m} + 1/2$. The portion of the distribution corresponding to the excited state starts to spirally circulate around the displaced equilibrium position at $x/2\xi = \mathrm{Re}\,\beta$ and $p\xi/\hbar = \mathrm{Im}\,\beta$ and its population decays simultaneously at rate Γ, as described in the second term of Eq. (4.75). The black spiral visualizes the trajectory of the center of probability of this part while the dashed and solid white rings mark the variance of the Gaussian components moving in the harmonic potential of the ground and excited state, respectively [for $t = 0$ in Fig. 4.2 b) the two rings overlap] . The contribution of the last term of Eq. (4.75) is hardly visible, but results, for example at $t = 2\tau/3$, in a small asymmetry with respect to the axis connecting the centers of the two Gaussians. At $t = \tau$, the components moving in the ground and excited state potentials strongly overlap again, leading to the partial revival of the electronic coherence in Fig. 4.2 a).
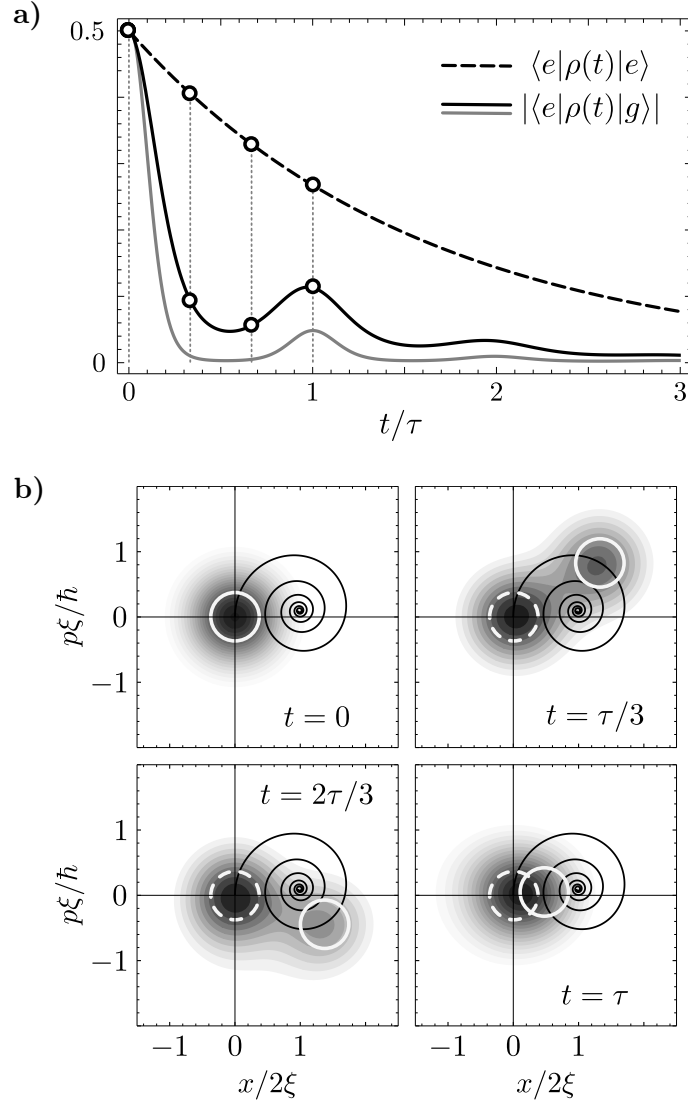
Figure 4.2: **a)** *shows the time evolution of the excited state population (dashed line) and the modulus of the coherences (solid lines) for the initial atomic state $(|g\rangle + |e\rangle)/\sqrt{2}$ in units of the oscillator period $\tau = 2\pi/\nu$ when the oscillator is initially in thermal equilibrium. The parameters are $\gamma = 0.2\nu$, $\Gamma = 0.1\nu$, $\Gamma^* = 0$ and $\eta = 1\nu$. The black curves show the case $\bar{m} = 0.05$ while the gray one corresponds to $\bar{m} = 1$. The density plots **b)** show the Wigner function of the oscillator state at the times indicated by the circles in **a)**. The dashed white ring represents the variance and location of the $|g\rangle\langle g|$-projection of the oscillator state in phase space, whereas the solid white ring analogously represents the $|e\rangle\langle e|$-projection which follows a trajectory along the spiral around β. The excited state population dies off and the system ultimately ends up in the stationary state $|g\rangle\langle g|\mu_{\text{th}}$.*

The advantage of the eigenvalue decomposition of the Liouvillian becomes apparent most clearly when calculating the spectral properties of the system. The method we use here was already applied for a systematic analysis of the fluorescence light of laser cooled atoms [Bie04] and is now carried over to the case of solid state quantum emitters. In Eq. (1.54) we already introduced the spectrum of absorption under stationary conditions for a weak probe laser of frequency ω_L illuminating the defect center, which is determined by [Mol72, CT77]

$$\mathcal{A}(\omega_L) = \mathrm{Re} \int_0^\infty \mathrm{d}t \, \langle [\sigma_-(0), \sigma_+(t)] \rangle_{\mathrm{st}} e^{-i\omega_L t} \,. \tag{4.76}$$

In this form the correlation function is evaluated without the probe. The time evolution of the operators is determined by the Liouvillian $\mathcal{L}$, Eq. (4.17), and can be calculated using the quantum regression theorem Eq. (1.30) to rewrite $\langle [\sigma_-, \sigma_+(t)] \rangle_{\mathrm{st}} = \mathrm{Tr}\{\sigma_+ e^{\mathcal{L}t}[\varrho_{\mathrm{st}}, \sigma_-]\}$. The stationary state of the undriven system is $\varrho_{\mathrm{st}} = |g\rangle\langle g|\mu_{\mathrm{th}}$, and hence, the second term of the commutator vanishes such that the spectrum takes on the form

$$\mathcal{A}(\omega_L) = \mathrm{Re} \sum_\lambda \frac{1}{i\omega_L - \lambda} \mathrm{Tr}\{\sigma_+ \hat{\varrho}_\lambda\} \mathrm{Tr}\{\breve{\varrho}_\lambda^\dagger \mu_{\mathrm{st}} \sigma_-\} \,. \tag{4.77}$$

In the last step we expanded the spectrum in terms of the eigensystem of $\mathcal{L}$, Eqs. (4.47)-(4.56), and performed the integration. The traces in Eq. (4.77) are readily evaluated because we encountered them already in the previous subsection when we calculated the dynamics of the system. They give

$$\mathrm{Tr}\{\sigma_+ \hat{\varrho}_{m,k}^{(-)}\} \mathrm{Tr}\{\breve{\varrho}_{m,k}^{(-)\dagger} \mu_{\mathrm{st}} \sigma_-\} = A_{m,k}^- B_{m,k}^- \,, \tag{4.78}$$

with the explicit form of the quantities $A_{m,k}^-$ and $B_{m,k}^-$ specified in App. B.1 and the products $W_{m,k} = A_{m,k}^- B_{m,k}^-$ shown in Eq. (4.66). The decomposed spectrum

$$\mathcal{A}(\omega_L) = \mathrm{Re} \sum_{m,k} \frac{W_{m,k}}{i\omega_L - \lambda_{m,k}^{(-)}} \tag{4.79}$$

is a superposition of curves associated with each eigenvalue $\lambda_{m,k}^{(-)}$, weighted by the function $W_{m,k}$ which also determines the shape: For real $W_{m,k}$ the spectral contribution is a Lorentzian, for purely imaginary weight it is a Fano-like profile, and in the general case it is a mixture of both, positioned at $\omega_L = \mathrm{Im}\,\lambda_{m,k}^{(-)}$ with a width given by $\mathrm{Re}\,\lambda_{m,k}^{(-)}$. From the k-dependency of the eigenvalues $\lambda_{m,k}^{(-)}$ it follows that the spectrum is built up by a series of peaks separated by the mechanical frequency ν and situated around the renormalized transition frequency $\widetilde{\omega}$. The peaks are distinguishable for $\Gamma, \gamma \ll \nu$ and otherwise overlap. Each peak, corresponding to a fixed value of k, is a sum of several contributions of increasing width for rising values of m. In the zero-
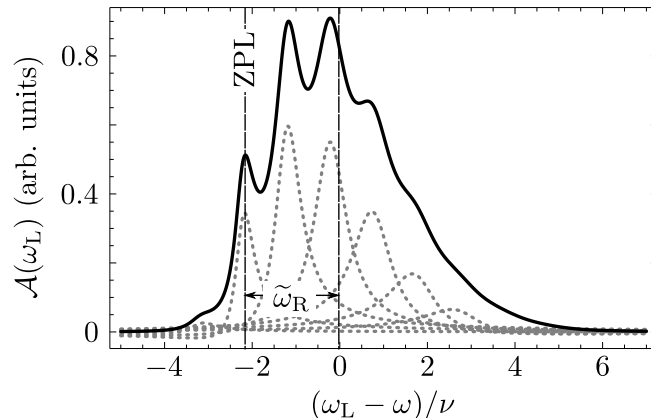
Figure 4.3: *The absorption spectrum of the defect center under weak excitation, according to* Eq. (4.79), *for the parameters* $\gamma = 0.2\nu$, $\Gamma = 0.01\nu$, $\Gamma^* = 0$, $\eta = 1.5\nu$ *and* $\bar{m} = 0.05$. *The gray dotted curves show the main contributions of the eigenvalue decomposition* (4.79) *of the spectrum, namely the terms corresponding to* $m = 0$ *and* $k = -5, ..., 1$. *ZPL denotes the position of the zero-phonon line shifted by* $\widetilde{\omega}_{\mathrm{R}}$ *from the bare transition frequency* ω *of the electronic states.*

temperature limit, *viz.* for $\bar{m} \to 0$, the $k > 0$ peaks vanish and only the terms with $m = 0$ contribute, as can be seen from Eq. (4.66). In this limit the weight factors take on the form

$$W_{m,k} = \delta_{m,0} \frac{\left[\beta^{*2}\right]^{|k|}}{|k|!} e^{-\beta^{*2}} \tag{4.80}$$

for $k \leq 0$ and are zero otherwise. It goes over into a Poissonian distribution when β becomes real. For vanishing thermal occupation of the phonon mode, only phonons can be created during the absorption process and consequently, the spectral components for $k > 0$ disappear. Note that the absorption and excitation spectrum of the two-level system coincide in the situation discussed here. We further remark that the integral representation of the absorption spectrum (4.76), involving the two-time correlation function in terms of the function $\Psi(t)$, can be advantageous in some cases, for example in the high temperature limit, when the expansion, Eq. (4.77), converges only slowly.

In Fig. 4.3 we show the absorption spectrum, Eq. (4.79), as a function of the probe frequency ω_{L} for a temperature close to zero. The spectrum is composed of several resolved peaks. The zero-phonon line corresponding to a pure electronic transition without creation or annihilation of phononic excitations is shifted by the relaxation frequency $\widetilde{\omega}_{\mathrm{R}} = \widetilde{\omega} - \omega$ from the frequency of the bare transition $|e\rangle \leftrightarrow |g\rangle$. More peaks are visible at multiple distances of the oscillator frequency and extend towards higher frequencies, forming the vibronic sidebands corresponding to absorption processes accompanied by the creation of phonons. Phonons to be annihilated are only rarely present at low temperatures entailing strongly suppressed signals on the lower

frequency side of the zero-phonon line. The dashed curves show the most relevant terms of the sum in Eq. (4.79), that is the individual spectral components associated with a certain eigenvalue which compose together the total spectrum. Note that the single contributions can become negative, only the superposition generally yields a valid spectrum.

We conclude this section by discussing the spectral properties of a photon *emitted* from the defect center. The emission spectrum reads [Scu97]

$$\mathcal{E}(\omega_{\mathrm{p}}) = \mathrm{Re} \int\limits_0^\infty \mathrm{d}t \int\limits_0^\infty \mathrm{d}\tau \, \langle \sigma_+(t+\tau)\sigma_-(t)\rangle e^{-i\omega_{\mathrm{p}}\tau} \,. \tag{4.81}$$

We assume here that the two-level system is initially excited and the oscillator is in the corresponding equilibrium $\mu_0 = D(\beta)\mu_{\mathrm{th}}D^\dagger(\beta)$. This is a reasonable assumption if the lifetime of the excited state Γ^{-1} is much larger than the thermalization time scale γ^{-1} of the phonon mode. Again the quantum regression theorem and the completeness relation of the eigenelements are applied to bring the spectrum into the form

$$\mathcal{E}(\omega_{\mathrm{p}}) = \mathrm{Re} \sum_{\lambda,\lambda'} \frac{\mathrm{Tr}\{\sigma_+\hat{\varrho}_\lambda\}\mathrm{Tr}\{\check{\varrho}_\lambda^\dagger \sigma_-\hat{\varrho}_{\lambda'}\}\mathrm{Tr}\{\check{\varrho}_{\lambda'}^\dagger|e\rangle\langle e|\mu_0\}}{(\lambda - i\omega_{\mathrm{p}})\lambda'} \,. \tag{4.82}$$

The further evaluation uses

$$\mathrm{Tr}\{\sigma_+\hat{\varrho}_{m,k}^{(-)}\} = A_{m,k}^- \,, \tag{4.83}$$

$$\mathrm{Tr}\{\check{\varrho}_{m',k'}^{(\rightsquigarrow)\dagger}|e\rangle\langle e|\mu_0\} = \delta_{m',0}\delta_{k',0}\mathrm{Tr}\{\check{\varrho}_{m',k'}^{(\rightsquigarrow)\dagger}\mu_{\mathrm{th}}\} \,, \tag{4.84}$$

and thus $\lambda' = -\Gamma$. The remaining trace in Eq. (4.82) can be calculated using the techniques of App. B.1 and yields $(-1)^l B_{m,k}^+ \exp[-i\,\mathrm{Im}\,\beta^2]$, *viz.* Eq. (B.15). The resulting spectrum

$$\mathcal{E}(\omega_{\mathrm{p}}) = \frac{1}{\Gamma}\mathrm{Re} \sum_{m,k} \frac{W'_{m,k}}{i\omega_{\mathrm{p}} - \lambda_{m,k}^{(-)}} \tag{4.85}$$

contains the weight factors $W'_{m,k} = W^*_{m,-k}$, signifying the fact that the emission spectrum is a mirrored version of the absorption spectrum [Mah00] with respect to the modified transition frequency $\widetilde{\omega}$.

We modeled the vibronic interaction of defect centers in crystals using a single-mode description including the radiative damping and pure dephasing of the electronic degree of freedom as well as the damping of the vibrational mode by a thermal reservoir with a temperature corresponding to a mean vibrational quantum number $\bar{m}$. The model can therefore be considered as an extension the Huang-Rhys model we intro-
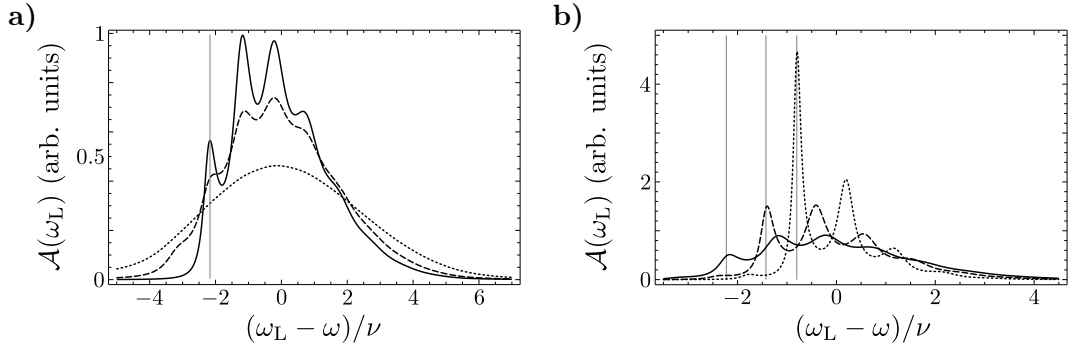
a)

b)

Figure 4.4: **a)** *The temperature dependence of the absorption spectrum for $\bar{m} = 0$ (solid line), $\bar{m} = 0.25$ (dashed line) and $\bar{m} = 1$ (dotted line).* **b)** *Dependence of the absorption on the coupling strength for $\eta = 1.5\nu$ (solid line), $\eta = 1.2\nu$ (dashed line) and $\eta = 0.9\nu$ (dotted line). The vertical lines are drawn at the corresponding zero-phonon lines, i.e. at the renormalized atomic frequency $\widetilde{\omega}$. The other parameters are the same as in* Fig. 4.3.

duced in Chapter 3, which is the limiting case of our model when both linewidths, Γ and γ, tend to zero.

From the temporal behavior treated in Sec. 4.3.1 follows that the vibronic coupling results in an effective dephasing mechanism for the electronic subsystem: It leaves the dynamics of the population unaffected but expedites the decay of the electronic coherences. This decay of the coherences is superimposed by an oscillatory behavior whose origins can be traced back to the motion of the vibrational degree of freedom in Wigner phase space. In the spirit of master equations, the dynamics of the two-level system can be considered as being dephased by a structured environment with harmonic time evolution, when tracing out the vibrational coordinates. The different types of dynamics concerning the populations and coherences is formally resembled in the classes of eigenvalues, Eqs. (4.54)-(4.56): The excited state simply decays with the natural rate Γ. In contrast, the electronic coherences oscillate with a renormalized frequency $\widetilde{\omega} = \omega - \widetilde{\omega}_{\mathrm{R}}$ and decay with the increased, temperature-dependent rate $\widetilde{\Gamma} = \Gamma + \widetilde{\Gamma}_{\mathrm{R}}$. The relaxation frequency $\widetilde{\omega}_{\mathrm{R}} = |\beta|^2 \nu$ goes over into $\omega_{\mathrm{R}} = S\nu$, proportional to the Huang-Rhys factor S, when the linewidth γ tends to zero. For finite linewidth, the damping rate γ additionally modifies the transition frequency of the two-level system, reflecting the fact that the electronic subsystem indirectly couples to the Markovian environment which damps the oscillator. Compared to the uncoupled case, the decay rate is increased by $\widetilde{\Gamma}_{\mathrm{R}} = |\beta|^2 \gamma (2\bar{m} + 1)$.

For the spectra, again a comparison with the Huang-Rhys model [Hua50, Dav81] suggests itself. This single-mode Hamiltonian model presented in Chapter 3 results in absorption spectra, see Figs. 3.2 and 3.3, consisting of Dirac-δ-shaped spikes displaced from the renormalized frequency $\omega - \omega_{\mathrm{R}}$ by multiples of the vibrational frequency ν, whose envelope (related to the intensities) is described by a Poissonian distribution $\mathcal{I}_l = e^{-S} S^l / l!$, when l numbers the vibronic sidebands. The generalized formulation applied here reflects these characteristics formally in Eq. (4.80), with the Huang-Rhys parameter replaced by the complex parameter β^{*2} quantifying the vibronic interaction

strength. For finite temperature, the Poissonian-like distribution breaks down and the intensity of the lth vibronic sideband is given by

$$\mathcal{I}_l = \sum_{m=0}^{\infty} \text{Re} \int_{-\infty}^{\infty} d\omega_L \frac{W_{m,l}}{i\omega_L - \lambda_{m,l}^{(-)}} = \pi \sum_{m=0}^{\infty} \text{Re}\, W_{m,l}\,. \qquad (4.86)$$

The sum over m can be carried out using the explicit form of the weight factors $W_{m,l} = A_{m,l}^- B_{m,l}^-$, given in Eq. (4.66), and the representation (4.67) leading to

$$\mathcal{I}_l = \pi\, e^{-(2\bar{m}+1)\text{Re}\beta^2} \sqrt{\frac{\bar{m}+1}{\bar{m}}}^l I_l\left(2|\beta|^2 \sqrt{\bar{m}(\bar{m}+1)}\right) \cos\theta_l \qquad (4.87)$$

with $\theta_l = \text{Im}\,\beta^2 + \arg\beta^{2l}$. This is a meaningful expression when the vibronic sidebands are resolved, that is for $\gamma, \Gamma \ll \nu$. The total spectral weight, *i.e.* the sum over l, gives the value π. The dependency of the absorption spectrum on the temperature is depicted in Fig. 4.4 a). For low temperature $\bar{m} \approx 0$ (solid line), the spectrum consists of the zero phonon line at $\omega_L = \omega - \widetilde{\omega}_R$ with $\widetilde{\omega}_R \approx 2\nu$ for the parameters considered here. Towards higher frequencies the vibronic sidebands are stretched out, starting to mutually overlap due to the swelling width of increasing orders. For a higher temperature, $\bar{m} = 0.25$, the individual lines are only hardly distinguishable and extend also towards lower frequencies on the red side of the zero-phonon line. The position of the zero phonon line is not temperature dependent, in contrast to its width given by $\text{Re}\,\lambda_{m,0}^{(-)}$, Eq. (4.55). Finally for $\bar{m} = 1$ only a broad spectral shape is present, centered approximately at the bare transition frequency ω of the two-level system. For $\nu \gg \gamma, \Gamma$ this single peak approaches a Gaussian form around $\omega_L = \omega$ whose width is proportional to $\sqrt{\bar{m}}$. Fig. 4.4 b) shows the absorption spectrum at low temperature for three different vibronic coupling strengths, $\eta = 0.9\nu$, 1.2ν, and 1.5ν, corresponding to the dotted, dashed, and solid curves, respectively. The peak strength follows the quasi-Poissonian distribution (4.80), with more peaks appearing for larger coupling: then higher order phonon processes become more likely. The position of the zero-phonon line moves towards lower frequencies for larger couplings in accordance with the renormalized frequency $\widetilde{\omega}$ defined in Eq. (4.55) and the simplified physical picture of Fig. 4.1. Moreover, the curves in Fig. 4.4 b) demonstrate that an increased coupling goes along with a broadening of the spectral components, as described by $\widetilde{\Gamma}$, Eq. (4.55).

The master equation description of this work can also be related to the independent boson model [Mah00], in which a linear coupling to essentially a continuum of phononic modes is taken into account. The phase diffusion in the temporal evolution of the phononic modes is at the heart of the dephasing mechanism there, being replaced in the present description by a Markovian reservoir. Consequently, the spectral function describing the frequency dependent coupling strength of the phononic continuum in that model is replaced here by a single parameter, namely the damping rate γ of the singled out phononic mode. Depending on the intended application, the more detailed independent boson model or the one-parametric simplified description presented here

can be advantageous.

Finally we comment on the applicability of the model for NV$^-$ centers in diamond. As already mentioned, the presence of a few localized modes of similar frequencies suggests to highlight these modes – or ultimately a single mode – as it was done here. A thermal reservoir damping the mode has clear physical origins in the continuum of the delocalized phononic modes. The Markovian description, however, is a simplification which works reasonably well for rendering the basic properties of the NV$^-$ dynamics, but does not include the details of the temperature dependency of the zero-phonon line, for example. This would at least require to replace the flat spectral function implicitly applied here, if not more involved processes [Fu09] have to be included, depending on the desired accuracy of the description. A temperature-dependent damping rate $\gamma(T)$ can however be used to mimic such behaviour. Of course, effects stemming from the dynamical *Jahn-Teller effect* are absent. Nevertheless, the model renders the basic properties of the spectra of NV$^-$ centers, especially in the room temperature regime and goes beyond simple pure dephasing models or artificial fitting models. Note that the room temperature spectra still correspond to $\bar{m} \ll 1$ due to the high *Debye-temperature* of diamond.

We formulated a compact theoretical description for the dynamics of defect centers in crystals. This master equation description is based on a linear vibronic coupling in the Franck-Condon, single phonon mode and two-level approximation and includes radiative and phononic Markovian damping. The overall solution of the master equation is given in terms of the eigenelements and eigenvalues of the Liouville operator. This solution covers both, the electronic and phononic degree of freedom and can be further reduced to a master equation of the electronic two-level system only by tracing out the undesired degree of freedom. We demonstrated the calculation of the absorption and emission spectrum at different temperatures, which take on a insightful form and reproduce the basic features of real spectra, for example for NV$^-$ centers in diamond. The physical picture at the heart of the presented model was reviewed in detail by means of the dynamics of both involved degrees of freedom.

In the form presented here, the model can be easily extended by adding more vibrational modes in order to increase the accuracy of the theory, if desired. Moreover, such an extension would also be interesting from the point of view of a systematic approximation of open quantum dynamics [Woo14]. It is also entirely conceivable to extend the treatment to include quadratic vibronic coupling or more electronic levels.

We believe that the model, based on an easy but clear physical picture, will be helpful for investigations of defect centers in quantum-optical applications, for example as single-photon sources, when the influence of the vibronic sidebands becomes important. With the analytic solution provided here it can deliver a basis for the description of coupled cavity-defect-center systems or similar hybrid setups.

PART III

Cavity optomechanics

The interaction of light with matter lies at the heart of many developments in modern physics. It were, for instance, the investigations of black-body radiation and the photoelectric effect that played a major role in the invention of quantum mechanics. This interaction comprises the coupling of the electric or magnetic field of light to the internal degrees of freedom of atoms, as successfully described by quantum electrodynamics, and allows, among others, high-precision spectroscopy, optical trapping and coherent manipulation of the electronic states.

On the other hand, light, although massless, carries a momentum. This momentum entails mechanical effects that are, for example, routinely employed in today's laboratories to cool trapped atoms down towards the ground state of their center-of-mass motion using laser light [Neu78, Met01]. For objects more massive than single atoms the momentum of the electromagnetic field of light can exert a *radiation pressure force*. This fact was predicted and experimentally observed [Leb01, Nic01] already before the advent of quantum mechanics, and early speculations even go back to Kepler.

The astonishing achievements in the control of single atomic systems [Lei03, Mes06] lead to increasing interest in the manipulation of macroscopic objects [Ash06] using this radiation pressure. To control the quantum state of truly macroscopic objects is not only interesting for applications, such as displacement and force detection [Cav80, Bra95, Gav12] near the fundamental quantum limit, but also from the point of view of testing the foundations of quantum mechanics on a larger scale than the atomic one. In this context the interaction can be used, for instance, to bring macroscopic objects into quantum superpositions and investigate how these superpositions behave under the influence of gravitation.

However, the radiation pressure force exerted by a single photon is exceedingly small. In order to develop an intuition we can consider a photon with wavenumber k being reflected on a mirror whereby the momentum $2\hbar k$ is transferred. For a continuous light ray of power P illuminating the mirror the rate of photon impacts is given by $P/\hbar ck$, leading to a force $F = 2P/c$. Since the speed of light c appears in the denominator of this expression its magnitude is very small, *e.g.* even a kilowatt beam only exerts a force of roughly 10^{-5} N. The smallness of this force implies that extremely low-weight mechanical objects have to be used in order to exhibit an appreciable influence of the radiation pressure on the mechanical degree of freedom.

A possible way to enhance the interaction is to confine the light field between two mirrors, such that in a simplified picture a photon can bounce off the mirrors many times instead of being reflect only once, as it would in free-space experiments. The paradigm setup of *cavity optomechanical systems* [Mey13, Asp14, Bow15] is an optical Fabry-Pérot cavity with one fixed and one *moving* end-mirror. The light field inside the optical resonator exerts a radiation pressure force on the end-mirror and transfers momentum to its motional degree of freedom. Due to the smallness of the radiation pressure the typical mechanical objects employed in optomechanical experiments are nano-cantilevers [HM04, Fav07] or microtoroids [Car05, Sch06] with effective masses of $\sim 10^{-11}$ kg, to mention only two examples. For a detailed review introducing a variety of optomechanical devices we refer to Ref. [Asp14] and references therein. Among

the tremendous progress toward full quantum control over the mechanical degree of freedom in such systems we mention the successful demonstration of laser cooling of the cavity's mirror motion toward the ground state of the confining potential [Gig06, Sch08, Roc10, Cha11], reaching phonon occupations of down to ~ 0.35 [Teu11]. For a theoretical analysis of the optomechanical cooling we refer to Refs. [WR04, WR08b].

This recent experimental success in cavity optomechanics also pioneers near-future experiments with extended, *hybrid systems* [Kur14, Rog14]. An obvious extension of the paradigmatic optomechanical system can be achieved by adding a single two-level system which couples to the cavity light field by dipole interaction, thereby combining cavity optomechanics with cavity quantum electrodynamics. Besides conventional quantum electrodynamics experiments with macroscopic cavities investigations of such systems are of particular importance for solid-state systems, such as two-level systems in optomechanical crystals [Eic09, RM12, Bre12]. In circuit electromechanical setups the coupling to two-level systems has already been demonstrated [LaH09, Pir13, Lec15, Pir15] successfully.

The richness in the dynamics of such highly non-linear hybrid systems has only been started to be explored theoretically in several general investigations of the coherent motion [Wan08, Cha09, Ram13, Mir15] and can, for example, be exploited to prepare non-classical states, similar as in nonlinear optical setups [Poy96, Rit04].

With the work presented in this part we provide a detailed theoretical treatment of such optomechanical hybrid systems in which we especially focus on an effect where the presence of the mechanical degree of freedom strongly changes the atom-cavity interaction leading to a suppression of Rabi-oscillations. This effect is analyzed for a coherent evolution as well as for a hybrid system subject to dissipation.

In general the dissipative dynamics of optomechanical systems can be described by a Born-Markov master equation. In a subsequent work presented at the end of this part we leave aside the two-level atom again and concern ourselves with this master equation. In the spirit of the damping basis that was introduced in Sec. 1.3 we derive the solution of the optomechanical master equation in terms of this damping basis and thereby provide a tool for the analytic treatment of dissipative optomechanics.

The structure of this part is the following: In Chapter 5 we introduce the basic theoretical description of generic optomechanical systems. Chapter 6 then deals with the dynamics of hybrid-optomechanical setups including the suppression of Rabi-oscillations. A derivation of the damping basis of the Liouville operator associated with the master equation for dissipative optomechanical systems is finally shown in Chapter 7.

In this chapter we briefly recapitulate the theoretical description of generic optomechanical systems in order to lay the ground work for the later treatment of optomechanical hybrid systems and the optomechanical master equation. In Sec. 5.1 we present a phenomenological derivation of the optomechanical Hamiltonian governing the coherent dynamics. The eigenbasis of this Hamiltonian and the time evolution of initial states which are relevant for a subsequent chapter are summarized in Sec. 5.2.

We consider an end-mirror of mass M whose center-of-mass motion is confined in a harmonic potential of frequency ν. The motion of the mirror then imposes boundary conditions on the electromagnetic field inside the cavity that vary with time. A Hamiltonian formulation of this problem with time-dependent boundary conditions, as found in Ref. [Law95], would go beyond the scope of this thesis, so that we give a more intuitive approach that leads to the same Hamiltonian. The motion of the movable mirror inherently changes the cavity length, making the cavity frequency ω a function of the mirror position x, measured with respect to its equilibrium position, *i.e.* $\omega(x)$. For small elongations of the mirror, compared to the cavity length L, a Taylor expansion in terms of x/L suggests itself, leading to

$$H = \hbar\omega(x)a^\dagger a + \hbar\nu b^\dagger b \approx (\hbar\omega - Fx)a^\dagger a + \hbar\nu b^\dagger b \,, \tag{5.1}$$

with $F = -\partial\omega(x)/\partial x|_{x=0}$. Additionally we introduced the cavity annihilation and creation operators a and $a^\dagger$ and the corresponding mechanical oscillator operators b and $b^\dagger$. The latter are related to the mirror position via $x = \xi(b + b^\dagger)$, with $\xi = \sqrt{\hbar/2M\nu}$. The quantity F can be thought of as the single photon radiation pressure force on the mirror. Defining the optomechanical coupling strength $\chi = F\xi/\hbar$ one arrives at the standard Hamiltonian of an optomechanical system which reads

$$H_{\mathrm{om}} = \hbar\omega a^\dagger a + \hbar\nu b^\dagger b - \hbar\chi a^\dagger a(b + b^\dagger) \,. \tag{5.2}$$

This Hamiltonian captures the basic interplay between the mirror motion and the cavity field: the radiation pressure results in a photon-number dependent displacement of the mirror which in turn changes the cavity's frequency.

The Hamiltonian (5.2) can be diagonalized using the photon-number dependent displacement transform $D(-\beta a^\dagger a)$ [Bos97] with the relative coupling strength

$$\beta = \frac{\chi}{\nu} \tag{5.3}$$

and the mechanical displacement operators $D(\alpha) = \exp[\alpha b^\dagger - \alpha^* b]$. In the displaced picture the two oscillators are decoupled and the eigenstates are products of cavity Fock states $|n\rangle$ and mechanical Fock states $|m\rangle_{\mathrm{mec}}$. In the original picture the eigenstates of H_{om} are then given by

$$|n\rangle\, D(n\beta)|m\rangle_{\mathrm{mec}} \tag{5.4}$$

with the corresponding eigenvalues $n\hbar\omega + m\hbar\nu - n^2\beta^2\hbar\nu$. The separability of these eigenstates entails the fact that any initial state in which the cavity is in a single number state always remains separable. If we consider the cavity to be in the state $|n\rangle$ and the mechanical oscillator in the coherent state $|\alpha\rangle_{\mathrm{mec}}$ the propagation of the mechanical oscillator is given by the coherent state [Bos97]

$$|\eta(t)\rangle_{\mathrm{mec}} = |n\beta(1 - e^{-i\nu t}) + \alpha e^{-i\nu t}\rangle_{\mathrm{mec}}\,, \tag{5.5}$$

apart from an additional phase factor. Figure 5.1 a) shows the trajectories in Wigner phase space for the values $n = 1$ and $n = 2$ of the cavity photon number and the mechanical ground state $\alpha = 0$. The radiation pressure of the cavity photons pushes the mirror out of its equilibrium position, resulting in a modified cavity length and thereby a modified frequency. In the modified potential the initial ground state of the mechanical oscillator moves like a coherent state on circular orbits in phase space centered around $x = 2\beta\xi$ and $p = 0$ whose radii are proportional to β. In Fig. 5.1 b) the trajectories of the probability density of the wave packet in the position representation are depicted. The turning points are marked by the maximum displacements from the equilibrium position which are given by

$$\langle x \rangle^{(n)}_{\mathrm{max}} = 2\xi \operatorname{Re}[n\beta(1 - e^{-i\nu t})] = 4n\beta\xi\,. \tag{5.6}$$

They are reached after half a mechanical period, *i.e.* at the time $t = \pi/\nu$. In the single-photon strong coupling regime, a regime that will be discussed in a later chapter in which $\beta \gtrsim 1$ is fulfilled, this displacement amounts to a significant change in the cavity frequency during the dynamics, a fact that will be particularly important in the following.
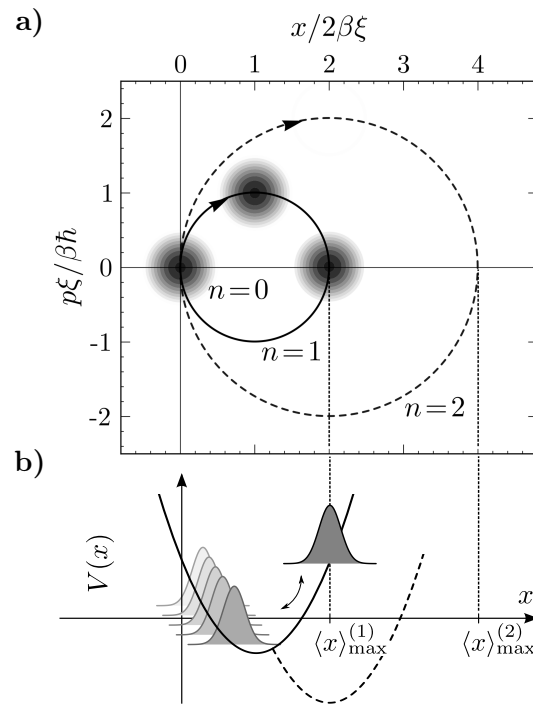
Figure 5.1: **a)** *Circular trajectories of the mechanical oscillator's Wigner function for cavity photon numbers $n = 1$ (solid) and $n = 2$ (dashed) if the mirror was initially prepared in its ground state $|0\rangle_{\mathrm{mec}}$. The radii are proportional to β while for $n = 0$ the Wigner function rests centered around the origin.* **b)** *Trajectory of the oscillator wave packet in the harmonic potential modified by the radiation pressure. The $\langle x \rangle_{\mathrm{max}}^{(n)}$ mark the maximal elongations.*

Suppression of Rabi oscillations in hybrid optomechanical systems

In the Jaynes-Cummings model [Jay63], a single atomic dipole interacting with a single photon of an electromagnetic field mode in a cavity periodically exchanges the excitation between the electronic and photonic degree of freedom. In this chapter we ask ourselves the following questions: How does this behavior change, when the cavity's mirrors are not fixed, but can move in time as an additional quantum dynamical degree of freedom? And, how does the quantumness of the mirror motion manifest itself in the dynamics?

When adding a single atom to the optomechanical cavity, the resulting hybrid system does not only incorporate the radiation forces of the cavity-mirror interaction, but also includes the dipole interaction between a near-resonant atomic transition and the cavity field, drastically altering the dynamics as a whole. In this chapter we focus on the possibility to dynamically suppress the Rabi oscillation of the atomic population due to the mirror motion. The idea behind can best be illustrated having a classical picture in mind, *i.e.* when the mirror is moving parametrically along a given trajectory. Then, an initially resonant atom-cavity interaction becomes disturbed by the mirror motion due to the change of the cavity's resonance frequency being a function of the cavity length. If the mirror elongation is large enough, the modified atom-cavity detuning can lead to reduced Rabi oscillations of the quantum electrodynamic subsystem. We will develop this simple classical picture beyond the trivial parametric motion towards a fully dynamical one in the quantum regime. The Wigner function will be used to represent the dynamics of the mechanical degree of freedom, which can exhibit strong non-classical characteristics deep in the non-linear parameter regime. Even when dissipation and a variation of the initial state is included, the characteristic features of this suppression can be distinguished.

We briefly note that especially solid-state systems (leaving aside the two-level system in contemporary realizations) are candidates for reaching the so-called single-photon strong coupling regime [Nun11], where the radiation force of a single photon is strong enough to displace the harmonically oscillating mechanical element by more than the extension of its ground-state wavepacket. This regime is entered, when the mechanical frequency becomes much smaller than the optomechanical coupling. Then, the non-linearity of the radiation force becomes clearly apparent and manifests itself in phenomena like the photon blockade effect [Rab11], which is caused by an effective photon-photon interaction mediated by the mechanical degree of freedom.

The present chapter has the following structure: In Sec. 6.1 we introduce the hybrid system that we investigate. In the subsequent Sec. 6.2 we present the coherent dynamics of the system, including two limiting cases of the parameters that allow for an analytic treatment, and analyze the suppression of Rabi-oscillations induced by the mirror motion. The behavior of this suppression effect under dissipation is treated in Sec. 6.3 and the influence of the initial state of the hybrid system is presented in Sec. 6.4 before we conclude in Sec. 6.5.

The main results of this chapter have been published in

- TIMO HOLZ, RALF BETZHOLZ, AND MARC BIENERT,
  "Suppression of Rabi oscillations in hybrid optomechanical systems",
  Phys. Rev. A **92**, 043822 (2015),
  Copyright (2015) by the American Physical Society.

We consider an optomechanical resonator with a two-level atom placed at a fixed position within the resonator. The transition frequency between the ground state $|g\rangle$ and the excited state $|e\rangle$ is assumed to be resonant with the frequency ω of the cavity when its end mirror is in the equilibrium position. The atomic dipole couples via Jaynes-Cummings interaction [Jay63] to the electromagnetic field of the cavity while the cavity interacts with the mechanical oscillator of frequency ν and mass M by radiation pressure. We denote the dipole-cavity interaction strength and the optomechanical coupling strength by g and χ, respectively. A schematic picture of this hybrid quantum system is shown in Fig. 6.1. The total Hamiltonian of the hybrid

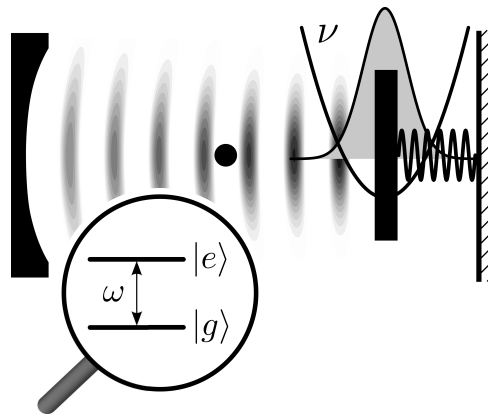**Figure 6.1:** *Hybrid optomechanical setup consisting of a single-mode cavity with a moving end-mirror confined in a harmonic potential of frequency ν and a resonant two-level atom at a fixed position. The cavity couples to the mechanical oscillator by radiation pressure with a coupling strength χ and to the two-level atom via dipole interaction of strength g.*

systems reads

$$H = H_{\mathrm{om}} + H_{\mathrm{tls}} + H_{\mathrm{JC}}\,,\tag{6.1}$$

where the operator H_{om} labels the standard Hamiltonian of optomechanics [Law95] that was introduced in Eq. (5.2). We use the same notation as before and write a and $a^\dagger$ for the annihilation and creation operators of the cavity mode, and b and $b^\dagger$ for the mechanical oscillator whose position operator relative to the equilibrium is $x = \xi(b + b^\dagger)$, with the harmonic oscillator length scale $\xi = \sqrt{\hbar/2M\nu}$. The Hamiltonians of the two-level system and the Jaynes-Cummings interaction are given by

$$H_{\mathrm{tls}} = \hbar\omega|e\rangle\langle e|\,,\tag{6.2}$$

$$H_{\mathrm{JC}} = \hbar g\big[a^\dagger|g\rangle\langle e| + a|e\rangle\langle g|\big]\,,\tag{6.3}$$

respectively.

For the coherent dynamics of the hybrid system including cavity, atom and mechanical oscillator, we focus on the initial state $|\psi(t = 0)\rangle = |e\rangle|0\rangle|0\rangle_{\mathrm{mec}}$, where the atom is in the excited state, the cavity is empty and the mirror is in its ground state. Experimentally such a state can be prepared with the help of ground-state cooling of the mechanical oscillator and standard optical pumping for the atomic state. Ground-state cooling for an optomechanical crystal was already demonstrated [Cha11] and is expected to be realizable in similar hybrid systems in near-future experiments.

   The position of the mirror determines the frequency of the cavity, which can be seen most clearly when rewriting the Hamiltonian (6.1) in the form

$$H = \hbar\left[\omega - \frac{\chi}{\xi}x\right]a^\dagger a + \hbar\nu b^\dagger b + H_{\mathrm{tls}} + H_{\mathrm{JC}}\,.\tag{6.4}$$

The mechanical oscillator in its maximally elongated mean position, Eq. (5.6), results in an effective detuning $\bar\delta_n = 4n\beta\chi$ between the cavity and the atom. From this consideration follows that for a distinct effect of the mirror's motion on the Rabi oscillation one has to be in the strong-coupling regime with $\beta \gtrsim 1$. In this regime we cannot resort to the approximate solution of single polariton optomechanics [Res14].

Nevertheless, to provide first insight into the dynamics we start our investigation with two limiting cases, namely a small dipole-cavity coupling $g \ll \chi,\nu$ and a small optomechanical coupling $\beta \ll 1$, that allow for an approximate analytical treatment.

Slow Rabi oscillations

In the case of small Jaynes-Cummings coupling, *i.e.* $g \ll \nu, \chi$, we focus on the parameter region $\beta \approx 1$ for strong optomechanical coupling and restrict the following discussion to the subspace of only one excitation in the quantum electrodynamical subsystem, remarking that the generalization is straightforward. In the interaction picture and after displacing the Hamiltonian (6.1) with $D(-\beta|g,1\rangle\langle g,1|)$ it takes on the form

$$\tilde{H} = \hbar g \Big[e^{i\beta^2 \nu t} D(\beta e^{i\nu t})|e,0\rangle\langle g,1| + \text{H.c.} \Big], \qquad (6.5)$$

apart from a constant energy, in the relevant subspace spanned by the two atom-cavity states $|g,1\rangle = |g\rangle|1\rangle$ and $|e,0\rangle = |e\rangle|0\rangle$. A rotating-wave approximation can be performed after expanding the displacement operator in a power series and taking only those terms that rotate with the smallest occurring frequency, which is given by $(\beta^2 - 1)\nu$ for $\beta \approx 1$. In the expansion of $D(\beta \exp[i\nu t])$ these surviving terms contain a single operator b more than $b^\dagger$. Applying this procedure to (6.5) leads to the approximate Hamiltonian

$$\tilde{H}_{\text{RWA}} = \hbar g \Big[e^{i(\beta^2-1)\nu t} f(b^\dagger b) b|e,0\rangle\langle g,1| + \text{H.c.} \Big] \qquad (6.6)$$

where the function $f(m)$ can be obtained by evaluating the matrix elements $_{\text{mec}}\langle m|D(\beta)|m+1\rangle_{\text{mec}}$ of the displacement operator [Cah69b] which explicitly results in the expression

$$f(m) = \frac{-\beta}{m+1} e^{-\beta^2/2} L_m^{(1)}(\beta^2) \qquad (6.7)$$

with the generalized Laguerre polynomials $L_m^{(\alpha)}(x)$ [Abr65]. Within this approximation the Hamiltonian is a Jaynes-Cummings-type interaction between the atom-cavity subsystem and the mechanical oscillator with an additional phonon number dependent factor that does not alter the eigenstates, *i.e.* the dressed states [Har06]. In the original picture the Hamiltonian then reads

$$H_{\text{RWA}} = \hbar \nu b^\dagger b - \hbar \chi |g,1\rangle\langle g,1|(b + b^\dagger) + \hbar g \big[f(b^\dagger b) b D^\dagger(\beta)|e,0\rangle\langle g,1| + \text{H.c.} \big] \qquad (6.8)$$

and its eigenstates are dressed states in which the state $|g,1\rangle|m\rangle_{\text{mec}}$ is displaced by $D(\beta)$ while the state $|e,0\rangle|m+1\rangle_{\text{mec}}$ remains undisplaced. For the initial state where the atom is prepared in its excited state and the mechanical oscillator in its ground state, *i.e.* $|\psi(t=0)\rangle = |e,0\rangle|0\rangle_{\text{mec}}$, the time evolution results in the reduced density operators

$$\mu_{\text{RWA}}(t) = \big[\cos^2(\Omega t) + \cos^2 \vartheta \sin^2(\Omega t) \big] |0\rangle_{\text{mec}}\langle 0|$$
$$+ \sin^2 \vartheta \sin^2(\Omega t) D(\beta)|1\rangle_{\text{mec}}\langle 1|D^\dagger(\beta) \qquad (6.9)$$

and

$$\rho_{\mathrm{RWA}}(t) = \left[\cos^2(\Omega t) + \cos^2\vartheta \sin^2(\Omega t)\right]|e,0\rangle\langle e,0| + \sin^2\vartheta \sin^2(\Omega t)|g,1\rangle\langle g,1| \quad (6.10)$$

for the mechanical oscillator and the atom-cavity subsystem, respectively. Here, we defined $\tan\vartheta = \Omega/(\beta^2 - 1)\nu$ and $\Omega = 2gf(0)$. We compared these approximate results with numerical propagation and found especially good agreement for the case $\beta = 1$, where the rotating-wave approximation is best fulfilled. From these outcomes we conclude: *(i)* The motion of the mechanical oscillator leads to non-classical states being composed of two contributions, namely an incoherent superposition of the vacuum and a displaced Fock state. They correspond to the radiation pressure of zero and one photon which are associated with the two trajectories $n = 0$ and $n = 1$ of Fig. 5.1a) in the uncoupled case and become mixed due to the coherent Rabi oscillations between $|g,1\rangle$ and $|e,0\rangle$. *(ii)* For $\beta \neq 1$ one finds detuned Rabi oscillations of the atom-cavity subsystem, while they are strictly sinusoidal for $\beta = 1$. *(iii)* The regime considered here is not sufficient for observing a suppression of Rabi oscillations of the atomic population. Nevertheless, it provides a first insight into the coupled dynamics of the system and the origin of the emergence of non-classicalities in the state of the mechanical oscillator.

Small optomechanical coupling

In a frame displaced by $D(-\beta/2)$ and restricted to the subspace spanned by the usual Jaynes-Cummings dressed states [Har06]

$$|\pm\rangle = \frac{1}{\sqrt{2}}[|g,1\rangle \pm |e,0\rangle] \qquad (6.11)$$

of the resonant atom-cavity subsystem the Hamiltonian (6.1), apart from a constant energy $\hbar\beta^2\nu/2$, can be written as the Hamiltonian of the driven Rabi model [Rab36]

$$\begin{aligned}
\tilde{H}_{\mathrm{Rabi}} =& \hbar\nu b^\dagger b + \hbar g \left[|+\rangle\langle+| - |-\rangle\langle-|\right] \\
& - \frac{\beta}{2}\hbar\nu \left[|+\rangle\langle-| + |-\rangle\langle+|\right](b + b^\dagger) + \frac{\beta^2}{2}\hbar\nu \left[|+\rangle\langle+| + |-\rangle\langle-|\right].
\end{aligned} \qquad (6.12)$$

Even in the absence of the last term, constituting a drive of the dressed state transition with a strength proportional to β^2, where this model allows for analytic expressions of the eigenvalues and eigenstates [Bra11, Zho13], the solutions are not easy-to-handle and reveal little physical insight.

   We therefore follow the treatment presented in Ref. [Res14] for an approximation in the regime of small values of the optomechanical coupling ratio. In this regime, for $\beta \ll 1$, one can discard the driving term in Hamiltonian (6.12) and perform a rotating-wave approximation leading to dynamics that are governed by the Hamiltonian [Res14]

$$\tilde{H}_\beta = \hbar\nu b^\dagger b + \hbar g \left[|+\rangle\langle+| - |-\rangle\langle-|\right] - \frac{\beta}{2}\hbar\nu \left[b|+\rangle\langle-| + b^\dagger|-\rangle\langle+|\right]. \qquad (6.13)$$

The Hamiltonian (6.13) is again of Jaynes-Cummings form, with the ladder operators $|\pm\rangle\langle\mp|$ playing the role of the atomic rising and lowering operators and the mechanical oscillator taking over the cavity part. In the rotating wave approximation we additionally assumed that the requirement $|2g - \nu| \ll 2g + \nu$ is fulfilled. In the case of a resonant interaction, $2g = \nu$, the double dressed states

$$|0,0\rangle = |-\rangle|0\rangle_{\mathrm{mec}} \quad (\text{for } m = 0),$$ (6.14)

$$|\pm, m\rangle = \frac{1}{\sqrt{2}}\left[|+\rangle|m-1\rangle_{\mathrm{mec}} \pm |-\rangle|m\rangle_{\mathrm{mec}}\right]$$ (6.15)

are the eigenstates of the Hamiltonian (6.13) with the corresponding eigenenergies $\varepsilon_0 = -\hbar\nu/2$ and

$$\varepsilon_m^{(\pm)} = \left[m - \frac{1}{2} \mp \frac{\beta}{2}\sqrt{m}\right]\hbar\nu$$ (6.16)

for $m \geq 1$. The initial state $|\psi(t = 0)\rangle = |e, 0\rangle|0\rangle_{\mathrm{mec}}$ can be propagated with help of the eigenbasis (6.14) and (6.15) of the Hamiltonian (6.13) and leads to

$$
\begin{aligned}
|\tilde{\psi}(t)\rangle = e^{-\frac{\beta^2}{8}} \sum_{m=0}^{\infty} \frac{\left(-\frac{\beta}{2}e^{-i\nu t}\right)^m}{\sqrt{2m!}} &\left\{ -i\sin\left(\sqrt{m}\frac{\beta}{2}\nu t\right)e^{i\frac{\nu}{2}t}|+\rangle|m-1\rangle_{\mathrm{mec}} \right. \\
&+ \left[\cos\left(\sqrt{m+1}\frac{\beta}{2}\nu t\right)e^{-i\frac{\nu}{2}t}|+\rangle - \cos\left(\sqrt{m}\frac{\beta}{2}\nu t\right)e^{i\frac{\nu}{2}t}|-\rangle\right]|m\rangle_{\mathrm{mec}} \\
&+ \left. i\sin\left(\sqrt{m+1}\frac{\beta}{2}\nu t\right)e^{-i\frac{\nu}{2}t}|-\rangle|m+1\rangle_{\mathrm{mec}} \right\}
\end{aligned}
$$ (6.17)

in the displaced frame. More insight reveals the $m = 0$ term,

$$
\begin{aligned}
|\psi(t)\rangle \approx \frac{e^{-\frac{\beta^2}{8}}}{\sqrt{2}} &\left\{ \left[\cos\left(\frac{\beta}{2}\nu t\right)e^{-i\frac{\nu}{2}t}|+\rangle - e^{i\frac{\nu}{2}t}|-\rangle\right]|\beta/2\rangle_{\mathrm{mec}} \right. \\
&+ \left. i\sin\left(\frac{\beta}{2}\nu t\right)e^{-i\frac{\nu}{2}t}|-\rangle D\left(\tfrac{\beta}{2}\right)|1\rangle_{\mathrm{mec}} \right\},
\end{aligned}
$$ (6.18)

written here in the original frame, showing the dominant behaviour of $|\psi(t)\rangle$ for $\beta \ll 1$: The first term describes the usual Rabi-oscillations of the atom-cavity system when $\beta \to 0$, whereas the second term represents an oscillating displaced number state of the mechanical oscillator, associated with the dressed state $|-\rangle$. Nevertheless, the condition $\beta \ll 1$ for the validity of the Hamiltonian (6.13) prevents clear signatures of non-classicality of the evolved state in this limit.

The time evolution of the excited state population $P_e(t) = \mathrm{Tr}\{|e\rangle\langle e|\psi(t)\rangle\langle\psi(t)|\}$, using the state (6.18), can be further approximated by

$$P_e(t) \approx \frac{1}{2}\left[1 + \cos\left(\frac{\beta}{2}\nu t\right)\cos(\nu t)\right]$$ (6.19)

which shows a sinusoidally modulated Rabi oscillation with a beat frequency of $\beta\nu/2$ describing the onset of the suppression of Rabi-oscillations for small values of β.

We now focus on the strong-coupling regime $\beta \gtrsim 1$ where the approximate Hamiltonians (6.6) and (6.13) are not valid and one has to deal with the original hybrid Hamiltonian, Eq. (6.1) instead. We therefore restrict ourselves in the following on the discussion of numerical results.

The case $g = \nu$

We first focus on the case $g = \nu$ and $\beta = 1$. We start again from the same initial state $|\psi(t = 0)\rangle = |e, 0\rangle|0\rangle_{\text{mec}}$ and propagate it numerically using the Hamiltonian (6.1). In Fig. 6.2 we show the time evolution of the excited state population $P_e(t) = \text{Tr}\{|e\rangle\langle e|\psi(t)\rangle\langle\psi(t)|\}$. The strictly periodic Rabi oscillation of the uncoupled case (dashed) undergoes a drastic change. Instead of the sinusoidal time evolution the excited state population exhibits a strong suppression before it rises up again at a time appreciably longer than the Rabi period π/g. This behavior continues quasi-periodically for the considered parameters and can be qualitatively understood with the following intuitive explanation: As time evolves the atom initially prepared in the excited state populates the cavity with a single photon leading to a rising radia-
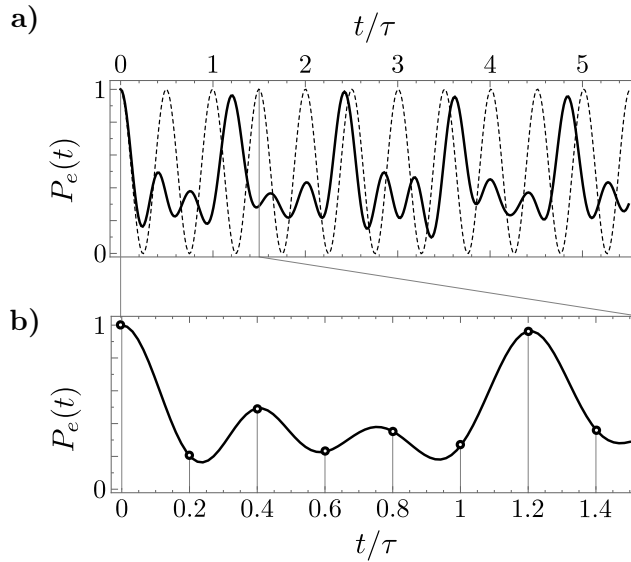

Figure 6.2: **a)** *Time evolution of the excited state population for the initial state $|e, 0\rangle|0\rangle_{\text{mec}}$. The population experiences a strong suppression before a first revival at a time larger then a Rabi period. The parameters are $\beta = 1$ and $g = \nu$. For comparison the unperturbed Rabi oscillations ($\beta = 0$) are shown in the dashed line.* **b)** *Inset on a time scale until the first revival occurs. The circles indicate instances of time which will be referred to later.*

tion pressure inside the cavity pushing the mirror significantly out of its equilibrium position and driving it along the trajectory $n = 1$ in Fig. 5.1 a). Its displacement is accompanied by an effective dynamical detuning between atom and cavity suppressing the Rabi oscillations. After approximately one mechanical oscillator period $\tau = 2\pi/\nu$ the atom-cavity resonance condition is fulfilled again and the Rabi oscillation continues. This simple picture, however, does not explain all details in Fig. 6.2: The behavior is not strictly periodic in the mechanical period τ and $P_e(t)$ does not show a full revival.

To systematically analyze the suppression of the Rabi oscillations for different values of β using the same initial state $|\psi(t=0)\rangle = |e,0\rangle|0\rangle_{\mathrm{mec}}$ as before we show in Figure 6.3 a) the time evolution of the population of the excited state in dependence of β color-coded in a density plot for $g = \nu$, where dark shading indicates high values of the population in $|e\rangle$. For the dotted white lines in the lower part of Fig. 6.3 a) we used the perturbative results of Sec. 6.2.1 to show the times T_n of the n-th maximum of the perturbed Rabi oscillation for the borderline parameters chosen here. These times can be approximated by the expression $T_n \approx n\pi[1 - \widetilde{m}_n\beta^2/2]/g$, where the $\widetilde{m}_n$ play the role of average phonon numbers. As β increases this quadratic behaviour ceases and distinct maxima of the population emerge separated by gaps approximately given by the mechanical period τ, being significantly longer than a Rabi period $\tau/2$ for the parameters chosen here. For even larger $\beta \lesssim 3$ the first revival stabilizes while subsequent revivals of the population show interference-like patterns and decline.

In order to provide deeper insight into this behaviour we show in Figs. 6.3 b) and c) the Wigner function of the mechanical oscillator for two different values of β and eight different instances of time as marked by the open circles in the density plot Fig. 6.3 a) [and in Fig. 6.2 b) for $\beta = 1$]. For both cases the mechanical oscillator starts in the vacuum state represented by the Gaussian Wigner function of minimal uncertainty. For $\beta = 1$ the phase space distribution begins to follow the trajectory belonging to the radiation pressure of a single photon inside the cavity until at $t \approx 2\tau/5$ the quasi probability distribution splits into two contributions and the non-classicality of this state manifests itself in the negative parts in between which are denoted by encircled areas. This behavior is caused by the coherent swapping between the states $|e,0\rangle$ and $|g,1\rangle$ of different radiation pressures corresponding to the two trajectories $n = 0$ and $n = 1$ in Fig. 5.1 a). At $t \approx 3\tau/5$ the two contribution are clearly distinguishable and merge again towards the end of the mechanical period at $t \approx \tau$ hence bringing atom and cavity back into resonance. One can observe, however, that the Wigner function is mostly localized around $t \approx 6\tau/5$, *i.e.* after more than one mechanical period. We conjecture that this delay stems from the Rabi oscillations taking place simultaneously with the oscillation of the mechanical element. After that, the quasi-periodic behavior starts into another round. For $\beta = 2$ the time evolution of the Wigner function is coined by the appearance of strong interferences in phase space for almost all instances of time as shown in Fig. 6.3 c). Only at $t = 0$ and the first revival at $t \approx 1.3\tau$ it is positive, already at the next revival at $t \approx 2.6\tau$ negativities and a delocalized Wigner function can be observed. This spread in phase space and the interferences explain incomplete population of the excited state and the fading of
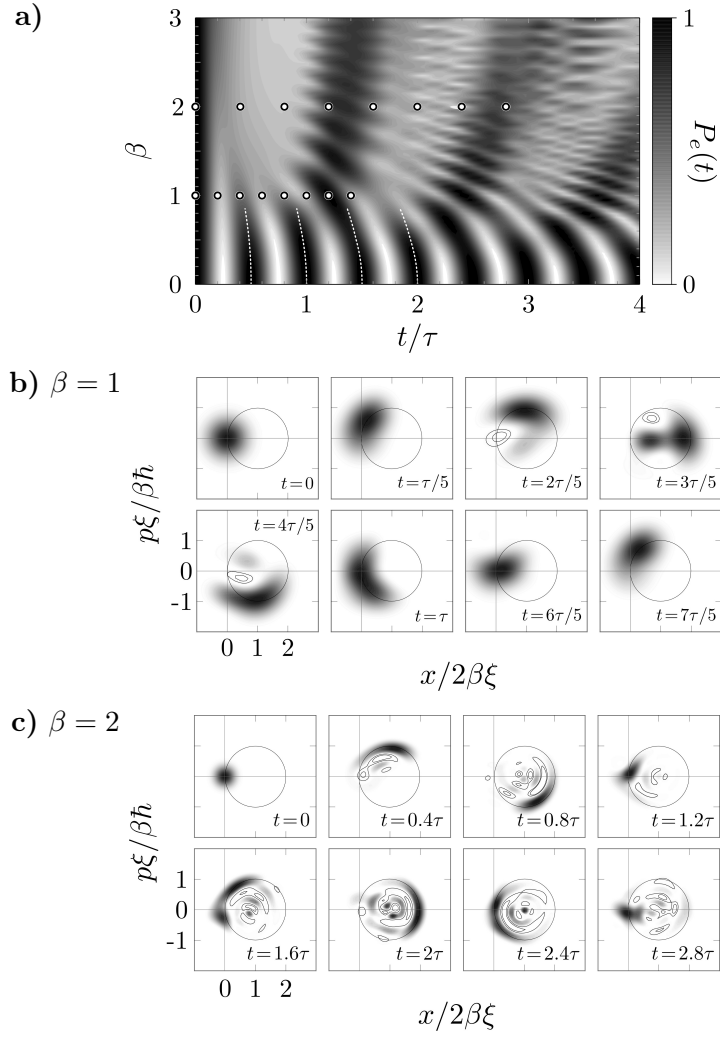
Figure 6.3: a) *Dependence of the Rabi oscillations on the optomechanical coupling ratio β for $g = \nu$. The dotted lines show the dependence of the times at which the population exhibits maxima in dependence of β calculated using a perturbative treatment of the optomechanical coupling.* **b)** *Wigner function of the mechanical oscillator for the eight instances denoted by the circles in* **a)** *along the line $\beta = 1$.* **c)** *Wigner function of the mechanical oscillator for the eight instances denoted by the circles in* **a)** *along the line $\beta = 2$. Encircled areas denote regions where the Wigner function takes on negative values.*

the later revivals: no sharp mirror position and thereby no defined resonance between atom and cavity can be found for later times. We also checked if the suppression effect persists for higher photon numbers and found indeed very similar characteristics.

The case $g = \nu/2$

We briefly consider the case $g = \nu/2$, whose limit for small β was analyzed in Sec. 6.2.1. The numerical results in this case for $\beta = 1$ are presented in Fig. 6.4.The excited state population in subfigure a) alternatingly displays incomplete and almost full revivals separated by roughly $\Delta t = 1.75\tau$. In contrast to the previous case $g = \nu$, the Wigner functions of the mechanical oscillator shown in Fig. 6.4 b) exhibits much more pronounced negativities. This phase space structure of the mechanical oscillator can be interpreted as an extrapolation of the simple superposition of vacuum and Fock state $|1\rangle_{\text{mec}}$, Eq. (6.18), being present for $\beta \to 0$, towards $\beta = 1$.
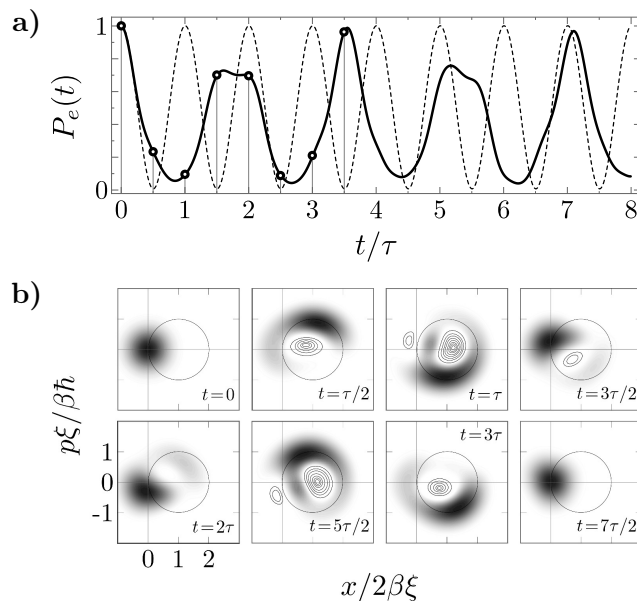

Figure 6.4: **a)** *Time evolution of the excited state population for the initial state $|e, 0\rangle |0\rangle_{\text{mec}}$ for $\beta = 1$ and $g = \nu/2$. The unperturbed Rabi oscillations ($\beta = 0$) are shown in the dashed line.* **b)** *Wigner function of the mechanical oscillator state at the eight instances denoted by open circles in* **a)**. *The encircled areas indicate regions where the Wigner functions takes on negative values, more circles correspond to more negative values.*

Before we go over to the dissipative dynamics we point out the connection of our model to the photon blockade in optomechanical systems. The photon blockade [Rab11] results from the interaction between the cavity field mode and the mechanical object due to the radiation pressure which lifts the degeneracy of the equidistant spectrum of the harmonic oscillators. Descriptively expressed, if a resonant photon is scattered into the cavity, a second photon is effectively detuned from resonance and therefore reflected with increased probability. When the entering photon stems from a second cavity which coherently couples to the optomechanical resonator in the form of a beam-splitter-like interaction, the analogy to the model presented here is established by replacing this second cavity with a two-level atom.

In this section we include spontaneous decay of the atom with rate Γ, cavity losses at rate κ and damping of the mechanical oscillator on a time scale $1/\gamma$ into account. In the regime considered in this work the dissipative dynamics can be described by the master equation $\partial_t \varrho = \mathcal{L}\varrho$ for the system density operator ϱ, with the Liouville operator

$$\mathcal{L}\varrho = \frac{1}{i\hbar}[H, \varrho] + \mathcal{L}_{\text{tls}}\varrho + \mathcal{L}_{\text{cav}}\varrho + \mathcal{L}_{\text{mec}}\varrho \qquad (6.20)$$

in Born-Markov approximation. The strong optomechanical coupling requires a treatment where the damping of the cavity and the mechanical oscillator cannot be treated independently [Pon04, Hu15]. The non-unitary parts of the dynamics are given by

$$\mathcal{L}_{\text{tls}}\varrho = \frac{\Gamma}{2}\mathcal{D}[|g\rangle\langle e|]\varrho\,, \qquad (6.21)$$

$$\mathcal{L}_{\text{cav}}\varrho = \frac{\kappa}{2}\mathcal{D}[a]\varrho + 4\gamma\frac{k_{\text{B}}T}{\hbar\nu}\mathcal{D}[\beta a^\dagger a]\varrho\,, \qquad (6.22)$$

$$\mathcal{L}_{\text{mec}}\varrho = \frac{\gamma}{2}\bar{m}\mathcal{D}[b^\dagger - \beta a^\dagger a]\varrho + \frac{\gamma}{2}\big(\bar{m}+1\big)\mathcal{D}[b - \beta a^\dagger a]\varrho\,, \qquad (6.23)$$

where we again use the notation $\mathcal{D}[X]\varrho = 2X\varrho X^\dagger - X^\dagger X\varrho - \varrho X^\dagger X$ to describe Lindblad terms and denote the mean thermal phononic occupation at temperature T by $\bar{m} = (\exp[\hbar\nu/k_{\text{B}}T] - 1)^{-1}$. As initial state we chose the same state as before, viz. $\varrho(t = 0) = |\psi(t = 0)\rangle\langle\psi(t = 0)|$, and calculated its time evolution by numerical diagonalization of the Liouville operator $\mathcal{L}$ in Eq. (6.20) on a truncated Hilbert space.

When the dissipative dynamics is dominated by the mechanical damping, i.e. $\gamma \gg \kappa, \Gamma$, the mechanical oscillator approaches its thermal state and thereby averages out the Rabi oscillations of the atom-cavity subsystem towards a constant value of the atomic population as shown in Fig. 6.5 a) for $\gamma = 0.1\nu$ (solid) and $\gamma = 0.4\nu$ (dashed). Nevertheless, the suppressed Rabi oscillation are observable even for such mechanical decay rates which are much larger than in typical existing or planned optomechanical setups with Q-factors in the order of $10^3 - 10^6$ [Coh15, Wil15, Kip14].

For high-Q mechanical oscillators the relevant time scale for damping is given by the atomic and cavity decay. Such a situation is depicted in Fig. 6.5 b) for $\kappa = \Gamma = 0.1\nu$ and $\beta = 2$ (solid) where we also show the undamped case (dashed) for comparison. For such high values of β where the Wigner function exhibits pronounced negativities one might suppose that the virtually undamped mechanical oscillator is capable to support a non-classical quasi-stationary state. However, the snapshots in Fig. 6.5 c) reveal that the time evolution disembogues into a non-trivial quasi-stationary Wigner function where all negativities are averaged out due to the randomness of the spontaneous emission and cavity losses. We remark that in an experiment where the emitted photon is recorded the negativity of the Wigner function persist for such a single quantum trajectory [Ple98].
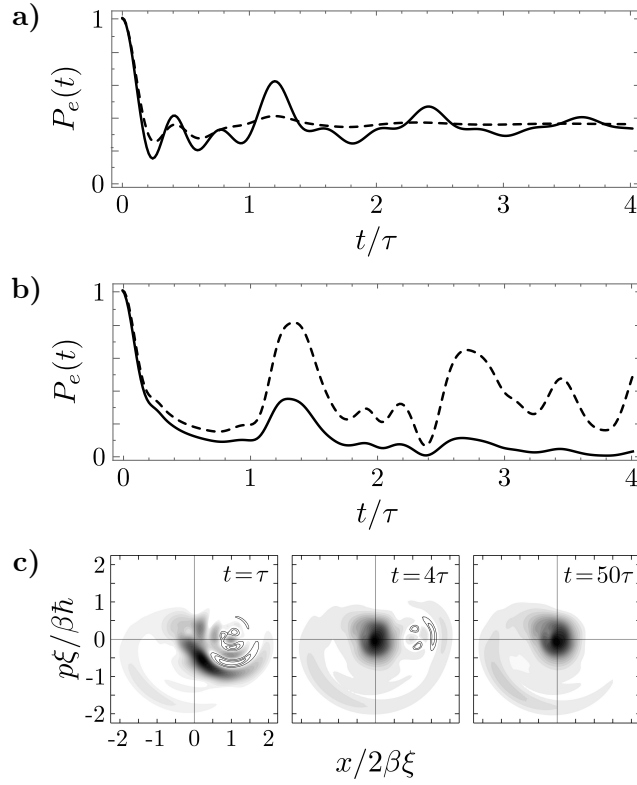
Figure 6.5: *Time evolution of the excited state population under dissipative dynamics for $g = \nu$.* **a)** *The bad oscillator case ($\Gamma = \kappa = 0$) for $\beta = 1$. The mean phononic occupation is $\bar{m} = 0.25$ and the mechanical decay rates are $\gamma = 0.1\nu$ (solid) and $\gamma = 0.4\nu$ (dashed).* **b)** *The good oscillator case ($\gamma = 0$) with the atomic and cavity decay rates $\Gamma = \kappa = 0.1\nu$ (solid) and the undamped case (dashed) for $\beta = 2$.* **c)** *Wigner function of the mechanical oscillator for the good resonator case of **b)** at times $t = \tau$, $t = 4\tau$ and $t = 50\tau$. Encircled areas denote negativities of the Wigner function.*

We eventually analyze the dependence of the modification of the Rabi oscillations on the initial state. Current technology provides techniques which allow for the preparation of atomic and cavity states to a high degree of fidelity. The initial state of the mechanical oscillator is prepared by laser cooling and the most relevant initial states to be considered are hence displaced thermal states of the form

$$\mu_{\alpha,\bar{m}} = D(\alpha) \left[\frac{1}{\bar{m}+1} \left(\frac{\bar{m}}{\bar{m}+1} \right)^{b^\dagger b} \right] D^\dagger(\alpha), \tag{6.24}$$

such that $\varrho(t = 0) = |e, 0\rangle\langle e, 0|\mu_{\alpha,\bar{m}}$. The initial mechanical displacement is characterized by the complex value α and the extension in phase space is proportional to the mean thermal occupation $\bar{m}$. The variance of the mechanical number operator in
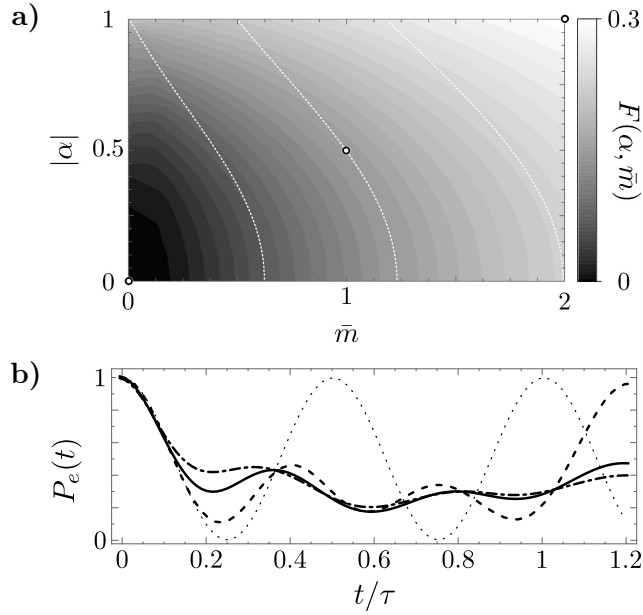
Figure 6.6:   **a)** *Density plot of the measure $F(\alpha, \bar{m})$ for the suppression of the Rabi oscillation in dependence of $|\alpha|$ and $\bar{m}$ of the initial state (for each modulus $|\alpha|$ an average over eight equidistant polar angles was performed). The dashed lines indicate the constant values of the phonon number variance $\Delta m^2 = 1, 2.75, 6$.* **b)** *Shows two exemplary evolutions of the excited state population for the initial states denoted by open circles in* **a)** *with $|\alpha| = 0.5$, $\bar{m} = 1$ (solid line) and $|\alpha| = 1$, $\bar{m} = 2$ (dashed-dotted line) corresponding to the values $F = 0.15$ and $F = 0.25$, respectively. As references the case of the usual initial state, viz. $\alpha = 0$, $\bar{m} = 0$, for $\kappa = \Gamma = 0$ is shown in the dashed line and the unperturbed Rabi oscillations in the dotted line. The parameters are $g = \nu$, $\beta = 1$, $\gamma = 0$ and $\kappa = \Gamma = 0.05\nu$.*

these states has the value $\Delta m^2 = \bar{m}(\bar{m}+1) + (2\bar{m}+1)|\alpha|^2$. We restrict ourself to the familiar case of $g = \nu$ and $\beta = 1$. In order to compare the behavior of the modified Rabi oscillations with the ideal case, *i.e.* an initial mechanical vacuum, we adopt the measure

$$F(\alpha, \bar{m}) = \int_0^{6\tau/5} \mathrm{d}t \, [P_e^{(0,0)}(t) - P_e^{(\alpha,\bar{m})}(t)]^2 \,, \tag{6.25}$$

representing the mean quadratic deviation of the atomic population $P_e^{(\alpha,\bar{m})}(t)$, belonging to $\mu_{\alpha,\bar{m}}$, from the ideal case $P_e^{(0,0)}(t)$, integrated over a time window where the suppression takes place. In Fig 6.6 a) we show a density plot of $F(\alpha, \bar{m})$ for $|\alpha| \leq 1$ and $\bar{m} \leq 2$ in the good resonator case with $\kappa = \Gamma = 0.05\nu$ and coupling strengths $g = \nu$ and $\beta = 1$. For the complex parameter α we preformed an average over eight equidistant polar angles for each modulus $|\alpha|$. From the density plot a quite stable behavior of the suppressed Rabi oscillations can be read off, which only marginally diminishes for temperatures corresponding to $\bar{m} \lesssim 0.25$ and displacements up to $|\alpha| = 0.5$, but even higher temperatures and displacements are tolerable.

To clarify the expressiveness of the deployed measure we additionally depict the time-evolution of the atomic population in Fig 6.6 b) for the different initial states indicated by open circles in Fig. 6.6 a), *i.e.* $|\alpha| = 0.5$, $\bar{m} = 1$ and $\alpha = 1$, $\bar{m} = 2$ which correspond to $F = 0.15$ (solid line) and $F = 0.25$ (dashed-dotted line), respectively. Strongly displaced thermal states hence do not exhibit an appreciable maximum in the region around $t = 6\tau/5$, as found in the ideal case (dashed line *and* Fig. 6.2). The higher the displacement and mean thermal occupation the flatter the curves for the time evolution of the excited state population become, thereby drastically diminishing the visibility of the suppression effect. Nevertheless, within a quite large region in the parameter space of the initial states, the effect remains clearly distinguishable.

We identified a distinctive feature in the highly non-linear regime of a hybrid optomechanical system which manifests itself in the suppression of Rabi oscillations of the atom-cavity subsystem and dynamically produces non-classical Wigner functions in the mechanical degree of freedom. The presented phenomenon is linked to blockade effects of non-linear systems, particularly to the photon blockade of optomechanics. We analyzed the dynamics of this suppression and gave a qualitative and intuitive explanation using the time evolution of the mechanical Wigner function. We also pointed out that even under the influence of dissipation the main features of the effect are still observable.

For the case of a resonant atom-cavity interaction, the effect is clearly observable when $\beta \gtrsim 1$ and $g \approx \nu$. Since it is based on the coherent time evolution, strong coupling is required, meaning $\kappa, \Gamma \ll g$ and $\gamma \ll \nu$. The latter requirement is already achieved in the majority of optomechanical experiments with high-Q mechanical elements. Ground state cooling is required such that the initial state fulfills $\bar{m} \lesssim 1$. We exemplify these requirement based on current experiments, such as the experiment of Ref. [Cha11], with a mechanical frequency $\nu = 2\pi \cdot 4\,\mathrm{GHz}$, mechanical (optical) Q-factor of $Q = 10^5$ ($Q = 10^6$) and $\bar{m} \approx 1$, only lacking the necessary strong optomechanical coupling which should, along with the cavity-dipole coupling, also be in the GHz range. In upcoming hybrid-systems with diamond-based crystal cavities [RM12, Kip14], a resonant interaction with color centers with linewidths in the MHz range could be tailored, basically fulfilling the requirements for the observation of the suppression effect presented here.

With this work we provided deeper insight into the rather unexplored area of the non-linear dynamics of hybrid optomechanical systems being potentially pivotal for future quantum technological applications interfacing different quantum degrees of freedom.

The optomechanical damping basis

In Sec. 1.3 we introduced the spectral decomposition of the Liouville operator that generates the non-unitary dynamics of a system and in Chapter 4 we employed this method to solve the master equation we presented for the description of solid-state emitters. In the present chapter we extend this technique to the master equation describing optomechanical systems that were introduced in Chapter 5. Besides the unitary part that comes from the optomechanical Hamiltonian (5.2) the master equation comprises the coupling of the optical cavity to the free electromagnetic field and the damping of the mechanical oscillator. Similar to the damping basis for the solid-state emitter the solution in this chapter again greatly relies on the solution of the damped harmonic oscillator that we reviewed in Chapter 2.

The chapter has the following structure: In Sec. 7.1 we introduce the optomechanical Liouville operator and split it into *two* superoperators. In Sec. 7.2 we present the solution of the eigenvalue problem of the *first* superoperator and obtain, by letting the *second* one act on these solutions, the eigenbasis of the full Liouville operator in Sec. 7.3. In Sec. 7.4, as an example, we finally apply the damping basis to determine the time evolution for a certain type of initial states.

A manuscript summarizing the results presented in this chapter is currently in preparation:

- JUAN MAURICIO TORRES, RALF BETZHOLZ, AND MARC BIENERT,
  "The optomechanical damping basis".

In addition to the unitary dynamics generated by the Hamiltonian (5.2) we incorporate cavity losses at rate κ and mechanical damping [Cle03, WR08a] by a finite temperature reservoir at rate γ. We treat these two decay processes independently, a fact that has to be examined critically in the case of strong optomechanical coupling [Hu15], leading to the master equation $\partial_t \varrho = \mathcal{L}\varrho$ for the system's density operator ϱ with the Liouville operator

$$\mathcal{L}\varrho = \frac{1}{i\hbar}[H_{\mathrm{om}}, \varrho] + \frac{\kappa}{2}\mathcal{D}[a]\varrho + \frac{\gamma}{2}(\bar{m}+1)\mathcal{D}[b]\varrho + \frac{\gamma}{2}\bar{m}\mathcal{D}[b^\dagger]\varrho. \qquad (7.1)$$

Here, $\bar{m} = (\exp[\hbar\nu/k_{\mathrm{B}}T] - 1)^{-1}$ again denotes the thermal occupation of the mechanical oscillator at the reservoir temperature T. As before, our aim is to solve the eigenvalue equations for the left and right eigenelements, *viz.*

$$\mathcal{L}\hat{\varrho}_\Lambda = \Lambda\hat{\varrho}_\Lambda \,, \tag{7.2}$$

$$\check{\varrho}_\Lambda^\dagger \mathcal{L} = \Lambda\check{\varrho}_\Lambda^\dagger \,. \tag{7.3}$$

For what follows it proves convenient to split the Liouville operator into two parts according to

$$\mathcal{L} = \mathcal{M} + \mathcal{J} \,, \tag{7.4}$$

where the photonic *jump operator* $\mathcal{J}$ has the form

$$\mathcal{J}\varrho = \kappa a\varrho a^\dagger \tag{7.5}$$

and carries its name because it describes jumps from the cavity Fock states $|n\rangle$ to $|n-1\rangle$. The remaining superoperator can be regrouped in the form

$$\mathcal{M}\varrho = -i\omega[a^\dagger a, \varrho] - \frac{\kappa}{2}a^\dagger a\varrho - \frac{\kappa}{2}\varrho a^\dagger a + \mathcal{L}_{\mathrm{mec}}\varrho + i\chi[a^\dagger a(b + b^\dagger), \varrho] \tag{7.6}$$

with the Liouville operator $\mathcal{L}_{\mathrm{mec}}$ from Eq. (2.7), describing the damping of the mechanical oscillator, whose eigenbasis was presented in Chapter 2. Since we are now dealing with two damped harmonic oscillators, the mechanical one and the optical one, we denote the eigenvalues of $\mathcal{L}_{\mathrm{mec}}$ by

$$\lambda_{m,k}^{(\mathrm{mec})} = -ik\nu - \left[m + \frac{|k|}{2}\right]\gamma \,. \tag{7.7}$$

In the next step we diagonalize the operator $\mathcal{M}$ and use the action of $\mathcal{J}$ on its eigenbasis to derive the form of the eigenbasis of the full Liouvillian.

In this section we present the solution of the eigenvalue equations of the operator $\mathcal{M}$. Denoting the eigenvalues, right and left eigenelements by Λ, $\hat{\rho}$, and $\check{\rho}^\dagger$, respectively. The eigenvalue equations read

$$\mathcal{M}\hat{\rho}_{m,k}^{(n,l)} = \Lambda_{m,k}^{(n,l)}\hat{\rho}_{m,k}^{(n,l)} \,, \tag{7.8}$$

$$\check{\rho}_{m,k}^{(n,l)\dagger}\mathcal{M} = \Lambda_{m,k}^{(n,l)}\check{\rho}_{m,k}^{(n,l)\dagger} \,, \tag{7.9}$$

where we have already anticipated the four indices $n, m = 0, 1, 2, \dots$ and $l, k = 0, \pm 1, \pm 2, \dots$ of the eigenelements and eigenvalues. The only cavity operator involved in $\mathcal{M}$ is the photonic number operator $a^\dagger a$. This means that it does not couple different diagonals of the cavity density operator in the Fock-state basis and suggests the

ansatz

$$\hat{\rho}_{m,k}^{(n,l)} = \big|n + (|l| + l)/2\big\rangle\big\langle n + (|l| - l)/2\big|\hat{\xi}_{m,k}^{(n,l)}\,, \tag{7.10}$$

$$\check{\rho}_{m,k}^{(n,l)\dagger} = \big|n + (|l| - l)/2\big\rangle\big\langle n + (|l| + l)/2\big|\check{\xi}_{m,k}^{(n,l)\dagger}\,. \tag{7.11}$$

In the next step we derive the explicit shape of the mechanical oscillator operators $\xi_{m,k}^{(n,l)}$.

First, we focus on the case $l \geq 0$ in Eq. (7.10) letting $\mathcal{M}$ act on the ansatz we chose for the right eigenelements results in

$$\mathcal{M}\hat{\varrho}_{n,l} = \mathcal{M}|n + l\rangle\langle n|\hat{\xi}_{m,k}^{(n,l)} = |n + l\rangle\langle n|\mathcal{M}_{n,l}\hat{\xi}_{m,k}^{(n,l)} \tag{7.12}$$

with the newly defined superoperators $\mathcal{M}_{n,l}$ which act on the operators on the mechanical Hilbert space associated with the photonic (n, l)-space. Their action is given by

$$\mathcal{M}_{n,l}\hat{\xi}_{m,k}^{(n,l)} = \lambda_{n,l}^{(\mathrm{cav})}\hat{\xi}_{m,k}^{(n,l)} + \mathcal{L}_{\mathrm{mec}}\hat{\xi}_{m,k}^{(n,l)} + in\chi[b + b^\dagger, \hat{\xi}_{m,k}^{(n,l)}] + il\chi(b + b^\dagger)\hat{\xi}_{m,k}^{(n,l)}\,. \tag{7.13}$$

We note that the action of $\mathcal{M}$ already produces the term $\lambda_{n,l}^{(\mathrm{cav})} = -il\omega - \kappa[n + |l|/2]$, the eigenvalue of the damped cavity oscillator, although we have not included the jump term. This hints at the fact that the full Liouville operator $\mathcal{L}$ has the same spectrum as $\mathcal{M}$, which is familiar from the damped harmonic oscillator master equation (2.7), where the Liouville operator for $\bar{m} = 0$ with and without the jump term has the same spectrum. Except for the last term in Eq. (7.13) the operator $\mathcal{M}_{n,l}$ is the master equation for a driven and damped harmonic oscillator, where the driving term can be removed straightforwardly by a suitable displacement. The last term in Eq. (7.13) is more intricate but can nevertheless be handled with the *asymmetric displacement*

$$\hat{\tilde{\xi}}_{m,k}^{(n,l)} = e^{\eta_l b}D(\alpha_{n,l})\hat{\xi}_{m,k}^{(n,l)}D^\dagger(\beta_{n,l})e^{-\eta_l b}\,, \tag{7.14}$$

in the same fashion as the transform Eq. (4.28). Our aim is to choose $\alpha_{n,l}$, $\beta_{n,l}$, and η_l in such a manner that in the asymmetrically displaced picture the action of the operator $\mathcal{M}_{n,l}$ is of the form

$$\tilde{\mathcal{M}}_{n,l}\hat{\tilde{\xi}}_{m,k}^{(n,l)} = \Big[\lambda_{n,l}^{(\mathrm{cav})} + \mathcal{L}_{\mathrm{mec}}\hat{\tilde{\xi}}_{m,k}^{(n,l)} + \varepsilon_{n,l}\Big]\hat{\tilde{\xi}}_{m,k}^{(n,l)} \tag{7.15}$$

because this is nothing but the damped harmonic oscillator case with additional constant terms. The correct choice (details of the calculation can be found in App. C.1)

is given by

$$\alpha_{n,l} = - n\beta - l\frac{|\beta|^2}{\chi}\left[\nu + i\frac{\gamma}{2}(2\bar{m} + 1)\right],\tag{7.16}$$

$$\beta_{n,l} = \alpha_{n,l} + l\beta^*,\tag{7.17}$$

$$\eta_l = il\frac{|\beta|^2}{\chi}\gamma(2\bar{m} + 1)\tag{7.18}$$

with the same definition of the dimensionless, complex coupling strength

$$\beta = \frac{\chi}{\nu - i\gamma/2}\tag{7.19}$$

that we used in the description of solid-state emitters in the previous part, Eq. (4.23). In terms of this quantity the additional eigenvalue shift in Eq. (7.15) can be expressed as

$$\varepsilon_{n,l} = l|\beta|^2\left[i\nu(2n + |l|) - \frac{\gamma}{2}(2\bar{m} + 1)l\right]\tag{7.20}$$

and the eigenvalue equation Eq. (7.15) is readily solved by the harmonic oscillator eigenelements (2.53), *i.e.* $\hat{\breve{\xi}}_{m,k}^{(n,l)} = \hat{\mu}_{m,k}$. The last step is to revert the asymmetrical displacement of Eq. (7.14) to obtain the eigenelements of $\mathcal{M}_{n,l}$ which read

$$\hat{\rho}_{m,k}^{(n,l)} = |n + l\rangle\langle n|D^\dagger(\alpha_{n,l})e^{-\eta_l b}\hat{\mu}_{m,k}e^{\eta_l b}D(\beta_{n,l})\tag{7.21}$$

with the corresponding eigenvalues

$$\Lambda_{m,k}^{(n,l)} = \lambda_{n,l}^{(\mathrm{cav})} + \lambda_{m,k}^{(\mathrm{mec})} + \varepsilon_{n,l}.\tag{7.22}$$

We found that the eigenvalues of $\mathcal{M}$ consist of the damped harmonic oscillator eigenvalues for the mechanical and the optical oscillator and an extra term that is due to the interaction between the two degrees of freedom. The left eigenelements $\check{\rho}_{n,l}^{\dagger m,k}$ are obtained by a treatment that goes along the same lines resulting in

$$\check{\rho}_{m,k}^{(n,l)\dagger} = |n\rangle\langle n + l|\check{\xi}_{m,k}^{(n,l)\dagger} = |n\rangle\langle n + l|D^\dagger(\beta_{n,l})e^{-\eta_l b}\check{\mu}_{m,k}^\dagger e^{\eta_l b}D(\alpha_{n,l})\tag{7.23}$$

with the same parameters $\alpha_{n,l}$, $\beta_{n,l}$, and η_l as for their right counterparts. Alternatively, one can use the orthogonality relation (1.41) between the left and right eigenelements to arrive at the same result.

For $l < 0$ one could use the same procedure as before with an appropriate ansatz, *viz.* Eq. (7.8) for $l < 0$. Fortunately, this is not necessary since we can use the property $[\mathcal{M}\rho]^\dagger = \mathcal{M}\rho^\dagger$ and the fact that the Hermitian conjugate of an eigenelement is again

an eigenelement to the complex conjugate eigenvalue, which in our case reads

$$\Lambda_{m,k}^{(n,l)*} = \lambda_{m,-k}^{(\text{mec})} + \lambda_{n,-l}^{(\text{cav})} + \varepsilon_{n,-l} = \Lambda_{m,-k}^{(n,-l)} \,. \tag{7.24}$$

Using these two properties we can establish that for $l < 0$ the eigenvalue equation

$$\mathcal{M} \left[\hat{\rho}_{m,-k}^{(n,-l)} \right]^{\dagger} = \Lambda_{m,k}^{(n,l)} \left[\hat{\rho}_{m,-k}^{(n,-l)} \right]^{\dagger} \tag{7.25}$$

is fulfilled for the eigenelements (7.21). Combined with the property $\hat{\mu}_{m,k}^{\dagger} = \hat{\mu}_{m,-k}$ of the harmonic oscillator eigenelements, which is easily verified in Eq. (2.53), this finally leads to

$$\hat{\rho}_{m,k}^{(n,l)} = \begin{cases} |n+l\rangle\langle n|\hat{\xi}_{m,k}^{(n,l)}, & \text{for } l \geq 0 \\ |n\rangle\langle n+|l||\hat{\xi}_{m,k}^{(n,l)}, & \text{for } l < 0 \end{cases} \tag{7.26}$$

$$= \begin{cases} |n+l\rangle\langle n|D^{\dagger}(\alpha_{n,l})e^{-\eta_l b}\hat{\mu}_{m,k}e^{\eta_l b}D(\beta_{n,l}), & \text{for } l \geq 0 \\ |n\rangle\langle n+|l||D^{\dagger}(\beta_{n,|l|})e^{\eta_{|l|} b^{\dagger}}\hat{\mu}_{m,k}e^{-\eta_{|l|} b^{\dagger}}D(\alpha_{n,|l|}), & \text{for } l < 0 \,. \end{cases} \tag{7.27}$$

Again the left eigenelements are found using the orthogonality relation, resulting in

$$\check{\rho}_{m,k}^{(n,l)\dagger} = \begin{cases} |n\rangle\langle n+l|\check{\xi}_{m,k}^{(n,l)\dagger}, & \text{for } l \geq 0 \\ |n+|l|\rangle\langle n|\check{\xi}_{m,k}^{(n,l)\dagger}, & \text{for } l < 0 \end{cases} \tag{7.28}$$

$$= \begin{cases} |n\rangle\langle n+l|D^{\dagger}(\beta_{n,l})e^{-\eta_l b}\check{\mu}_{m,k}^{\dagger}e^{\eta_l b}D(\alpha_{n,l}), & \text{for } l \geq 0 \\ |n+|l|\rangle\langle n|D^{\dagger}(\alpha_{n,|l|})e^{\eta_{|l|} b^{\dagger}}\check{\mu}_{m,k}^{\dagger}e^{-\eta_{|l|} b^{\dagger}}D(\beta_{n,|l|}), & \text{for } l < 0 \,. \end{cases} \tag{7.29}$$

We now include the jump operator $\mathcal{J}$ which makes the situation more complicated since the jumps induce a coupling between different photonic subspaces. As we briefly mentioned before we will show that the operators $\mathcal{L}$ and $\mathcal{M}$ have the same spectrum, meaning that $\mathcal{L}$ is already triangular in the eigenbasis of $\mathcal{M}$. This means that in this basis we have to find the correct linear combinations of eigenelements such that $\mathcal{L}$ is diagonal.

Taking into account that the jumps induced by $\mathcal{J}$ are always downwards on the same diagonal in the Fock-state basis we make the ansatz

$$\mathcal{L}\hat{\varrho}_{m,k}^{(n,l)} = \Lambda_{m,k}^{(n,l)} \hat{\varrho}_{m,k}^{(n,l)} \tag{7.30}$$

with the eigenvalues (7.24) and the eigenelements

$$\hat{\varrho}_{m,k}^{(n,l)} = \sum_{r=0}^{n} |r+l\rangle\langle r|\hat{\zeta}_{m,k}^{(n,r,l)} , \tag{7.31}$$

where the operators $\hat{\zeta}_{m,k}^{(n,r,l)}$ have yet to be determined. We first focus on $l \geq 0$ and note that the transfer to the case $l < 0$ is straightforward. Letting $\mathcal{L} = \mathcal{M} + \mathcal{J}$ act on this ansatz transforms the eigenvalue problem (7.30) into

$$\sum_{r=0}^{n} \left[|r+l\rangle\langle r|\left(\mathcal{M}_{r,l} - \Lambda_{m,k}^{(n,l)}\right)\hat{\zeta}_{m,k}^{(n,r,l)} + \kappa\sqrt{r(r+l)}|r+l-1\rangle\langle r-1|\hat{\zeta}_{m,k}^{(n,r,l)} \right] = 0 . \tag{7.32}$$

This equality has to be fulfilled for each value of r separately, $i.e.$ in each subspace associated with the cavity operator $|r+l\rangle\langle r|$. For $r = n$ this simply gives the condition

$$\mathcal{M}_{n,l}\hat{\zeta}_{m,k}^{(n,n,l)} = \Lambda_{m,k}^{(n,l)}\hat{\zeta}_{m,k}^{(n,n,l)} , \tag{7.33}$$

which is the eigenvalue equation of the operator $\mathcal{M}_{n,l}$ that was solved in the previous section. Therefore, we can establish that

$$\hat{\zeta}_{m,k}^{(n,n,l)} = \hat{\xi}_{m,k}^{(n,l)} , \tag{7.34}$$

with the operators $\hat{\xi}_{m,k}^{(n,l)}$ defined in Eq. (7.26). Going one step downwards then leads to an equation in the space associated with $|n+l-1\rangle\langle n-1|$. This can be generalized to

$$\hat{\zeta}_{m,k}^{(n,n-j,l)} = \frac{\kappa\sqrt{(n-j+1)(n+l-j+1)}}{\Lambda_{m,k}^{(n,l)} - \mathcal{M}_{n-j,l}}\hat{\zeta}_{m,k}^{(n,n-j+1,l)} . \tag{7.35}$$

This first order recurrence relation with the initial condition (7.34) has the solution

$$\hat{\zeta}_{m,k}^{(n,q,l)} = \kappa^{n-q}\sqrt{\frac{n!}{q!}\frac{(n+|l|)!}{(q+|l|)!}}\left[\prod_{j=q}^{n-1} \frac{1}{\Lambda_{m,k}^{(n,l)} - \mathcal{M}_{j,l}}\right]\hat{\xi}_{m,k}^{(n,l)} \tag{7.36}$$

for $q = 0, 1, ..., n-1$, with the convention $\prod_{j=1}^{N} \mathcal{X}_j = \mathcal{X}_1\mathcal{X}_2\cdots\mathcal{X}_N$ for products of superoperators.

The action to the left of the jump operator on an arbitrary operator X is given by

$$X\mathcal{J} = \kappa a^\dagger X a \tag{7.37}$$

and is generally meaningful only in a trace. This means that it induces a jump upwards in the photon number. Since the Hilbert space is infinite dimensional we make the ansatz

$$\check{\varrho}_{m,k}^{(n,l)\dagger}\mathcal{L} = \Lambda_{m,k}^{(n,l)}\,\check{\varrho}_{m,k}^{(n,l)\dagger} \tag{7.38}$$

with

$$\check{\varrho}_{m,k}^{(n,l)\dagger} = \sum_{r=n}^{\infty}|r\rangle\langle r+l|\check{\zeta}_{m,k}^{(n,r,l)\dagger}\,. \tag{7.39}$$

In the same way as for the right eigenelements we let $\mathcal{L}$ act to the left on this ansatz, thereby giving the eigenvalue equation

$$\sum_{r=n}^{\infty}\Big[|r\rangle\langle r+l|\check{\zeta}_{m,k}^{(n,r,l)\dagger}\Big(\mathcal{M}_{r,l}-\Lambda_{m,k}^{(n,l)}\Big)$$
$$+\kappa\sqrt{(r+1)(r+l+1)}|r+1\rangle\langle r+l+1|\hat{\zeta}_{m,k}^{(n,r,l)\dagger}\Big] = 0 \tag{7.40}$$

which has to be satisfied in each photonic subspace. Again this leads to a first order recurrence relation whose solution, with the appropriate initial condition

$$\check{\zeta}_{m,k}^{(n,n,l)\dagger} = \check{\xi}_{m,k}^{(n,n,l)\dagger}\,, \tag{7.41}$$

is given by

$$\check{\zeta}_{m,k}^{(n,q,l)\dagger} = \kappa^{q-n}\sqrt{\frac{q!}{n!}\frac{(q+|l|)!}{(n+|l|)!}}\check{\xi}_{m,k}^{(n,l)\dagger}\left[\prod_{j=1}^{q-n}\frac{1}{\Lambda_{m,k}^{(n,l)}-\mathcal{M}_{n+j,l}}\right] \tag{7.42}$$

with $q = n+1, n+2, ...$ and the same convention for products as above.

With the results (7.36) and (7.42), substituted back into ansatz (7.31) and (7.39), respectively, we have derived the formal expression for the eigenbasis of the optomechanical Liouville operator and the corresponding eigenvalues are given by (7.22). The expressions for the eigenelements are formal in the sense that they still contain superoperators. In App. C.2 we show how Eqs. (7.36) and (7.42) can be rewritten in a more explicit form without superoperators.

In order to gain some insight into the non-unitary dynamics of an optomechanical system we can investigate the time evolution of a certain class of initial states. Let us consider the system to be initially in a state of the form

$$\varrho(0) = \sum_{n=0}^{N}|n\rangle\langle n|\mu_n(0) \tag{7.43}$$

with some mechanical oscillator density operators μ_n. This state is diagonal in the cavity photon number states and therefore remains of a diagonal shape throughout the dynamics. The master equation $\partial_t \varrho = [\mathcal{M} + \mathcal{J}]\varrho$ then explicitly reads

$$\frac{\partial}{\partial t}\varrho(t) = \sum_{n=0}^{N}|n\rangle\langle n|\mathcal{M}_n\mu_n(t) + \kappa\sum_{n=1}^{N}n|n-1\rangle\langle n-1|\mu_n(t)\,, \tag{7.44}$$

where we wrote $\mathcal{M}_{n,0} := \mathcal{M}_n$ for convenience. In each photonic subspace this results in the reduced mechanical dynamics

$$\frac{\partial}{\partial t}\mu_n(t) = \mathcal{M}_n\mu_n(t) + \kappa(n+1)(1-\delta_{n,N})\mu_{n+1}(t) \tag{7.45}$$

which is a system of coupled differential equations whose first equation, *i.e.* for $n = N$, is decoupled and can be solved according to

$$\mu_N(t) = e^{\mathcal{M}_N t}\mu_N(0)\,. \tag{7.46}$$

The subsequent equation is then given by

$$\frac{\partial}{\partial t}\mu_{N-1}(t) = \mathcal{M}_{N-1}\mu_{N-1}(t) + \kappa N e^{\mathcal{M}_N t}\mu_N(0)\,. \tag{7.47}$$

Here, for simplicity we assume initial conditions in which the system density operator is a product of a single cavity Fock state $|N\rangle\langle N|$ and a thermal state $\mu_{\mathrm{th}} = \hat{\mu}_{0,0}$ of the mechanical oscillator, *viz.*

$$\mu_n(0) = \delta_{n,N}\mu_{\mathrm{th}}\,. \tag{7.48}$$

The linearity of the Liouville operator directly implies that the results obtained with this initial state can be generalized to any state that is a product of the mechanical thermal state and a cavity state that is diagonal in the number state basis, *i.e.* states of the form $\varrho(0) = \sum_k c_k|k\rangle\langle k|\mu_{\mathrm{th}}$, with $\sum_k c_k = 1$. The solution of Eq. (7.47) with the initial condition (7.48) is then

$$\mu_{N-1}(t) = \kappa N\int_0^t \mathrm{d}\tau\, e^{\mathcal{M}_{N-1}(t-\tau)}e^{\mathcal{M}_N \tau}\mu_{\mathrm{th}}\,. \tag{7.49}$$

Iteratively applying this procedure to the coupled system of differential equations (7.44) results in the solution

$$\mu_n(t) = \kappa^{N-n}(N-n)!\binom{N}{n}e^{\mathcal{M}_n t}\left[\prod_{j=1}^{N-n}\int_0^{\tau_{j-1}}\mathrm{d}\tau_j\, e^{-\mathcal{M}_{n+j-1}\tau_j}e^{\mathcal{M}_{n+j}\tau_j}\right]\mu_{\mathrm{th}} \tag{7.50}$$

with the definition $\tau_0 = t$ and the same product convention as before. The successive application of the superoperator exponentials can be carried out using the diagonalization of the operators $\mathcal{M}_n$, given by Eqs. (7.27) and (7.29). In particular, we can
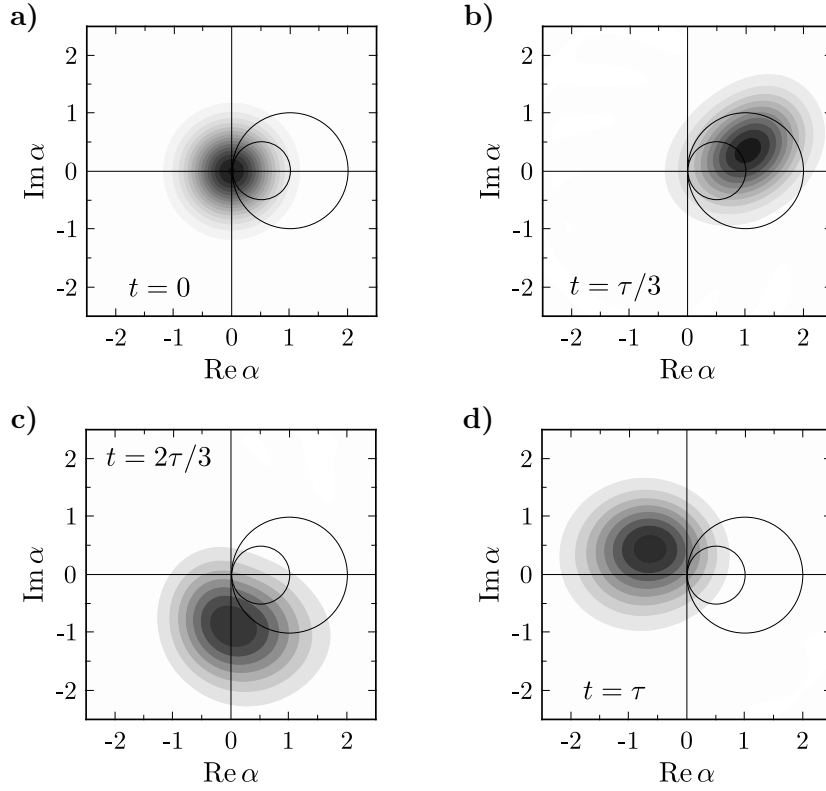
Figure 7.1: *Wigner function $W(\alpha, t)$ of the mechanical oscillator's reduced density operator $\mu(t)$ for the initial state $\varrho(0) = |2\rangle\langle 2|\mu_{\text{th}}$ at different times:* **a)** $t = 0$, **b)** $t = \tau/3$, **c)** $t = 2\tau/3$ *and* **d)** $t = \tau$, *with the mechanical period $\tau = 2\pi/\nu$. The parameters are $\chi = \nu/2$, $\gamma = \nu/50$ and $\kappa = \nu/2$ and the circles correspond to the one- and two-photon trajectories from* Fig. 5.1.

incorporate the exponential of eigenvalues into the overlap of displaced eigenelements and the thermal state in the same manner as in Eq. (4.73). Using the properties of displacement operators produces a time-dependent displacement of the mechanical steady-state density operator which can be cast into the form

$$\mu_n(t) = \kappa^{N-n}(N-n)! \binom{N}{n} e^{-n\kappa t} \prod_{j=1}^{N-n} \int_0^{\tau_{j-1}} \mathrm{d}\tau_j \, e^{-\kappa\tau_j} \times$$

$$D\left(n\beta + \sum_{k=1}^{N-n} \beta(t-\tau_k) - N\beta(t)\right) \mu_{\text{th}} D^\dagger\left(n\beta + \sum_{l=1}^{N-n} \beta(t-\tau_l) - N\beta(t)\right). \quad (7.51)$$

Due to the diagonal shape of the state in the cavity Fock basis the time evolution of the mechanical oscillator's reduced density operator $\mu(t) = \text{Tr}_{\text{cav}}\{\varrho(t)\}$, given by the trace over the cavity degrees of freedom, has the simple form $\mu(t) = \sum_n \mu_n(t)$. In Fig. 7.1 we illustrate the time evolution of the oscillator state for $N = 2$ using its Wigner function $W(\alpha, t)$ for different times, given in units of the mechanical oscillation

period $\tau = 2\pi/\nu$. Without damping the Wigner function would follow the circular trajectory from Fig. 5.1 for $n = 2$. However, cavity photons are lost with a rate κ, leading to a trajectory that lies between the $n = 1$ and $n = 2$ circles at first, as seen in Fig. 7.1 b). As time goes on, the probability that *both* cavity photons are lost increases which leads to an unmodified mechanical oscillator potential in which the Wigner function circles around the *origin*, see Fig. 7.1 c) and d).

We presented a treatment of the master equation describing the dynamics of an optomechanical system in terms of the spectral decomposition of the associated Liouville operator. In this treatment we showed the derivation of the full system of eigenelements relying on the solution of the eigenvalue problem of the damped harmonic oscillator. The formal shape of the eigenelements, Eqs. (7.31), (7.36), (7.39), and (7.42), still contain expressions involving superoperators, however, in App. C.2 we show how they can be made explicit, *i.e.* recast into a form without superoperators.

This explicit form can, among other applications, be practical for numeric calculations since they make the numeric diagonalization of the Liouville operator over a truncated Hilbert space unnecessary. Especially for higher temperatures the dimension of the truncated Hilbert space has to be chosen sufficiently large, and can thereby make the numeric treatment of the Liouville operator a challenging task. With our solution of the optomechanical master equation we thereby hope to provide a basic tool for the analytic investigation of the non-unitary dynamics of optomechanical systems.

PART IV

Non-harmonic trapping potentials

CHAPTER 8

Laser cooled atom in a non-harmonic potential

In 1953, Dicke investigated the effect of photon recoil on the spectrum of light scattered by atoms [Dic53]: When the atoms emit single photons, they experience a recoil and thereby change their motional state. The required energy for this acceleration is taken from the photons, which show a shifted frequency after the scattering event. In order to describe this effect most clearly, Dicke presented its calculation based on a simple confining potential, namely an infinite square well.

Trapping atoms in confining potentials has meanwhile become state of the art in experiments and exploiting the momentum recoil due to the spontaneous emission of single photons is routinely applied in laser cooling in today's laboratories[CT98, Phi98, Chu98, Met01]. Laser cooling is achieved when the laser parameters are chosen such that photon scattering processes that diminish the atomic motional energy prevail over transitions that heat the motion [Win79, Dal85]. For trapped ions or ground-state cooled atoms, it is justified to approximate the trapping potential harmonically. In the Lamb-Dicke limit [Jav81] the atomic wavepacket is spatially confined on a scale much smaller than the laser wavelength. Laser cooling theory then predicts that light scattering drives the atomic motion towards a thermal state [Lin84a]. In the spectrum of resonance fluorescence [Raa00] two distinct peaks emerge, the motional sidebands, as the Stokes- and anti-Stokes components of the scattered light.

In this chapter we investigate the light scattering at an atom trapped in a non-harmonic potential in the Lamb-Dicke regime. By this analysis we extend the theoretical tools for the description of laser cooling [Lin84b, Cir92] and the corresponding spectrum of resonance fluorescence [Cir93, Lin86, Bie04] to the case of non-harmonic potentials. Compared to the previous works, the details of the theoretical treatment for arbitrarily shaped potentials are presented and compared to the well-known harmonic case. This extension becomes relevant, for example, for atoms cooled in optical lattices [Gat97, Ham98, Blo08], where the harmonic approximation can be insufficient, especially at higher temperatures. Similarly, in cavity cooling experiments [Hor97, Pin00, Mau04, Rit13] the trapping potential's anharmonicity can manifest itself in the cooling dynamics and the spectrum of scattered light.

The work presented here focuses on the expansion of the theoretical description, guided by Dicke's original work based on a particle in a box. The infinite square well, but also the Morse potential, are used to exemplify the application of the extended theory. Both potentials support an analytic solution of the eigenvalue problem given

by the time independent Schrödinger equation for the center-of-mass motion, allowing for a clear and comprehensive treatment of laser cooling and the analysis of the scattered light. The Morse potential describes the dynamics of the relative coordinate of diatomic molecules [Mor29b, Mor29a] and therefore is of essential interest for the cooling [Mor07, Ngu11] and spectroscopy [Roy13] of such systems.

The presented approach allows to identify details in the perturbative description in the Lamb-Dicke regime that are connected with the non-degeneracy of transition frequencies between the motional eigenstates. For both potentials the resulting steady state of the center-of-mass motion cannot be written in terms of a thermal distribution and the motional sidebands consist of a series of peaks of finite width whose spectral position is connected to the transition frequencies between the relevant vibrational states.

The chapter is organized as follows: In Sec. 8.1 we introduce the system and present in Sec. 8.2 the elements of the theory of light scattering that are necessary to describe the signatures of the atomic motion in the spectrum of resonance fluorescence. In order to discuss the results and to illustrate the deviations from harmonic trapping potentials, we present in Sec. 8.3 the laser cooling performance and the motional sidebands of the scattered light for the two previously mentioned potentials. Finally, in Sec. 8.4 we draw the conclusions.

A manuscript about the contents of this chapter has been submitted:

- RALF BETZHOLZ AND MARC BIENERT,
  "Resonance fluorescence of a laser-cooled atom in a non-harmonic potential",
  Preprint: `http://arxiv.org/abs/1605.05951`.

We investigate the radiation scattered by a single laser-cooled two-level atom. Along the x-direction the atom's center of mass is tightly trapped in a non-harmonic potential $V(x)$ and we restrict ourselves to the one-dimensional problem. The relevant electronic states are the ground state $|g\rangle$ and the excited state $|e\rangle$ which are energetically separated by the transition frequency ω_0. A running wave laser with wave number k irradiates the atom under an angle ϕ with respect to the motional axis and drives the dipole transition between the two levels with Rabi frequency Ω. The laser with frequency ω_L is detuned from the atomic transition by $\Delta = \omega_L - \omega_0$. The scattered photons are recorded by a narrow-band detector positioned at an angle ψ from the axis of motion. The rate of spontaneous emission of the two-level system is given by Γ. Figure 8.1 depicts a sketch of the setup.

We assume that the coupling of the light field to the atomic motion is in a regime where the size of the center-of-mass wave packet is much smaller than the laser wavelength. Formally this can be expressed by the necessary condition
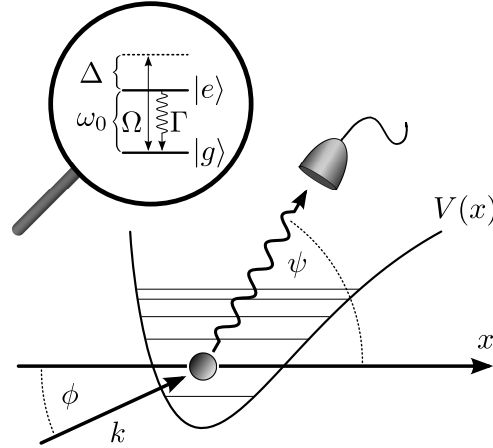
$$\eta = k\xi \ll 1 \,, \tag{8.1}$$

Figure 8.1: *Two-level atom with excited state linewidth Γ. The transition is detuned from an incidence laser with wave number k by Δ. The center of mass is confined along the x-direction in the non-harmonic potential $V(x)$. A detector is placed in the far field at an angle ψ while the laser illuminates the atom under the angle ϕ with respect to the motional axis.*

for the smallness parameter η, where $\xi = \sqrt{\langle x^2 \rangle_0 - \langle x \rangle_0^2}$ denotes the position uncertainty of the atomic ground-state wave function in the potential $V(x)$. The requirement on the atomic localization puts constraints on the occupation of higher excited motional states: Only a sufficiently low mean occupation number $\bar{m}$ of energy eigenstates in the trapping potential is allowed for the treatment presented in this work to be valid. We note that for harmonic trapping η corresponds to the Lamb-Dicke parameter [Jav81, Lin84b, Ste86].

The Hamiltonian of the system is composed of an internal part H_I describing the electronic states, an external part H_E accounting for the atomic center-of-mass motion and the coupling $W(x)$ of those two degrees of freedom by the mechanical effects of the laser light, *viz.*

$$H = H_\mathrm{I} + H_\mathrm{E} + W(x). \tag{8.2}$$

In the frame rotating with the laser frequency the internal Hamiltonian is given by

$$H_\mathrm{I} = -\hbar \Delta \sigma_+ \sigma_-, \tag{8.3}$$

where $\sigma_+ = |e\rangle\langle g|$ and $\sigma_- = |g\rangle\langle e|$ represent the atomic raising and lowering operators, respectively. The external Hamiltonian reads

$$H_\mathrm{E} = \frac{p^2}{2M} + V(x) \tag{8.4}$$

with the atomic mass M and the momentum operator p. The coupling of the electronic

and motional degrees of freedom due to the laser field takes on the form

$$W = \hbar \frac{\Omega}{2} \left[\sigma_+ e^{ikx\cos\phi} + \sigma_- e^{-ikx\cos\phi} \right] . \tag{8.5}$$

To complete the description, we take electronic relaxation processes into account using a master-equation formalism. The time evolution of the system's density operator ϱ, covering the internal *and* external degrees of freedom, including spontaneous emission, obeys $\partial_t \varrho = \mathcal{L}\varrho$ and is generated by the Liouville operator $\mathcal{L}$ which has the form

$$\mathcal{L}\varrho = \frac{1}{i\hbar}[H, \varrho] + \frac{\Gamma}{2} \int_{-1}^{1} du\, w(u) \mathcal{D}[\sigma_- e^{-ikxu}]\varrho \tag{8.6}$$

with our usual abbreviation $\mathcal{D}[X]\varrho = 2X\varrho X^\dagger - X^\dagger X \varrho - \varrho X^\dagger X$ for superoperators of Lindblad form. The normalized radiation pattern $w(u)$ for the considered transition describes the probability of emitting a photon at an angle $\psi = \arccos u$ while the exponential accounts for momentum recoils due to spontaneously emitted photons projected on the axis of motion. The specific form of the symmetric function $w(u)$ depends on the details of the electronic transition [Lin84b].

Under stationary conditions the spectral signal at the detector is given by [Lin86, Cir93]

$$\mathcal{S}(\omega) = \text{Re} \int_0^\infty dt\, e^{-i(\omega - \omega_{\text{L}})t} \langle D_+(t) D_-(0) \rangle_{\text{st}} , \tag{8.7}$$

where in the far field the two mutually adjoint generalized atomic lowering and raising operators have the form

$$\begin{aligned} D_-(t) &= \sigma_-(t) e^{-ikx\cos\psi} , \\ D_+(t) &= \sigma_+(t) e^{ikx\cos\psi} , \end{aligned} \tag{8.8}$$

respectively. The exponential term in Eq. (8.8) accounts for the recoil of the photon of wave number k spontaneously emitted along the direction specified by ψ, projected on the axis of motion.

A convenient way to evaluate the power spectrum (8.7) is to employ the spectral decomposition of the Liouville operator defined in Eq. (8.6), the so-called damping basis [Bri93, Bar00]. This method has already been applied for the description of light scattering [Cir93, Bie04, Bie07, Tor11] and laser cooling [Lin84b, Cir92] of harmonically trapped atoms in the Lamb-Dicke limit.

Formally the solution of the master equation (8.6) can be achieved by solving the eigenvalue equations of $\mathcal{L}$ for the left and right eigenelements which read

$$\mathcal{L}\hat{\varrho}_\lambda = \lambda \hat{\varrho}_\lambda \,, \tag{8.9}$$

$$\check{\varrho}_\lambda^\dagger \mathcal{L} = \lambda \check{\varrho}_\lambda^\dagger \,. \tag{8.10}$$

A small value of η suggests an expansion of the Liouville operator $\mathcal{L}$ with techniques described in [Bie04, Bie07]. Up to second order in η we write the Liouville operator as $\mathcal{L} = \mathcal{L}_0 + \mathcal{L}_1 + \mathcal{L}_2$, where the subscript indicates the order. The individual terms read

$$\mathcal{L}_0 \varrho = \mathcal{L}_I \varrho + \mathcal{L}_E \varrho \,, \tag{8.11}$$

$$\mathcal{L}_1 \varrho = \frac{1}{i\hbar}[W_1 x, \varrho] \,, \tag{8.12}$$

$$\mathcal{L}_2 \varrho = \frac{1}{i\hbar}[W_2 x^2, \varrho] + \alpha \frac{\Gamma}{2} k^2 \sigma_- \mathcal{D}[x] \varrho \sigma_+ \tag{8.13}$$

with the definition $\alpha = \int_{-1}^{1} du\, w(u)u^2$. In the case of a dipole pattern $w(u)$ one finds the value $\alpha = 2/5$ [Lin84b] which we will use in the subsequent text. The internal and external Liouville operators we defined in the zeroth order of the expansion are given by

$$\mathcal{L}_I \varrho = \frac{1}{i\hbar}[H_I + W_0, \varrho] + \frac{\Gamma}{2}\mathcal{D}[\sigma_-]\varrho \,, \tag{8.14}$$

$$\mathcal{L}_E \varrho = \frac{1}{i\hbar}[H_E, \varrho] \,. \tag{8.15}$$

The expansion

$$W_n = \frac{1}{n!}\left.\frac{\partial^n W}{\partial x^n}\right|_{x=0} \tag{8.16}$$

of the interaction Hamiltonian up to second order is explicitly given by

$$W_0 = \hbar \frac{\Omega}{2}\left(\sigma_+ + \sigma_-\right) \,, \tag{8.17}$$

$$W_1 = i\hbar\frac{\Omega}{2}k\cos\phi\left(\sigma_+ - \sigma_-\right) \,, \tag{8.18}$$

$$W_2 = -\hbar\frac{\Omega}{4}k^2\cos^2\phi\left(\sigma_+ + \sigma_-\right) \,. \tag{8.19}$$

We solve the eigenvalue equations (8.9) and (8.10) in zeroth order of η and then perform perturbation theory to obtain the eigenvalues and eigenelements in higher orders.

The zeroth order Liouville operator Eq. (8.11) does not couple the internal and

external degrees of freedom. Hence, the eigenelements

$$\hat{\varrho}_\lambda^{(0)} = \hat{\rho}_{\lambda_I}\hat{\mu}_{\lambda_E} \,, \tag{8.20}$$

$$\check{\varrho}_\lambda^{\dagger(0)} = \check{\rho}_{\lambda_I}^\dagger\check{\mu}_{\lambda_E}^\dagger \tag{8.21}$$

factorize, where ρ and μ denote eigenelements of the internal and external degrees of freedom, respectively. The eigenvalues are $\lambda_0 = \lambda_I + \lambda_E$, with λ_I and λ_E denoting the internal and external eigenvalues of $\mathcal{L}_I$ and $\mathcal{L}_E$, respectively. Therefore, we only have to solve the eigenvalue equations of the internal and external motion separately, which read

$$\mathcal{L}_I\hat{\rho}_{\lambda_I} = \lambda_I\hat{\rho}_{\lambda_I} \,, \quad \check{\rho}_{\lambda_I}^\dagger\mathcal{L}_I = \lambda_I\check{\rho}_{\lambda_I}^\dagger \,, \tag{8.22}$$

$$\mathcal{L}_E\hat{\mu}_{\lambda_E} = \lambda_E\hat{\mu}_{\lambda_E} \,, \quad \check{\mu}_{\lambda_E}^\dagger\mathcal{L}_E = \lambda_E\check{\mu}_{\lambda_E}^\dagger \,. \tag{8.23}$$

The eigenvalue equations for the internal Liouville operator can be readily solved using a matrix representation we presented in Sec. 1.3.5 where we also gave the explicit expression of the steady state ρ_{st} of the internal dynamics.

The external Liouvillian (8.11) on the other hand does not include any non-unitary terms and its eigenelements

$$\hat{\mu}_{n,m} = |n\rangle\langle m| \,, \tag{8.24}$$

$$\check{\mu}_{n,m}^\dagger = |m\rangle\langle n| \tag{8.25}$$

can be constructed from the energy eigenstates $|n\rangle$ satisfying

$$H_E|n\rangle = \varepsilon_n|n\rangle \,. \tag{8.26}$$

The corresponding external eigenvalues $\lambda_{n,m} = i\omega_{n,m}$ contain the transition frequencies

$$\omega_{n,m} = \frac{\varepsilon_m - \varepsilon_n}{\hbar} \tag{8.27}$$

between the energy eigenstates $|m\rangle$ and $|n\rangle$.

The perturbative corrections of interest for later calculations are the ones of first order, given by

$$\check{\varrho}_\lambda^{\dagger(1)} = \check{\varrho}_\lambda^{\dagger(0)}\mathcal{L}_1\left(\lambda_0 - \mathcal{L}_0\right)^{-1}\mathcal{Q}_\lambda \,, \tag{8.28}$$

$$\hat{\varrho}_\lambda^{(1)} = \left(\lambda_0 - \mathcal{L}_0\right)^{-1}\mathcal{Q}_\lambda\mathcal{L}_1\hat{\varrho}_\lambda^{(0)} \,. \tag{8.29}$$

Here subscripts of the eigenvalues and superscripts of the eigenelements again label the corresponding order of η. The projectors introduced in Eqs. (8.28) and (8.29) are given by $\mathcal{Q}_\lambda = 1 - \mathcal{P}_\lambda$ and $\mathcal{P}_\lambda = \hat{\varrho}_\lambda^{(0)} \otimes \check{\varrho}_\lambda^{\dagger(0)}$.

The time evolution of the operators in expression (8.7) for the spectrum of resonance fluorescence is determined by the Liouville operator $\mathcal{L}$ and can be calculated using the quantum regression theorem, which was derived in Sec. 1.2. Together with the eigenvalue equations (8.9) and (8.10) of the Liouville operator and the completeness relation (1.42) the spectrum formula (8.7) can be cast into the form

$$\mathcal{S}(\omega) = \mathrm{Re} \sum_{\lambda} \frac{w_{\lambda}}{i(\omega - \omega_{\mathrm{L}}) - \lambda}, \tag{8.30}$$

i.e. we can decompose the spectrum into contributions connected to the eigenvalues of the Liouville operator, weighted by

$$w_{\lambda} = \mathrm{Tr}\{D_{+}\hat{\varrho}_{\lambda}\}\mathrm{Tr}\{\check{\varrho}_{\lambda}^{\dagger}D_{-}\varrho_{\mathrm{st}}\}. \tag{8.31}$$

Depending on the real and imaginary parts of w_{λ} the spectrum consists of a superposition of Lorentzians and Fano profiles.

We are mainly interested in the signatures of the atomic motion in the spectrum of the scattered light. Therefore we only focus on contributions fulfilling the following criteria: *(i)* We only take the first non-vanishing correction, *i.e.* the second order in η, of the spectrum into account. *(ii)* We only consider eigenvalues with $\lambda_{\mathrm{I}} = 0$ giving the motional sidebands of the elastic peak (for the harmonic trapping potential the motional sidebands of the *inelastic* peaks were reported in Ref. [Bie06]). *(iii)* We do not report the contribution $\lambda_{\mathrm{I}} = 0$ and $\lambda_{\mathrm{E}} = 0$ resulting in a correction to the Rayleigh peak.

In order to evaluate the factors (8.31) we expand the generalized atomic lowering operators as $D_{-} = D_{-}^{(0)} + D_{-}^{(1)} + ...$ with

$$D_{-}^{(0)} = \sigma_{-}, \tag{8.32}$$

$$D_{-}^{(1)} = -ik \cos\psi \, \sigma_{-} x \tag{8.33}$$

and likewise the weight factors according to $w_{\lambda} = w_{\lambda}^{(0)} + w_{\lambda}^{(1)} + ...$ in orders of η. In this expansion the zeroth order weight factors give rise to the *Mollow-type spectrum* of a laser driven two-level system [Mol69]. It turns out that the first order does not contribute, while the second order takes on the form

$$w_{\lambda}^{(2)} = \sum_{\substack{\alpha+\beta+\gamma \\ +\delta+\epsilon=2}} \mathrm{Tr}\{D_{+}^{(\alpha)}\hat{\varrho}_{\lambda}^{(\beta)}\}\mathrm{Tr}\{\check{\varrho}_{\lambda}^{\dagger(\gamma)}D_{-}^{(\delta)}\varrho_{\mathrm{st}}^{(\epsilon)}\}. \tag{8.34}$$

The only contributions to the weight factors that fulfill the conditions *(i)-(iii)* read

$$w_{\lambda}^{(2)} = \mathrm{Tr}\{D_{-}^{(0)}\hat{\varrho}_{\lambda}^{(1)} + D_{-}^{(1)}\hat{\varrho}_{\lambda}^{(0)}\}\mathrm{Tr}\{[\check{\varrho}_{\lambda}^{\dagger(1)}D_{+}^{(0)} + \check{\varrho}_{\lambda}^{\dagger(0)}D_{+}^{(1)}]\varrho_{\mathrm{st}}^{(0)} + \check{\varrho}_{\lambda}^{\dagger(0)}D_{+}^{(0)}\varrho_{\mathrm{st}}^{(1)}\}, \tag{8.35}$$

where in $\varrho_{\text{st}}^{(0)} = \rho_{\text{st}} \mu_{\text{st}}$ the external steady state has the form

$$\mu_{\text{st}} = \sum_j p_j |j\rangle\langle j| \tag{8.36}$$

in the energy eigenbasis (8.26) of the external Hamiltonian. The populations $p_j = \text{Tr}_{\text{I}}\langle j|\rho|j\rangle$ in the energy eigenstates $|j\rangle$ are determined by laser cooling as discussed in the next section.

An outline of the evaluation of the factors (8.35) is presented in App. D.1. The spectrum of resonance fluorescence can then be brought into the form

$$\mathcal{S}_{\text{sb}}(\omega) = \text{Re} \sum_{n \neq m} \frac{\left[p_m|\tilde{r}(\omega_{n,m})|^2 + (p_n - p_m)\tilde{r}(\omega_{n,m})q(\omega_{n,m})\right]|\langle n|x|m\rangle|^2}{i(\omega - \omega_{\text{L}} - \omega_{n,m}) - \lambda_{n,m}^{(1)} - \lambda_{n,m}^{(2)}} \tag{8.37}$$

where $\tilde{r}(\omega) = r(\omega) - [\Delta + i\Gamma/2]\Omega k \cos\psi/2N$ and $N = \Gamma^2/4 + \Delta^2 + \Omega^2/2$. Furthermore, we defined the two functions [Cir93]

$$r(\omega) = \frac{1}{\hbar} \int_0^\infty \mathrm{d}t\, \mathrm{e}^{-i\omega t} \langle[\sigma_+(t), W_1(0)]\rangle_{\text{st}}, \tag{8.38}$$

$$q(\omega) = \frac{1}{\hbar} \int_{-\infty}^\infty \mathrm{d}t\, \mathrm{e}^{-i\omega t} \langle W_1(t)\sigma_-(0)\rangle_{\text{st}}. \tag{8.39}$$

Explicit expressions for $r(\omega)$ and $q(\omega)$ are given in App. D.2. In the denominator of Eq. (8.37) we used the perturbative expansion $\lambda_{n,m} = \lambda_{n,m}^{(0)} + \lambda_{n,m}^{(1)} + \lambda_{n,m}^{(2)}$ of the eigenvalues. The higher order contributions of this expansion introduce a finite linewidth of the motional sidebands, since the denominator of Eq. (8.37) is purely imaginary in zeroth order.

In the well studied case of a harmonic trapping potential the external eigenvalues $\lambda_{n,m}$ are degenerate due to the equidistant eigenenergies of the potential. In that specific case, perturbation theory for degenerate eigenvalues has to be performed. In the problem treated here the potential is assumed to show an appreciable anharmonicity such that generally only the eigenvalue $\lambda_{\text{E}} = 0$ is degenerate. Hence, perturbation theory for non-degenerate eigenvalues has to be applied. Such an approach is valid if the splitting of the eigenvalues due to the interaction with the laser is small compared to the energy differences of the vibrational levels [Mor03]. Explicitly the condition

$$\eta\Omega \ll \min_{n,n' \neq n}|\omega_{n,n'}| \tag{8.40}$$

has to be fulfilled.

The first order correction to the eigenvalues is given by

$$\lambda_1 = \text{Tr}\{\breve{\varrho}_\lambda^{\dagger(0)}\mathcal{L}_1\hat{\varrho}_\lambda^{(0)}\} \tag{8.41}$$

which for $\lambda_0 = \lambda_{n,m}$ can be written as $\lambda_{n,m}^{(1)} = i\delta\omega_{n,m}^{(1)}$ with

$$\delta\omega_{n,m}^{(1)} = \frac{\Gamma\Omega^2 k\cos\phi}{4N} \left[\langle n|x|n\rangle - \langle m|x|m\rangle\right].$$

(8.42)

This constitutes a shift of the peak positions but does not add a finite width. We further note that this shift vanishes in all even potentials due to the parity of the eigenstates. The second order correction

$$\lambda_2 = \mathrm{Tr}\big\{\check{\varrho}_\lambda^{\dagger(0)} \left[\mathcal{L}_2 + \mathcal{L}_1(\lambda_0 - \mathcal{L}_0)^{-1}\mathcal{Q}_\lambda\mathcal{L}_1\right] \hat{\varrho}_\lambda^{(0)}\big\}$$

(8.43)

shows a non-vanishing real part. Their evaluation is sketched in App. D.3 where it is shown that for $\lambda_0 = \lambda_{n,m}$ one obtains $\lambda_{n,m}^{(2)} = i\delta\omega_{n,m}^{(2)} - \gamma_{n,m}$ with the second order frequency shift

$$\delta\omega_{n,m}^{(2)} = \frac{\Delta\Omega^2 k^2 \cos^2\phi}{4N} \left(\langle n|x^2|n\rangle - \langle m|x^2|m\rangle\right)$$
$$- \mathrm{Im}\sum_j \left[s(\omega_{j,n})|\langle j|x|n\rangle|^2 - s(\omega_{j,m})|\langle j|x|m\rangle|^2\right]$$

(8.44)

and the real part

$$\gamma_{n,m} = \frac{1}{2}\sum_j (A_{j,n} + A_{j,m}) - D\langle n|x|n\rangle\langle m|x|m\rangle$$

(8.45)

describing finite width of the sidebands. In this expression we introduced the diffusion coefficient

$$D = \alpha\Gamma k^2 \mathrm{Tr}\{\sigma_+\sigma_-\rho_{\mathrm{st}}\} = \frac{\Gamma\Omega^2 k^2}{10N}$$

(8.46)

and the transition rates

$$A_{n,m} = [2\,\mathrm{Re}\,s(\omega_{n,m}) + D]\,|\langle n|x|m\rangle|^2$$

(8.47)

with the fluctuation spectrum

$$s(\omega) = \frac{1}{\hbar^2}\int_0^\infty \mathrm{d}t\, e^{i\omega t}\langle W_1(t)W_1(0)\rangle_{\mathrm{st}}.$$

(8.48)

Here, the two-time correlation function $s(\omega)$ (for explicit expressions see App. D.2) is evaluated in the steady state ρ_{st}, *viz.* $\langle X\rangle_{\mathrm{st}} = \mathrm{Tr}\{X\rho_{\mathrm{st}}\}$. In the next section we will see that the coefficients $A_{n,m}$ indeed describe the rate of population transfer between the energy eigenstate $|m\rangle$ and $|n\rangle$ due to the mechanical effects of light scattering. Inspecting $\gamma_{n,m}$ defined in Eq. (8.45) we find that the width of a sideband peak that originates in a transition from $|m\rangle$ to $|n\rangle$ involves a sum over the rates of transitions from $|m\rangle$ and $|n\rangle$ to all other states $|j\rangle$, *i.e.* $A_{j,m}$ and $A_{j,n}$. We note that since $\mathrm{Re}\,s(\omega) > 0$ one also finds $\gamma_{n,m} > 0$.

In zeroth order of η the steady state μ_{st} cannot be determined uniquely since the eigenvalue $\lambda_{\mathrm{E}} = 0$ is infinitely degenerate. This degeneracy is lifted in second order perturbation theory and the unique steady state of laser cooling can be found by adiabatic elimination of the internal degrees of freedom [Jav84, Lin84b, Ste86, Gar04]. This procedure applied to Eq. (8.6) yields the equation

$$\mathcal{P}_0 \left(\mathcal{L}_1 \mathcal{L}_0^{-1} \mathcal{Q}_0 \mathcal{L}_1 - \mathcal{L}_2 \right) \mathcal{P}_0 \rho_{\mathrm{st}} \mu_{\mathrm{st}} = 0 \tag{8.49}$$

for the external steady state μ_{st}. Using the representation (8.36) of μ_{st} and performing a partial trace $\mathrm{Tr}_{\mathrm{I}}\{\,\cdot\,\}$ over the internal degrees of freedom in Eq. (8.49) results in the a recursive equation for the probabilities p_j. One can rewrite this equation as

$$\sum_m A_{n,m} p_m - \sum_m A_{m,n} p_n = 0 \tag{8.50}$$

with $A_{n,m}$ defined in Eq. (8.47), see App. D.4. This set of equations determines the steady state of the atomic motion. In this rate equation the part of the coefficients $A_{n,m}$ including $s(\omega)$ reflects the rate of transitions induced by the laser field while the diffusive part connected with the diffusion coefficient D stems from spontaneous emission.

We conclude this section by a comparison with the harmonic trapping potential $V(x) = M\nu^2 x^2/2$ [Jav81, Lin84b, Ste86, Cir92]. The matrix elements of the position operator are only non-zero between neighboring energy states, $\langle n|x|m\rangle \propto \sqrt{m}\delta_{n,m-1} + \sqrt{m+1}\delta_{n,m+1}$, allowing only transitions between adjacent vibrational levels. This is directly reflected in the transition rates A_{nm} which are also non-zero only for $n = m \pm 1$, resulting in a recurrence relation Eq. (8.50) that has the form of the detailed balance condition

$$nA_+ p_{n-1} + (n+1)A_- p_{n+1} = [nA_- + (n+1)A_+]p_n \tag{8.51}$$

with $A_\pm = 2\,\mathrm{Re}\,s(\mp\nu) + D$ [Cir92]. The normalized solution is a thermal distribution $p_n = \bar{m}^n/(\bar{m}+1)^{n+1}$ with the mean occupation number $\bar{m} = A_+/(A_- - A_+)$. The steady state (8.36) of the atomic center-of-mass motion can be cast in the canonical form $\mu_{\mathrm{st}} = \exp(-\beta H_{\mathrm{osc}})/Z$ with the harmonic oscillator Hamiltonian H_{osc}, the partition function $Z = \mathrm{Tr}\{\exp(-\beta H_{\mathrm{osc}})\}$ and the inverse temperature β implicitly defined via $\bar{m} = [\exp(\beta\hbar\nu) - 1]^{-1}$. The harmonic potential is special in the sense that the effective dynamical equation (8.49) takes the shape of a master equation of a harmonic oscillator in contact with a thermal reservoir [Cir92], resulting in a thermal distribution as a steady state. In contrast, non-harmonic potentials do *not* lead to a recursive relation as Eq. (8.51) and generally do not lead to a thermal external state.

According to Eq. (8.37) the atomic motion causes the emergence of an infinite

number of motional sidebands, each approximately centered around a possible transition between eigenstates of the external motion. The property that only transitions between neighboring levels can occur together with the degeneracy of the transition frequencies results in a sideband spectrum Eq. (8.54) consisting of *two* peaks centered around $\pm\nu$. The widths of both peaks can be obtained by employing perturbation theory for degenerate eigenvalues and is given by the cooling rate $\gamma = A_- - A_+$, thereby giving a sideband spectrum of the form [Cir93]

$$\mathcal{S}_{\mathrm{sb}}(\omega) = \mathrm{Re}\frac{\bar{m}|\tilde{r}(\nu)|^2 + \tilde{r}(\nu)q(\nu)}{i(\omega - \omega_{\mathrm{L}} - \tilde{\nu}) + \gamma} + \mathrm{Re}\frac{(\bar{m}+1)|\tilde{r}(-\nu)|^2 - \tilde{r}(-\nu)q(-\nu)}{i(\omega - \omega_{\mathrm{L}} + \tilde{\nu}) + \gamma} \qquad (8.52)$$

with a renormalized frequency $\tilde{\nu}$.

We exemplify our results by means of two specific choices of the potential $V(x)$, namely the infinite square well and the Morse potential. For both potentials we will focus on two distinct parameter regimes of laser cooling: The regime of Doppler cooling ($\omega_{nm} \ll \Gamma$) and the regime of resolved sideband cooling ($\omega_{nm} \gg \Gamma$).

In the following we will assume the Rabi frequency to be small such that the atom is driven below saturation. In this case the function $s(\omega)$ in Eq. (8.48) can be expanded as

$$s(\omega) = \frac{\Omega^2}{4}k^2\cos^2\phi\,\frac{\Gamma/2 + i(\omega + \Delta)}{\Gamma^2/4 + (\omega + \Delta)^2} + \mathcal{O}(\Omega^4)\,. \qquad (8.53)$$

In the spectrum formula (8.37) we find $|\tilde{r}(\omega)|^2 = \mathcal{O}(\Omega^2)$ while $\tilde{r}(\omega)q(\omega) = \mathcal{O}(\Omega^4)$. In the low intensity limit $\Omega \ll \Gamma$ this implies that we can write the motional sidebands of the elastic peak in second order of η as

$$\mathcal{S}_{\mathrm{sb}}(\omega) = \sum_{n\neq m} \frac{\gamma_{n,m}p_m|\langle n|x|m\rangle|^2|\tilde{r}(\omega_{n,m})|^2}{(\omega - \omega_{\mathrm{L}} - \tilde{\omega}_{n,m})^2 + \gamma_{n,m}^2} \qquad (8.54)$$

where we introduced the renormalized frequencies $\tilde{\omega}_{n,m} = \omega_{n,m} + \delta\omega_{n,m}^{(1)} + \delta\omega_{n,m}^{(2)}$ that slightly shift the sideband peaks from the natural transitions between vibrational states.

In Ref. [Dic53] a study of the light scattered by atoms confined in a one-dimensional square well (see Fig. 8.2) of length L has been performed. We revisit this problem using the theory presented in the previous sections. As a first example we therefore
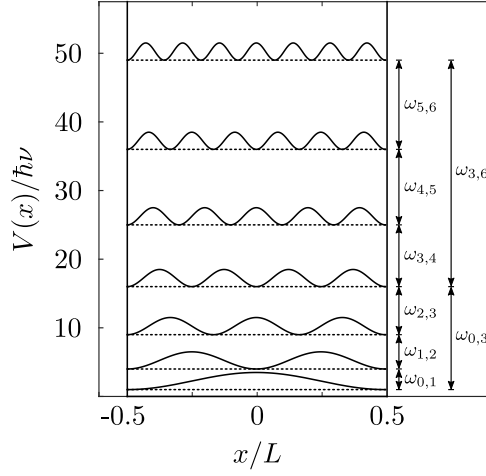
Figure 8.2: *Infinite square well potential with its first seven eigenenergies (dashed) and the corresponding probability densities $|\varphi_n(x)|^2$ (solid) with some transition frequencies of allowed transitions (in units of ν).*

consider the atom to be trapped in the symmetric potential

$$V(x) = \begin{cases} \infty, & \text{for } |x| \geq L/2 \\ 0, & \text{for } |x| < L/2 \,. \end{cases} \tag{8.55}$$

The eigensystem of H_{E} is given by

$$\varepsilon_n = (n+1)^2 \hbar\nu \,, \tag{8.56}$$

$$\varphi_n(x) = \begin{cases} \sqrt{\frac{2}{L}} \sin((n+1)\pi x/L), & \text{for odd } n \\ \sqrt{\frac{2}{L}} \cos((n+1)\pi x/L), & \text{for even } n \,. \end{cases} \tag{8.57}$$

for $n = 0, 1, 2, \dots$ with the frequency $\nu = \hbar\pi^2/2ML^2$. Figure 8.2 shows the potential well with the motional eigenenergies in units of $\hbar\nu$ and the probability densities of the associated wavefunctions $\varphi_n(x) = \langle x|n\rangle$. The transition frequency between neighboring eigenstates increases linearly with n according to

$$\omega_{n,n+1} = (2n+3)\nu \,. \tag{8.58}$$

With the help of the eigenstates (8.57) it is straightforward to calculate the matrix elements of the position operator which are needed to evaluate the coefficients $A_{n,m}$ and the eigenvalue corrections of Eqs. (8.42) and (8.43). They are given by

$$\langle n|x|m\rangle = -\frac{8(n+1)(m+1)(-1)^{(n+m+1)/2}L}{\pi^2[(n+1)^2 - (m+1)^2]^2} \tag{8.59}$$

for n, m of different parity and zero otherwise, being a consequence of the symmetry of

the potential. The matrix elements of x^2 are also readily evaluated and their diagonal elements read

$$\langle n|x^2|n\rangle = \frac{L^2}{12}\left[1 - \frac{6}{(n+1)^2\pi^2}\right].\tag{8.60}$$

For the ground state $n = 0$ this yields a smallness parameter, as introduced in Eq. (8.1), of

$$\eta = \frac{kL}{2\pi}\sqrt{\frac{\pi^2 - 6}{3}} \approx 0.18\,kL.\tag{8.61}$$

The parameter kL was already mentioned in Ref. [Dic53] to quantify the influence of the atomic motion on the emitted radiation.

The above mentioned matrix elements can now be used to determine the steady state of the atomic motion. Although the explicit shape of the rate equation (8.50) is easily obtained it is nevertheless necessary to solve the rate equation numerically due to the complexity of the coefficient matrix (see Eq. (D.19)).

Doppler regime

In the Doppler regime the transition frequencies between the lower eigenstates are small compared to the linewidth of the atomic transition. To fulfill this criterion we choose $\nu = \Gamma/30$ which corresponds to a lowest transition frequency of $\omega_{0,1} = \Gamma/10$.

Figure 8.3 a) shows the dependence of the mean steady state occupation $\bar{m} = \Sigma_m p_m m$ on the laser detuning Δ for $\Omega = \Gamma/5$. Optimal Doppler cooling occurs at the detuning $\Delta \approx -0.59\,\Gamma$ (indicated by a circle), where a steady state occupation of $\bar{m} \approx 1.24$ is reached. The optimal detuning takes a higher value than in the harmonic trapping potential where best Doppler cooling is achieved for approximately $\Delta = -\Gamma/2$ with $\bar{m} \approx 3$. This shows that in the square well potential the atomic motion is Doppler cooled well below the final value for harmonically trapped atoms.

In the inset of Fig. 8.3 a) we plot the negative logarithm of the populations p_m for optimal Doppler cooling against the eigenenergies ε_m. Since $-\log(p_m)$ does not show a linear dependence on ε_m the steady state of the atomic motion cannot be written in the form of a thermal state, *i.e.* $\mu_{\text{st}} \neq \exp(-\beta H_{\text{E}})/Z$ with $H_{\text{E}} = \sum_n (n+1)^2\hbar\nu|n\rangle\langle n|$.

In Fig. 8.3 b) we show the motional sidebands detected under an angle $\psi = \pi/2$ calculated using Eq. (8.54) for optimal cooling $\Delta = -0.6\,\Gamma$ and a smallness parameter of $\eta = 0.1$. The sideband spectrum consists of a series of Lorentzians centered around the transition frequencies between neighboring energy levels, *viz.* $\omega_{n,n+1} = (2n+3)\nu$ such that they are separated by 2ν. Their height decreases rapidly towards higher values of n, because of the lower populations p_n of higher motional states. Transitions between non-adjacent levels are not visible due to the smallness of the position operator's matrix elements and vanishing values of $r(\omega)$.
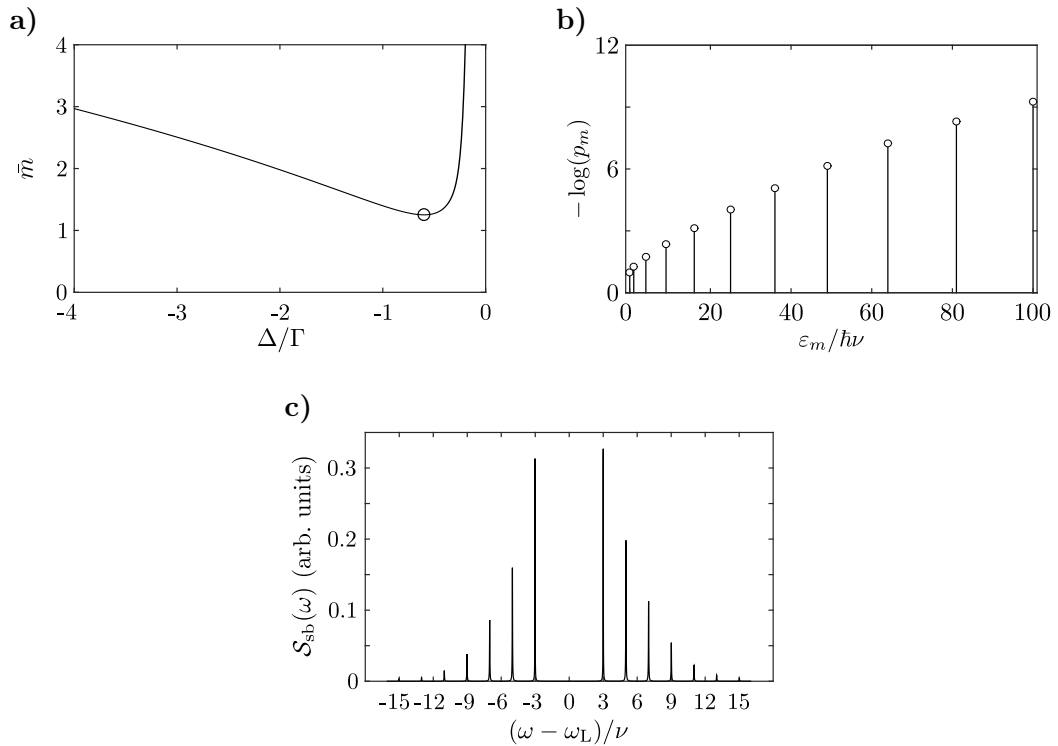
Figure 8.3: *Doppler cooling of an atom trapped in an infinite square well potential for $\nu = \Gamma/30$ ($\omega_{0,1} = \Gamma/10$), $\Omega = \Gamma/5$ and $\eta = 0.1$.* **a)** *Mean occupation $\bar{m}$ in dependence on the detuning Δ. The circle indicates optimal cooling for $\Delta \approx -0.6\,\Gamma$ resulting in $\bar{m} \approx 1.24$.* **b)** *Negative logarithm of the steady state occupations p_m ($m = 0, ..., 10$) for optimal cooling. In a thermal distribution the curve would be linear–clearly not the case here.* **c)** *Power spectrum Eq. (8.54) of the motional sidebands for $\psi = \pi/2$ consisting of Lorentzians centered around the transition frequencies $\omega_{n,n+1} = (2n + 3)\nu$. Transitions of the kind $n \rightarrow n \pm l$ with $l > 1$ are not visible due to their small heights.*

Resolved sideband regime

In the regime of resolved sideband cooling the transition frequency between the lowest energy states is much larger than the atomic linewidth. We choose $\nu = 10\,\Gamma/3$, which corresponds to a transition frequency $\omega_{0,1} = 10\,\Gamma$. Figure 8.4 a) shows again the dependence of the mean occupation on the laser detuning for $\Omega = \Gamma/5$. Optimal cooling to a mean occupation $\bar{m} \approx 0.068$ is achieved when the laser is red-detuned from the atomic transition by roughly the first transition frequency $\omega_{0,1}$, i.e $\Delta \approx -3.35\,\nu$. In contrast to Doppler cooling the cooling curve shows additional dips at the detunings $\Delta/\nu = -15, -21, -27, ...$, corresponding to frequencies where multiple transitions between motional eigenstates coincide, *e.g.* in the cases $\omega_{3,0} = \omega_{7,6} = -15\,\nu$ or $\omega_{4,1} = \omega_{10,9} = -21\,\nu$.

Due to ground state cooling, the spectrum shown in Fig. 8.4 b) is dominated by two peaks involving the lowest transition frequency $\pm\omega_{0,1} = \pm3\,\nu$. The inset shows
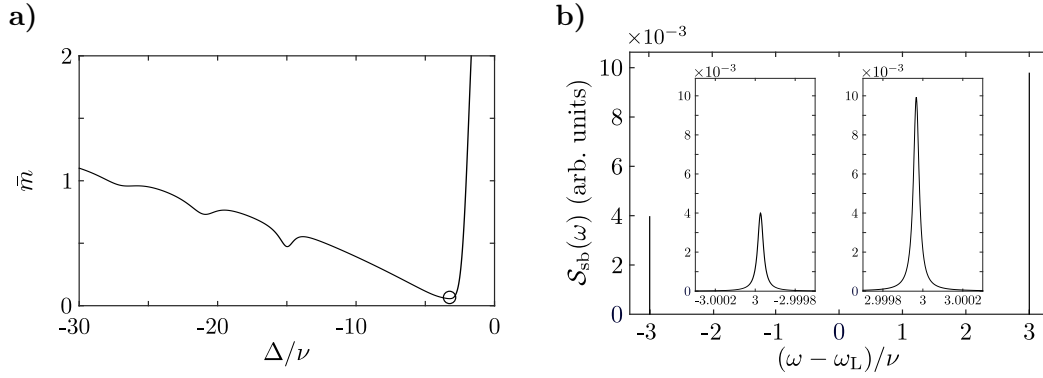
a)

b)

Figure 8.4: **a)** *Cooling of an atom trapped in an infinite square well potential in the resolved sideband regime for $\nu = 10\,\Gamma/3$ (corresponding to $\omega_{0,1} = 10\,\Gamma$) and $\Omega = \Gamma/5$. The mean occupation $\bar{m}$ in dependence of the laser detuning Δ takes its minimum $\bar{m} \approx 0.086$ at $\Delta \approx -3.35\,\nu$ (indicated by a circle), where sideband cooling of the $1 \to 0$ transition occurs.* **b)** *Power spectrum of the motional sidebands for $\psi = \pi/2$ and $\eta = 0.1$. The insets show magnifications of the first red and blue sideband which dominate the spectrum.*

a magnification of the red and blue sideband where also the frequency shift due to the interaction with the laser becomes visible. We also note that the half-width at half-maximum of both peaks is equal, due to the invariance of $\gamma_{n,m}$ under exchange of n and m, and that the asymmetry in the height vanishes when the spectrum is averaged over the detection angle ψ.

We turn to the discussion of the Morse potential [Mor29b, Mor29a] which is sketched in Fig. 8.5. It has possible applications in the laser cooling of the vibrational degrees of freedom of di-atomic molecules [Ngu11, Man13, Ham15]. Although the general results are well-known, we briefly summarize them for the sake of completeness.

The potential has the form

$$V(x) = U \left(1 - e^{-\kappa x}\right)^2 \tag{8.62}$$

with the depth U and the characteristic length scale $1/\kappa$. Its eigenenergies are given by [Pek34]

$$\varepsilon_n = \left[\left(n + \frac{1}{2}\right) - \frac{1}{2a}\left(n + \frac{1}{2}\right)^2\right]\hbar\nu \tag{8.63}$$

for $n = 0, 1, 2, ...$ with the frequency $\nu = \kappa\sqrt{2U/M}$ and the dimensionless parameter $a = \sqrt{2MU}/\hbar\kappa$. The corresponding energy eigenstates $|n\rangle$ in the position representa-
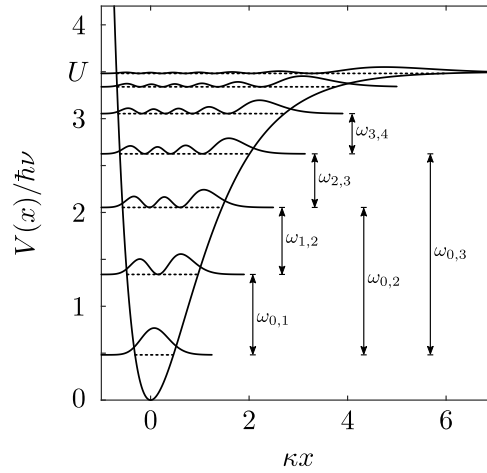
Figure 8.5: *The asymmetric Morse potential and the eigenenergies (dashed) and corresponding probability densities $|\varphi_n(x)|^2$ of its bound states for $a = 7$ with some transition frequencies of possible transitions (in units of ν).*

tion read [Dah88]

$$
\begin{aligned}
\varphi_n(x) &= \langle x|n \rangle \\
&= \mathcal{N}_n \zeta^{a-n-1/2} e^{-\zeta/2} L_n^{(2a-2n-1)}(\zeta)
\end{aligned}
\tag{8.64}
$$

with the abbreviation $\zeta = 2a \exp(-\kappa x)$ and the generalized Laguerre polynomials $L_n^{(\alpha)}(z)$ and the normalization constants $\mathcal{N}_n = [\kappa(2a - 2n - 1)n!/\Gamma(2a - n)]^{1/2}$ [Pek34, Sch32]. The highest bound state in this potential has the index $n = \lfloor a - 1/2 \rfloor$. Figure 8.5 shows the Morse potential and its eigenenergies in units of $\hbar\nu$ along with the probability densities of the bound states for $a = 7$. The transition frequency between adjacent energy eigenstates decreases according to

$$
\omega_{n,n+1} = \frac{a - 1 - n}{a}\nu
\tag{8.65}
$$

The matrix elements of the position operator required for the evaluation of the transition rates $A_{n,m}$ were reported in [Sch32, Gal80, San90] and can be written in the form

$$
\begin{aligned}
\langle n|x|m \rangle &= \frac{(-1)^{n+m}}{\kappa(n - m)(2a - n - m - 1)} \\
&\quad \times \left[\frac{m!}{n!} \frac{\Gamma(2a - m)}{\Gamma(2a - n)} (2a - 2n - 1)(2a - 2m - 1) \right]^{1/2},
\end{aligned}
\tag{8.66}
$$

with the *Gamma function* $\Gamma(z)$ [Abr65], for $n < m$, while for $n > m$ the two indices have to be interchanged on the right-hand side. The moments of the position operator in the eigenstates of the Morse potential are obtained from the generating

function [Gal80]

$$\langle n|e^{sx}|n\rangle = \frac{(2a-2n-1)n!}{\Gamma(2a-n)}e^{s\log(2a)/\kappa}$$
$$\times \sum_{j,l=0}^{n}\frac{(-1)^{j+l}}{j!l!}\binom{2a-2n-1}{n-j}\binom{2a-2n-1}{n-l}$$
$$\times \Gamma(2a-2n-1+j+l-s/\kappa) \tag{8.67}$$

by differentiation with respect to s. For the ground state $n = 0$ the first and second moments are

$$\langle 0|x|0\rangle = \frac{1}{\kappa}\big[\log(2a)-\psi^{(0)}(2a-1)\big], \tag{8.68}$$

$$\langle 0|x^2|0\rangle = \frac{1}{\kappa^2}\big[\psi^{(1)}(2a-1)+\langle 0|x|0\rangle^2\big] \tag{8.69}$$

with the *polygamma functions* $\psi^{(n)}(z)$ [Abr65], resulting in the ground-state variance $\xi^2 = \psi^{(1)}(2a-1)/\kappa^2$ and thereby a smallness parameter

$$\eta = \frac{k}{\kappa}\sqrt{\psi^{(1)}(2a-1)}. \tag{8.70}$$

Doppler regime

In Fig. 8.6 we show the mean steady state occupation $\bar{m}$ in dependence of Δ for $a = 30$ and $\Omega = \Gamma/5$ assuming that the transition frequency between the lowest two states is again given by $\omega_{0,1} = \Gamma/10$ which leads to $\nu = a/(a-1)\Gamma/10 \approx 0.1034\,\Gamma$. Optimal cooling is achieved for $\Delta \approx 0.509\,\Gamma$ with a mean occupation of $\bar{m} \approx 3.54$. In the inset we plot $-\log(p_m)$ against the eigenenergies ε_m. It can be seen that only the populations of the lower energy levels can be approximated by a thermal distribution while for higher states this is clearly not the case. In the calculation only the finite number $\lfloor a - 1/2 \rfloor + 1$ of bound states of the potential, here 30 for $a = 30$, are taken into account while free solutions are disregarded. This is a good approximation for states which are energetically well localized within the range of bound states.

In Fig. 8.6 b) we show the motional sidebands of an atom trapped in a Morse potential ($a = 30$) calculated using Eq. (8.54). We used the parameters of optimal cooling, *i.e.* $\Delta = -0.509\,\Gamma$, a detection angle $\psi = \pi/2$ and a smallness parameter $\eta = 0.1$. The decreasing transition frequency between neighboring states is reflected in the fact that in the sideband spectrum the modulus of the peak positions is smaller than the first transition frequency $\omega_{0,1}$. The thin gray curves under the sideband spectrum are the main components, according to the decomposition Eq. (8.54), corresponding to the transitions $n + 1 \to n$ for $n = 0, ..., 9$ on the blue sideband and $n - 1 \to n$ for $n = 1, ..., 10$ on the red sideband, which add up to the complete spectrum but overlap because of their finite width.
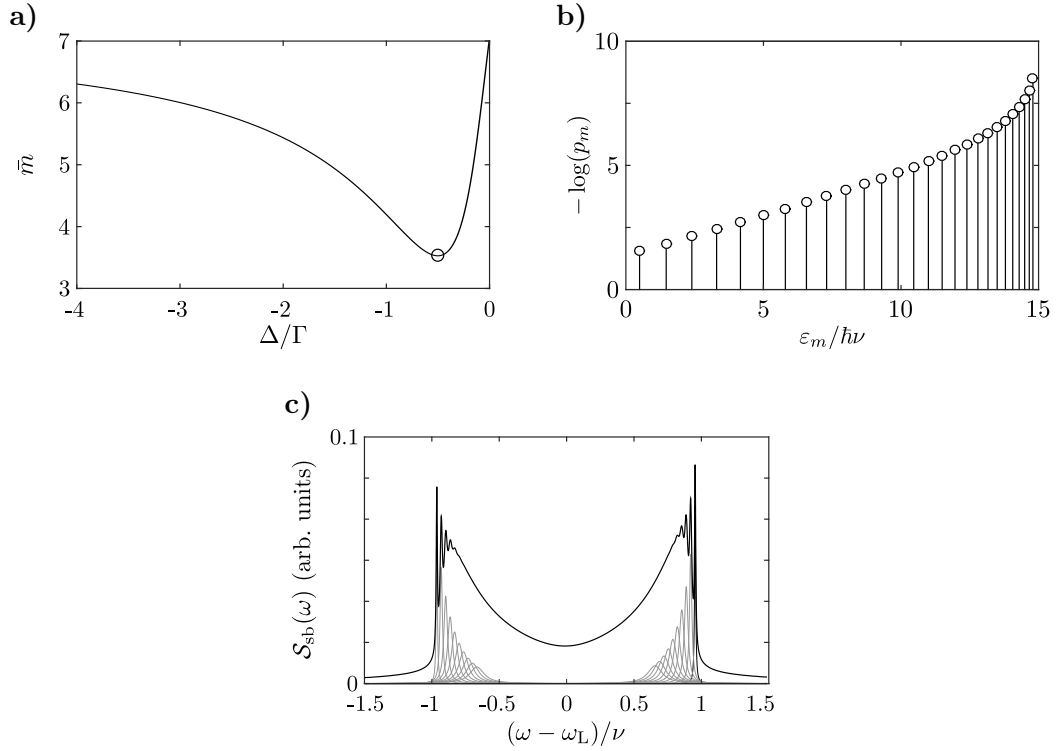
Figure 8.6: *Cooling of atoms trapped in a Morse potential in the Doppler regime for $a = 30$, $\nu = a\Gamma/10(a-1)$ (corresponding to $\omega_{0,1} = \Gamma/10$) and $\Omega = \Gamma/5$. **a)** Mean occupation $\bar{m}$ in dependence of the laser detuning Δ. The circle indicates optimal cooling occurring at $\Delta \approx -0.51\,\Gamma$ resulting in $\bar{m} = \Sigma_m m p_m \approx 3.54$. **b)** Negative logarithm of the steady state occupations p_m $(m = 0, ..., 24)$ for optimal cooling. In a thermal distribution the resulting curves would be linear–only approximately the case for the lower energy levels. **c)** Power spectrum of the motional sidebands. The thin lines correspond to the first ten transitions between neighboring states on both sidebands. The smallness parameter is given by $\eta = 0.1$ and the detector angle by $\psi = \pi/2$.*

Resolved sideband regime

In the resolved sideband case with $\nu = 10a\Gamma/(a-1)$, corresponding to $\omega_{0,1} = 10\,\Gamma$, optimal cooling occurs when the laser is red-detuned by the transition frequency ω_{01}, leading to a mean occupation $\bar{m} = 0.0026$. This is only slightly higher than in the harmonic case where $\bar{m} = 0.0016$ is achieved [calculated using $\bar{m} = A_+/(A_- - A_+)$, see Sec. 8.2.4]. The fact that in this case the cooling is more efficient than in the square well case is due to the comparatively small anharmonicity of the Morse potential in the lower energy levels. Figure 8.7 a) shows the mean occupation in dependence of the detuning Δ where again shallow dips are visible where multiple transition frequencies coincide, for example $\omega_{2,0} = \omega_{12,9} = -1.9\,\nu$, $\omega_{4,1} = \omega_{19,13} = -2.7\,\nu$, and $\omega_{3,0} = \omega_{21,14} = -2.8\,\nu$.

In this regime the motional sideband spectrum, depicted in Fig. 8.7 b), is also
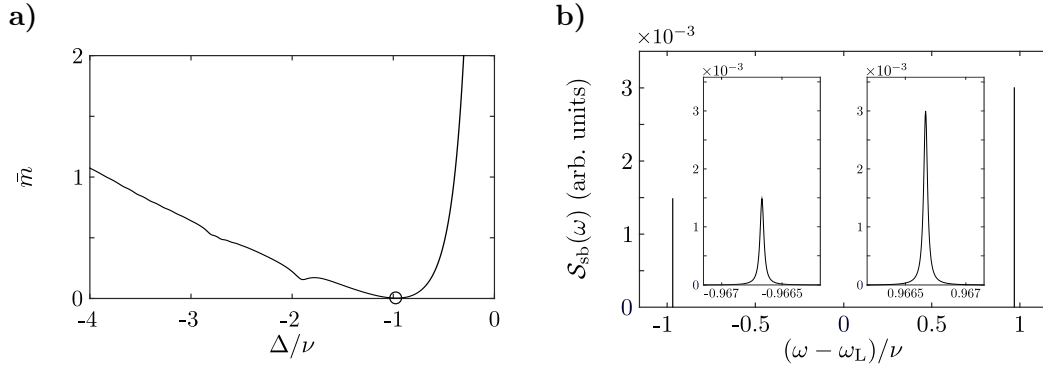
Figure 8.7: a) *Cooling of an atom trapped in a Morse potential in the resolved sideband regime for* $\nu = 10a/(a-1)\Gamma$ *(corresponding to* $\omega_{0,1} = 10\,\Gamma$*) and* $\Omega = \Gamma/5$. *The mean occupation* $\bar{m} = \Sigma_m m p_m$ *in dependence of the detuning* Δ *takes its minimum* $\bar{m} \approx 0.0026$ *at* $\Delta \approx -\omega_{0,1}$ *(indicated by a circle), where sideband cooling of the* $1 \to 0$ *transition occurs.* **b)** *Power spectrum of the motional sidebands for a smallness parameter* $\eta = 0.1$ *and* $\psi = \pi/2$.

mainly given by the two peaks arising from the transitions between the lowest energy states. The insets show a magnification of the red and blue sideband.

Following up on Dicke's original work on light scattered by atoms confined to an infinite square well and subsequent works on harmonically trapped atoms we present the spectrum of resonance fluorescence of laser cooled atoms trapped in arbitrary potentials. The treatment relies on a perturbative analysis of the power spectrum of the scattered light up to second order in the Lamb-Dicke parameter and is based on the solution of the corresponding master equation describing the laser cooling dynamics.

We applied the results to two exemplary potentials, the infinite square well and the Morse potential, and distinguished between different cooling regimes, namely Doppler cooling and resolved sideband cooling. In contrast to the harmonic trapping potential the steady state of the atomic motion does not take the form of a thermal distribution. The spectrum of the motional sidebands consists of a series of peaks centered around the transitions between eigenstates of the atomic center-of-mass motion. From our treatment also follow the widths of the individual peaks which are determined by the transitions rates between the motional states due to the interaction with the laser. In the case of separated motional sideband peaks, the temperature of the cooled atom can be extracted from the individual heights. When the peaks overlap, the resulting asymmetric envelope of the spectral signals stemming from the atomic motion can be used to determine the temperature by using our theoretical results.

Asymmetric motional sidebands have been observed in recent atom-cavity experiments where instead of the resonance fluorescence the spectrum of the cavity output was measured. In this case the atom is trapped in the sinusoidal optical-lattice po-

tential of the cavity mode. With the work presented here we lay the ground work for
further investigation of such periodic potentials offering possible means for tempera-
ture extraction in cavity-cooling experiments.

In this thesis we extended the toolbox for solving the Born-Markov master equation to various situations, namely solid-state quantum emitter, optomechanical systems and atoms trapped in non-harmonic potentials.

We started by proposing a model for the description of solid-state emitters and their interaction with lattice vibrations of the crystal in which they are embedded. We formulated this description in the form of a single Born-Markov master equation and derived the solution of this equation in the form of the eigensystem of the associated Liouville operator, the damping basis. In this master equation we included the lattice-phonon environment in the form of a single vibrational mode damped by a Markovian reservoir. We then showed how this eigenbasis can be used to calculated the dynamics of the emitter and its light scattering properties. Here, the electron-phonon interaction manifests itself in an additional dephasing of the emitter and in the emergence of the phonon sideband in the spectrum of absorbed and emitted photons. This phonon sideband shows the characteristic shape of solid-state single-photon sources such as Nitrogen-vacancy centers in diamond [Alb14]. Our model intrinsically contains the results obtained by the Huang-Rhys model [Hua50] for the absorption lineshape of crystal defect centers when both the linewidth of the emitter transition and the vibrational mode tend to zero. The solution we showed represents a general tool for the investigation of damped two-level systems interacting with a damped harmonic oscillator via a state-dependent displacement, for instance a single electron spin coupled to the quantized motion of a vibrating magnetized tip [Rab10],

We then lay our focus on optomechanical systems where we investigated the dynamics of a hybrid system consisting of a two-level atom coupled to the electric field of a noptomechanical cavity. In this system we analyzed an effect where the dipole-cavity interaction can be appreciably suppressed in the regime of strong optomechanical coupling. A possible realization of such a hybrid system are monolithic diamond structures in which a Nitrogen-vacancy center couples to a phoxonic crystal cavity [Kip14], *i.e.* a crystal cavity that can host localized mechanical vibrations and electric fields that are optomechanically coupled. In a more detailed description of this kind of system the master equation for solid-state emitter can be useful to account for the coupling of the Nitrogen-vacancy center to the surrounding crystal. To follow up on the first subject we transfered the methods we employed for solid-state emitters to the master equation describing a dissipative optomechanical system. As a result we derived the damping basis of the optomechanical master equation which can be a resource to avoid numerical overhead.

The third and last subject of this thesis was the analysis of a single laser-driven atom trapped in a non-harmonic potential. Here, we employed a perturbative treatment of the underlying master equation in the Lamb-Dicke regime to investigate the

cooling performance and the signatures of the atomic motion in the spectrum of spontaneously emitted photons. In particular, we presented the results for two specific potentials, the infinite square well and the Morse potential. In both cases the final stages of the laser cooling dynamics do not result in a thermal distribution of the motional state populations. These populations on the other hand influence the shape of the motional sidebands in the resonance fluorescence spectrum. Our example of the Morse potential could thereby be employed to obtain information on the motional degrees of freedom of diatomic molecules in molecule-cooling experiments. Similarly, in recent cavity cooling experiments, where the atom is trapped in the optical-lattice potential of the cavity mode, motional sidebands have been observed whose shape reflect the sinusoidal nature of the trapping potential.

The work presented here demonstrates the prediction power of the spectral decomposition of the Liouville operator in Born-Markov master equations. Open issues in this context are its application to non-Markovian reservoirs [Bar01] which are important in solid-state environments.

APPENDIX

Damped harmonic oscillator

We saw in Eq. (2.14) that the s-parametrized distribution can be expressed by the Fourier transform

$$W(\alpha, s) = \frac{1}{\pi^2} \int \mathrm{d}^2\beta \, e^{\frac{s-t}{2}|\beta|^2} \chi(\beta, t) e^{\alpha\beta^* - \alpha^*\beta} \tag{A.1}$$

of the characteristic function (2.13), where we used the definition of the exponential operator (2.12). Inserting the t-parametrized characteristic function in terms of the quasiprobability distribution, using Eq. (2.15), yields

$$W(\alpha, s) = \frac{1}{\pi^2} \int \mathrm{d}^2\beta \, e^{\frac{s-t}{2}|\beta|^2} \left\{ \int \mathrm{d}^2\upsilon \, W(\upsilon, t) e^{\beta\upsilon^* - \beta^*\upsilon} \right\} e^{\alpha\beta^* - \alpha^*\beta} . \tag{A.2}$$

Here, one has to check whether the integral over β exists, which is the case if the Fourier transform of $W(\upsilon, t, \mu)$ with respect to β multiplied by $\exp[\alpha\beta^* - \alpha^*\beta]$ decrease faster than the anti Gaussian $\exp[(s-t)|\beta|^2/2]$ (for $s > t$). We shortly summarize the three steps: *(i)* Fourier transform of $W(\upsilon, t)$ to obtain $\chi(\beta, t)$, *(ii)* multiplication with $\exp[(s-t)|\beta|^2/2]$ and *(iii)* Fourier transform of $\chi(\beta, s)$ to arrive at $W(\alpha, s)$.

The procedure mentioned in App. A.1 can be used to transform the Q-representations ($s = -1$) of the left and right eigenelements, given by Eqs. (2.46) and (2.52), into the corresponding P-functions ($t = 1$). For the *left* eigenelements we start with

$$\check{Q}_{m,k}(\upsilon) = W(\upsilon, -1, \hat{\mu}^\dagger_{m,k}) = \frac{1}{\pi} \frac{m!}{(m+|k|)!} \left[\frac{-\bar{m}}{\bar{m}+1} \right]^m \left\{ \begin{matrix} \upsilon^k \\ \upsilon^{*|k|} \end{matrix} \right\} L_m^{(|k|)}\left(\frac{|\upsilon|^2}{\bar{m}} \right) , \tag{A.3}$$

where we introduced the notation that the upper line stands for the case $k \geq 0$ and the lower one for $k < 0$. For the generating function of these functions we obtain

$$
\begin{aligned}
G_k[W(v, -1, \hat{\mu}^\dagger_{m,k}); z] &= \sum_{m=0}^\infty \frac{(m + |k|)!}{m!} W(v, -1, \hat{\mu}^\dagger_{m,k}) z^m \\
&= \frac{1}{\pi} \left[\frac{\bar{m} + 1}{\bar{m} + 1 + \bar{m}z} \right]^{|k|+1} \left\{ \begin{array}{c} v^k \\ v^{*|k|} \end{array} \right\} e^{\frac{z|v|^2}{\bar{m}+1+\bar{m}z}} ,
\end{aligned} \tag{A.4}
$$

where we used the generating function (2.18). The Fourier transform of this delivers the generating function of the characteristic function. It is easily performed under use of the integral

$$
\int \mathrm{d}^2\alpha \left\{ \begin{array}{c} \alpha^l \\ \alpha^{*l} \end{array} \right\} e^{-c|\alpha|^2} e^{\alpha\zeta^* - \alpha^*\zeta} = \frac{\pi}{c^{l+1}} \left\{ \begin{array}{c} (-\zeta)^l \\ \zeta^{*l} \end{array} \right\} e^{-\frac{|\zeta|^2}{c}} \tag{A.5}
$$

and reads

$$
G_k[\chi(\beta, -1, \check{\mu}^\dagger_{m,k}); z] = -\left[\frac{\bar{m}+1}{z} \right]^{|k|+1} \left\{ \begin{array}{c} (-\beta)^k \\ \beta^{*|k|} \end{array} \right\} e^{\frac{\bar{m}+1+\bar{m}z}{z}|\beta|^2} . \tag{A.6}
$$

According to step *(ii)* of App. A.1 we have to multiply this function with $\exp[|\beta|^2]$ and take the Fourier back transform, again using the same integral (A.5), to arrive at

$$
G_k[W(\alpha, 1, \check{\mu}^\dagger_{m,k}); z] = \frac{1}{\pi} \left[\frac{1}{z+1} \right]^{|k|+1} \left\{ \begin{array}{c} \alpha^k \\ \alpha^{*|k|} \end{array} \right\} e^{\frac{z}{(\bar{m}+1)(z+1)}|\alpha|^2} . \tag{A.7}
$$

The distribution itself is obtained by differentiating this generating function with respect to z and setting $z = 0$ afterwards. Here, again the generating function for Laguerre polynomials (2.18) comes in handy and we find

$$
\check{P}_{m,k}(\alpha) = \frac{(-1)^m}{\pi} \frac{m!}{(m+|k|)!} \left\{ \begin{array}{c} \alpha^k \\ \alpha^{*|k|} \end{array} \right\} L_m^{(|k|)} \left(\frac{|\alpha|^2}{\bar{m}+1} \right) . \tag{A.8}
$$

In the same fashion one can derive the P-distribution of the *right* eigenelements which reads

$$
\hat{P}_{m,k}(\alpha) = \frac{1}{\pi} \left[-\frac{\bar{m}+1}{\bar{m}} \right]^m \left[\frac{1}{\bar{m}} \right]^{|k|+1} \left\{ \begin{array}{c} \alpha^{*k} \\ \alpha^{|k|} \end{array} \right\} L_m^{(|k|)} \left(\frac{|\alpha|^2}{\bar{m}} \right) e^{-\frac{|\alpha|^2}{\bar{m}}} . \tag{A.9}
$$

From the definition of the P-distribution it is also straightforward to write the eigenelements in their *antinormally* ordered form.

The newly found generating function for products of hypergeometric functions and Laguerre polynomials has the form

$$\sum_{m=0}^{\infty} {}_2F_1\left(-m, N+1; 1; w\right) L_m^{(0)}(wy) z^m =$$

$$\frac{[1-z]^N e^{\frac{w[w-1]yz}{1-z+wz}}}{[1-z+wz]^{n+1}} L_N^{(0)}\left(\frac{-w^2 yz}{[1-z][1-z+wz]}\right) . \tag{A.10}$$

The proof can be carried out using *induction* and the properties of the Laguerre polynomials. In the generating function one has to identify $w = (\bar{m}+1)^{-1}$, $y = |\alpha|^2$ and $z = \exp[-\gamma t]$ to arrive at Eq. (2.59).

Solid-state quantum emitters

In Sec. 4.3 we need explicit expressions for the formulas

$$A_{m,k}^{\pm} = \text{Tr}\big\{D(\alpha_{\pm})e^{\pm\varsigma b}\hat{\mu}_{m,k}e^{\mp\varsigma b}D^{\dagger}(\beta_{\pm})\big\}\,, \tag{B.1}$$

$$B_{m,k}^{\pm} = \text{Tr}\big\{D(\beta_{\pm})e^{\pm\varsigma b}\breve{\mu}_{m,k}^{\dagger}e^{\mp\varsigma b}D^{\dagger}(\alpha_{\pm})\mu_{\text{th}}\big\} \tag{B.2}$$

following from overlaps of eigenelements of the Liouvillian $\mathcal{L}$, Eq. (4.17). Moreover,

$$C_{n,l}^{m,k}(\beta) = \text{Tr}\big\{\breve{\mu}_{n,l}^{\dagger}D(\beta)\hat{\mu}_{m,k}D^{\dagger}(\beta)\big\} \tag{B.3}$$

is helpful for the application of the damping basis.

To evaluate expression (B.1), we use the cyclic property of the trace and

$$e^{\mp\varsigma b}D^{\dagger}(\beta_{\pm})D(\alpha_{\pm})e^{\pm\varsigma b} = D(\pm\beta^{*})\exp[\mp\beta\varsigma]e^{i\text{Im}\,\alpha_{\pm}\beta_{\pm}^{*}}\,. \tag{B.4}$$

One arrives at

$$A_{m,k}^{\pm} = e^{i\text{Im}\alpha_{\pm}\beta_{\pm}^{*}}e^{-\frac{1}{2}|\beta|^{2}}\hat{\chi}_{m,k}(\mp\beta^{*}) \tag{B.5}$$

with the characteristic function

$$\hat{\chi}_{m,k}(\beta) = \text{Tr}\big\{D(\beta)e^{\frac{1}{2}|\beta|^{2}}\hat{\mu}_{m,k}\big\} = \int \text{d}^{2}\alpha\, e^{\alpha\beta^{*}-\alpha^{*}\beta}\hat{Q}_{nl}(\alpha) \tag{B.6}$$

of antinormally ordered expectation values [Cah69a], being the Fourier transform of the quasi-probability distribution $\hat{Q}_{m,k}(\alpha) = \langle\alpha|\hat{\mu}_{m,k}|\alpha\rangle/\pi$ defined in Eqs. (2.35) and (2.46). The remaining integral can be evaluated using the generating function Eq. (2.18) of the Laguerre polynomials and Gaussian integrals of the form (2.20).

After collecting all terms, one finds

$$A_{m,k}^+ = \frac{(-1)^m}{m!}[(\bar{m}+1)|\beta|^2]^m e^{-(\bar{m}+1)\mathrm{Re}\beta^2} e^{-\bar{m}\beta^{*2}} e^{(\bar{m}+\frac{1}{2})|\beta|^2} \left\{ \begin{matrix} (-\beta)^k \\ \beta^{*|k|} \end{matrix} \right\}, \qquad (B.7)$$

$$A_{m,k}^- = \frac{(-1)^m}{m!}[(\bar{m}+1)|\beta|^2]^m e^{-\bar{m}(\mathrm{Re}\beta^2+\beta^{*2})} e^{-\beta^2} e^{(\bar{m}+\frac{1}{2})|\beta|^2} \left\{ \begin{matrix} \beta^k \\ (-\beta^*)^{|k|} \end{matrix} \right\}. \qquad (B.8)$$

In this notation, the upper and lower line in the curly brackets again correspond to $k \geq 0$ and $k < 0$, respectively.

Equation (B.2) has the phase space representation

$$B_{m,k}^\pm = \pi \int \mathrm{d}^2\alpha \, \check{P}_{m,k}(\alpha) Q(\alpha) \qquad (B.9)$$

with the P-function of the left eigenelements, see Eq. (A.8), and the Q-function of the asymmetrically displaced thermal state, given by

$$\check{P}_{m,k}(\alpha) = \frac{(-1)^m}{\pi} \frac{m!}{(m+|k|)!} \left\{ \begin{matrix} \alpha^k \\ \alpha^{*|k|} \end{matrix} \right\} L_m^{|k|}\left(\frac{|\alpha|^2}{\bar{m}+1}\right), \qquad (B.10)$$

$$Q(\alpha) = \frac{1}{\pi} \langle \alpha | e^{\pm\varsigma b} D(\alpha_\pm) \mu_{\mathrm{th}} D(\beta_\pm) e^{\mp\varsigma b} | \alpha \rangle, \qquad (B.11)$$

respectively. The Q-function can be evaluated explicitly by applying the Baker-Hausdorff relation and using the properties of coherent states. Then, in the function

$$\widetilde{B}_l^\pm(z) = \sum_{n=0}^\infty \frac{(n+|l|)!}{n!} B_{nl}^\pm z^n \qquad (B.12)$$

the summation is performed using Eq. (2.18), leading to an integral of the form

$$\int \mathrm{d}^2\alpha \left\{ \begin{matrix} \alpha^l \\ \alpha^{*|l|} \end{matrix} \right\} e^{\alpha\zeta^* - \alpha^*\xi} e^{-c|\alpha|^2} = \frac{\pi}{c^{l+1}} \left\{ \begin{matrix} (-\xi)^l \\ \zeta^{*|l|} \end{matrix} \right\} e^{-\frac{\xi\zeta^*}{c}}. \qquad (B.13)$$

For the "$-$"-case, the coefficients are

$$\xi = -\frac{\bar{m}}{\bar{m}+1}\beta, \quad \zeta^* = -\beta^*, \quad c^{-1} = (z+1)(\bar{m}+1). \qquad (B.14)$$

Finally, one obtains

$$B_{nl}^+ = \frac{(-1)^n}{(n+|l|)!}[\bar{m}|\beta|^2]^n e^{-i(\bar{m}+1)\mathrm{Im}\beta^2} e^{-(\bar{m}+\frac{1}{2})|\beta|^2} \left\{ \begin{matrix} [-(\bar{m}+1)\beta]^l \\ [\bar{m}\beta^*]^{|l|} \end{matrix} \right\}, \qquad (B.15)$$

$$B_{nl}^- = \frac{(-1)^n}{(n+|l|)!}[\bar{m}|\beta|^2]^n e^{-i\bar{m}\mathrm{Im}\beta^2} e^{-(\bar{m}+\frac{1}{2})|\beta|^2} \left\{ \begin{matrix} [\bar{m}\beta]^l \\ [-(\bar{m}+1)\beta^*]^{|l|} \end{matrix} \right\} \qquad (B.16)$$

from the generating function (B.12) by differentiation with respect to z and setting $z \to 0$ afterwards.

The evaluation of Eq. (B.3) goes along the lines sketched in App. B.1.2, this time, however, using the displaced right eigenelement, Eq. (2.53), with the function

$$Q_{m,k}^{(\beta)}(\alpha) = \frac{1}{\pi}\langle\alpha|D(\beta)\hat{\mu}_{m,k}D^{\dagger}(\beta)|\alpha\rangle. \qquad (B.17)$$

The generating function, Eq. (2.18), is applied twice to express the Laguerre polynomials in $\check{P}_{n,l}$ and $Q_{m,k}^{(\beta)}$ in terms of exponentials. The resulting integrals can be solved using

$$\int d^2\alpha \left\{ \begin{array}{c} \alpha^\nu(\alpha^*+\beta^*)^\mu \\ (\alpha+\beta)^\nu\alpha^{*\mu} \end{array} \right\} e^{\alpha\zeta^*-\alpha^*\xi}e^{-c|\alpha|^2}$$
$$= \frac{\pi}{c}e^{-\frac{\xi\zeta^*}{c}} \left\{ \begin{array}{c} c^{-\nu}(-\xi)^{\nu-\mu}\mu!\,L_\mu^{(\nu-\mu)}[\xi(\beta^*+\zeta^*/c)] \\ c^{-\mu}\zeta^{*\mu-\nu}\nu!\,L_\nu^{(\mu-\nu)}[-\zeta^*(\beta-\xi/c)] \end{array} \right\}. \qquad (B.18)$$

From differentiating the generating function then follows

$$C_{n,l}^{(m,k)}(\beta) = \binom{n}{m}\left[\frac{|\beta|^2}{\bar{m}+1}\right]^{n-m} \left\{ \begin{array}{c} \dfrac{1}{(n-m+|l|-|k|)!}\beta^{|l|-|k|} \\ \dfrac{(n-m)!}{(n-m-|k|)!(n-m+|l|)!}\dfrac{\beta^{*|l|}}{\beta^{|k|}} \end{array} \right\} \qquad (B.19)$$

where the upper line corresponds to $l \geq 0$, $k \geq 0$ and the lower line to $l < 0$, $k \geq 0$. The complex conjugate expressions are the results when both l and k change sign.

Optomechanics

In this appendix we elaborate on the symmetric displacement transform Eq. (7.14). We use the identities

$$e^{\eta b} D(\alpha) b D^\dagger(\alpha) e^{-\eta b} = b - \alpha, \tag{C.1}$$

$$e^{\eta b} D(\alpha) b^\dagger D^\dagger(\alpha) e^{-\eta b} = b^\dagger - \alpha^* + \eta \tag{C.2}$$

which follow immediately from the *Baker-Hausdorff formula* and write the action of the transformed $\tilde{\mathcal{M}}_{n,l}$ on an arbitrary operator ξ as

$$
\begin{aligned}
\tilde{\mathcal{M}}_{n,l}\xi = & e^{\eta_l b} D(\alpha_{n,l}) \left\{ \mathcal{M}_{n,l} D^\dagger(\alpha_{n,l}) e^{-\eta_l b} \xi e^{\eta_l b} D(\beta_{n,l}) \right\} D^\dagger(\beta_{n,l}) e^{-\eta_l b} \\
= & \lambda_{n,l}^{(\mathrm{cav})}\xi + \mathcal{L}_{\mathrm{mec}}\xi \\
& + \left\{ \left[-i\nu - \frac{\gamma}{2}(2\bar{m}+1) \right] \alpha_{n,l}(\alpha_{n,l}^* - \eta_l) + \left[i\nu - \frac{\gamma}{2}(2\bar{m}+1) \right] \beta_{n,l}(\beta_{n,l}^* - \eta_l) \right\}\xi \\
& + \left\{ \gamma(\bar{m}+1)\alpha_{n,l}(\beta_{n,l}^* - \eta_l) + \gamma\bar{m}\beta_{n,l}(\alpha_{n,l}^* - \eta_l) \right\}\xi \\
& + \left\{ -i\chi(n+l)(\alpha_{n,l} + \alpha_{n,l}^* - \eta_l) + i\chi n(\beta_{n,l} + \beta_{n,l}^* - \eta_l) \right\}\xi \\
& + \left\{ \left[i\nu + \frac{\gamma}{2}(2\bar{m}+1) \right] \alpha_{n,l}^* - \gamma(\bar{m}+1)\beta_{n,l}^* - \left[i\nu - \frac{\gamma}{2} \right]\eta_l + i\chi(n+l) \right\} b\xi \\
& + \left\{ -\gamma\bar{m}\alpha_{n,l}^* + \left[-i\nu + \frac{\gamma}{2}(2\bar{m}+1) \right] \beta_{n,l}^* + \left[i\nu - \frac{\gamma}{2} \right]\eta_l - i\chi n \right\}\xi b \\
& + \left\{ \left[i\nu + \frac{\gamma}{2}(2\bar{m}+1) \right] \alpha_{n,l} - \gamma\bar{m}\beta_{n,l} + i\chi(n+l) \right\} b^\dagger\xi \\
& + \left\{ -\gamma(\bar{m}+1)\alpha_{n,l} + \left[-i\nu + \frac{\gamma}{2}(2\bar{m}+1) \right] \beta_{n,l} - i\chi n \right\}\xi b^\dagger, \tag{C.3}
\end{aligned}
$$

where we have already grouped the different combinations of annihilation and creation operators and the operator ξ. With this expression we have already found the constant $\varepsilon_{n,l}$ in Eq. (7.15), which is nothing but the collection of all factors that multiply ξ

where no b and $b^\dagger$ are involved. It reads

$$
\begin{aligned}
\varepsilon_{n,l} = & \left[-i\nu - \frac{\gamma}{2}(2\bar{m}+1) \right] \alpha_{n,l}(\alpha_{n,l}^* - \eta_l) + \left[i\nu - \frac{\gamma}{2}(2\bar{m}+1) \right] \beta_{n,l}(\beta_{n,l}^* - \eta_l) \\
& + \gamma(\bar{m}+1)\alpha_{n,l}(\beta_{n,l}^* - \eta_l) + \gamma\bar{m}\beta_{n,l}(\alpha_{n,l}^* - \eta_l) \\
& - i\chi(n+l)(\alpha_{n,l} + \alpha_{n,l}^* - \eta_l) + i\chi n(\beta_{n,l} + \beta_{n,l}^* - \eta_l) \, .
\end{aligned}
\tag{C.4}
$$

As a brief reminder, we want to choose $\alpha_{n,l}$, $\beta_{n,l}$, and η_l such that all terms in Eq. (C.3) except for $\mathcal{L}_{\text{mec}}$ and $\varepsilon_{n,l}$ vanish. The terms involving $b^\dagger\xi$ and $\xi b^\dagger$, *i.e.* the second last and the last line in Eq. (C.3), can be written as the linear equations

$$
\begin{bmatrix} i\nu + \frac{\gamma}{2}(2\bar{m}+1) & -\gamma\bar{m} \\ -\gamma(\bar{m}+1) & -i\nu + \frac{\gamma}{2}(2\bar{m}+1) \end{bmatrix} \cdot \begin{bmatrix} \alpha_{n,l} \\ \beta_{n,l} \end{bmatrix} = \begin{bmatrix} -i\chi(n+l) \\ i\chi n \end{bmatrix} \, .
\tag{C.5}
$$

Whose formal solution is given by

$$
\begin{bmatrix} \alpha_{n,l} \\ \beta_{n,l} \end{bmatrix} = \frac{1}{\nu^2 + \gamma^2/4} \begin{bmatrix} -i\nu + \frac{\gamma}{2}(2\bar{m}+1) & \gamma\bar{m} \\ \gamma(\bar{m}+1) & i\nu + \frac{\gamma}{2}(2\bar{m}+1) \end{bmatrix} \cdot \begin{bmatrix} -i\chi(n+l) \\ i\chi n \end{bmatrix} \, .
\tag{C.6}
$$

Simplification of this expression gives the results for $\alpha_{n,l}$ and $\beta_{n,l}$ which can be used to identify η_l from the condition that the remaining terms in (C.3) vanish as well. This leads to

$$
\alpha_{n,l} = -n\frac{\chi}{\nu - i\gamma/2} - l\frac{\chi[\nu + i\frac{\gamma}{2}(2\bar{m}+1)]}{\nu^2 + \gamma^2/4} \, ,
\tag{C.7}
$$

$$
\beta_{n,l} = \alpha_{n,l} + l\frac{\chi}{\nu + i\gamma/2} \, ,
\tag{C.8}
$$

$$
\eta_l = l\frac{i\chi\gamma(2\bar{m}+1)}{\nu^2 + \gamma^2/4} \, ,
\tag{C.9}
$$

which can be rewritten in terms of $\beta = \chi/(\nu - i\gamma/2)$ yielding the expressions (7.16)-(7.18) and (7.20) from the main text.

We will write the eigenelements (7.36) in a form that might be useful for practical applications. We start by writing the product of superoperators according to

$$
\left[\prod_{j=q}^{n-1} \frac{1}{\Lambda_{m,k}^{(n,l)} - \mathcal{M}_{j,l}} \right] \hat{\xi}_{m,k}^{(n,l)} = \left[\prod_{j=q}^{n-2} \frac{1}{\Lambda_{m,k}^{(n,l)} - \mathcal{M}_{j,l}} \right] \frac{1}{\Lambda_{m,k}^{(n,l)} - \mathcal{M}_{n-1,l}} \hat{\xi}_{m,k}^{(n,l)} \, .
\tag{C.10}
$$

The inverse of the superoperators can be applied explicitly by expanding the operator $\hat{\xi}_{m,k}^{(n,l)}$ in the eigenbasis of $\mathcal{M}_{n-1,l}$. This is achieved by insert a completeness relation

of the eigenelements yielding

$$\frac{1}{\Lambda_{m,k}^{(n,l)} - \mathcal{M}_{n-1,l}} \hat{\xi}_{m,k}^{(n,l)} = \frac{1}{\Lambda_{m,k}^{(n,l)} - \mathcal{M}_{n-1,l}} \sum_{m',k'} \left(\hat{\xi}_{m',k'}^{(n-1,l)} \otimes \check{\xi}_{m',k'}^{(n-1,l)} \right) \hat{\xi}_{m,k}^{(n,l)}$$

$$= \sum_{m',k'} \frac{1}{\Lambda_{m,k}^{(n,l)} - \Lambda_{m',k'}^{(n-1,l)}} \mathrm{Tr}\left\{ \check{\xi}_{m',k'}^{(n-1,l)\dagger} \hat{\xi}_{m,k}^{(n,l)} \right\} \hat{\xi}_{m',k'}^{(n-1,l)} . \qquad (C.11)$$

The scalar product can be calculated using

$$e^{\eta_l b} D(\alpha_{n-1,l}) D^\dagger(\alpha_{n,l}) e^{-\eta_l b} = D^\dagger(\beta) e^{\frac{-i\nu\gamma\bar{m}|\beta|^2 l}{\nu^2+\gamma^2/4}} e^{\eta_l \beta} , \qquad (C.12)$$

$$e^{\eta_l b} D(\beta_{n,l}) D^\dagger(\beta_{n-1,l}) e^{-\eta_l b} = D(\beta) e^{\frac{i\nu\gamma(\bar{m}+1)|\beta|^2 l}{\nu^2+\gamma^2/4}} e^{-\eta_l \beta} \qquad (C.13)$$

leading to

$$\mathrm{Tr}\left\{ \check{\xi}_{m',k'}^{(n-1,l)\dagger} \hat{\xi}_{m,k}^{(n,l)} \right\} = C_{m',k'}^{m,k}(\beta) e^{\frac{i\nu\gamma|\beta|^2 l}{\nu^2+\gamma^2/4}} . \qquad (C.14)$$

Here, the overlaps $C_{m',k'}^{m,k}(\beta)$ were reported in Eq. (B.19) and we obtain

$$\frac{1}{\Lambda_{m,k}^{(n,l)} - \mathcal{M}_{n-1,l}} \hat{\xi}_{m,k}^{(n,l)} = e^{\frac{i\nu\gamma|\beta|^2 l}{\nu^2+\gamma^2/4}} \sum_{m',k'} \frac{C_{m',k'}^{m,k}(\beta)}{\Lambda_{m,k}^{(n,l)} - \Lambda_{m',k'}^{(n-1,l)}} \hat{\xi}_{m',k'}^{(n-1,l)} . \qquad (C.15)$$

Applying this to all superoperators in the product (C.10) yields the result

$$\hat{\zeta}_{m,k}^{(n,q,l)} = \kappa^{n-q} e^{\frac{i\nu\gamma|\beta|^2 l(n-q)}{\nu^2+\gamma^2/4}} \sqrt{\frac{n!}{q!} \frac{(n+|l|)!}{(q+|l|)!}}$$

$$\times \sum_{m_1,k_1} \cdots \sum_{m_{n-q},k_{n-q}} \frac{C_{m_1,k_1}^{m,k}(\beta)}{\Lambda_{m,k}^{(n,l)} - \Lambda_{m_1,k_1}^{(n-1,l)}} \cdots \frac{C_{m_{n-q},k_{n-q}}^{m_{n-q-1},k_{n-q-1}}(\beta)}{\Lambda_{m,k}^{(n,l)} - \Lambda_{m_{n-q},k_{n-q}}^{(q,l)}} \hat{\xi}_{m_{n-q},k_{n-q}}^{(q,l)} \quad (C.16)$$

which might be advantageous for numerical implementation since no superoperators are involved anymore.

We will outline the main steps in the evaluation of the weight factors (8.35) that contribute to the motional sidebands. They can be calculated according to

$$
\begin{aligned}
\mathrm{Tr}\big\{D_-^{(0)}\hat\varrho_\lambda^{(1)}+D_-^{(1)}\hat\varrho_\lambda^{(0)}\big\} &=\mathrm{Tr}\big\{\sigma_+\big[(\lambda_{n,m}-\mathcal{L}_0)^{-1}\mathcal{Q}_{n,m}\mathcal{L}_1+ik\cos\psi\,x\big]\rho_{\mathrm{st}}\hat\mu_{n,m}\big\}\\
&=-i\tilde r(\omega_{n,m})\mathrm{Tr}\{x\hat\mu_{n,m}\}\,,
\end{aligned}
\tag{D.1}
$$

where we used $\tilde r(\omega)$ defined in Sec. 8.2.2 and evaluated $\mathrm{Tr}\{\sigma_+\rho_{\mathrm{st}}\}=[\Delta+i\Gamma/2]\Omega/2N$ with help of the internal steady state (1.59),

$$
\begin{aligned}
\mathrm{Tr}\big\{\big(\check\varrho_\lambda^{\dagger(1)}D_+^{(0)}&+\check\varrho_\lambda^{\dagger(0)}D_+^{(1)}\big)\varrho_{\mathrm{st}}^{(0)}\big\}\\
&=\mathrm{Tr}\big\{\check\mu_{nm}^\dagger\big[\mathcal{L}_1(\lambda_{n,m}-\mathcal{L}_0)^{-1}\mathcal{Q}_{n,m}-ik\cos\psi\,x\big]\sigma_+\rho_{\mathrm{st}}\hat\mu_{n,m}\big\}\\
&=\frac{1}{i\hbar}\mathrm{Tr}\big\{W_1(\lambda_{n,m}-\mathcal{L}_\mathrm{I})^{-1}\mathcal{Q}_{n,m}\sigma_+\rho_{\mathrm{st}}\big\}\mathrm{Tr}\big\{\check\mu_{n,m}^\dagger[x,\mu_{\mathrm{st}}]\big\}\\
&\quad-ik\cos\psi\mathrm{Tr}\{\sigma_+\rho_{\mathrm{st}}\}\mathrm{Tr}\{\check\mu_{n,m}^\dagger x\}\,,
\end{aligned}
\tag{D.2}
$$

and

$$
\begin{aligned}
\mathrm{Tr}\big\{\check\varrho_\lambda^{\dagger(0)}D_+^{(0)}\varrho_{\mathrm{st}}^{(1)}\big\} &=-\mathrm{Tr}\big\{\check\mu_{n,m}^\dagger\sigma_+\mathcal{L}_0^{-1}\mathcal{Q}_0\mathcal{L}_1\rho_{\mathrm{st}}\mu_{\mathrm{st}}\big\}\\
&=ir^*(\omega_{n,m})\mathrm{Tr}\big\{\check\mu_{n,m}^\dagger x\mu_{\mathrm{st}}\big\}\\
&\quad-\frac{1}{i\hbar}\mathrm{Tr}\big\{\sigma_+(\lambda_{n,m}+\mathcal{L}_\mathrm{I})^{-1}\mathcal{Q}_{n,m}\rho_{\mathrm{st}}W_1\big\}\mathrm{Tr}\big\{\check\mu_{n,m}^\dagger[x,\mu_{\mathrm{st}}]\big\}\,.
\end{aligned}
\tag{D.3}
$$

where we have used the corrections Eq. (8.28), (8.29), (8.32) and (8.33) as well as the explicit form of $\mathcal{L}_1$ from Eq. (8.12) and the projector $\mathcal{Q}_{n,m}=1-\mathcal{P}_{\lambda_{n,m}}$. Addition of these terms yields the result

$$
w_\lambda^{(2)}=|\langle n|x|m\rangle|^2\Big[p_m\big|\tilde r(\omega_{nm})\big|^2+(p_n-p_m)\tilde r(\omega_{n,m})q(\omega_{n,m})\Big]\,,
\tag{D.4}
$$

where we already inserted the actual form of the motional steady state $\mu_{\mathrm{st}}=\Sigma_j p_j|j\rangle\langle j|$ and the two definitions Eqs. (8.38) and (8.39).

In this section we give explicit expressions for the two functions $r(\omega)$ and $q(\omega)$ from Eqs. (8.38) and (8.39) as well as $s(\omega)$ from Eq. (8.48). Using the quantum regression theorem (1.30) and $\int_0^\infty \mathrm{d}t \, \exp(-z + \mathcal{L})t = (z - \mathcal{L})^{-1}$ they can be rewritten as

$$
\begin{aligned}
r(\omega) =& \frac{1}{\hbar} \mathrm{Tr}\big\{ \sigma_+ (i\omega - \mathcal{L}_\mathrm{I})^{-1} [W_1, \rho_\mathrm{st}] \big\} \\
=& \frac{\Omega}{2} k \cos\phi \, \frac{\Gamma N \tilde{\Delta} + i[(\tilde{\Delta} + i\Gamma)|\tilde{\Delta}|^2 + \Delta\Omega^2]\omega - i|\tilde{\Delta}|^2\omega^2}{\Gamma N^2 + i[5\Gamma^2/4 + \Delta^2 + \Omega^2]N\omega - 2\Gamma N\omega^2 - iN\omega^3} \, ,
\end{aligned}
\tag{D.5}
$$

$$
\begin{aligned}
q(\omega) =& \frac{1}{\hbar} \mathrm{Tr}\big\{ W_1 (i\omega - \mathcal{L}_\mathrm{I})^{-1} \sigma_- \rho_\mathrm{st} \big\} - \frac{1}{\hbar} \mathrm{Tr}\big\{ \sigma_- (i\omega + \mathcal{L}_\mathrm{I})^{-1} \rho_\mathrm{st} W_1 \big\} \\
=& \frac{\Omega^3}{2} k \cos\phi \, \frac{i\Gamma^3 N \tilde{\Delta}^* - \Gamma^2 \tilde{\Delta}^* N\omega + a\omega^2 + b\tilde{\Delta}^*\omega^3 + [b - i\Gamma\tilde{\Delta}]\omega^4 + \tilde{\Delta}^*\omega^5 + \omega^6}{2\Gamma^2 N^3\omega + [\Gamma^2(9\Gamma^2/8 - 3\Delta^2 + \Omega^2) + 2(\Delta^2 + \Omega^2)^2]N\omega^3 + 4bN\omega^5} \, ,
\end{aligned}
\tag{D.6}
$$

$$
\begin{aligned}
s(\omega) =& -\frac{1}{\hbar^2} \mathrm{Tr}\big\{ W_1 (i\omega + \mathcal{L}_\mathrm{I})^{-1} W_1 \rho_\mathrm{st} \big\} \\
=& \frac{\Omega^2}{4} k^2 \cos^2\phi \, \frac{\Gamma^3\Omega^2/(4N) + d\omega + [i\Delta|\tilde{\Delta}|^2/N - 3\Gamma/2 - 2i\Delta]\omega^2 + i\omega^3}{-i\Gamma N\omega - [5\Gamma^2/4 + \Delta^2 + \Omega^2]\omega^2 + 2i\Gamma\omega^3 + \omega^4} \, ,
\end{aligned}
\tag{D.7}
$$

with the complex detuning $\tilde{\Delta} = \Delta + i\Gamma/2$ and the constants

$$
a = \Gamma^2(b + \Omega^2) - i\Gamma b\tilde{\Delta}^*, \quad b = 3\Gamma^2/4 - \Delta^2 - \Omega^2 \, ,
\tag{D.8}
$$

$$
d = \Gamma(\Delta - 3i\Gamma/2) + i\Gamma^2|\tilde{\Delta}|^2/N \, .
\tag{D.9}
$$

In the evaluation of the trace we employed the explicit form of the matrices $(i\omega \mp \mathcal{L}_\mathrm{I})^{-1}$ which can be obtained by using the Liouville operator (1.58).

We briefly go into the derivation of the perturbative corrections of the eigenvalues that lead to a non-vanishing real part which becomes immanent in the finite width of the sideband peaks. Their form is given by

$$
\lambda_2 = \mathrm{Tr}\big\{ \breve{\varrho}_\lambda^{\dagger(0)} \big[\mathcal{L}_2 + \mathcal{L}_1 (\lambda_0 - \mathcal{L}_0)^{-1} \mathcal{Q}_\lambda \mathcal{L}_1 \big] \hat{\varrho}_\lambda^{(0)} \big\} \, .
\tag{D.10}
$$

We will treat the two terms separately, starting with the first one that involves $\mathcal{L}_2$. For $\lambda_0 = \lambda_{nm}$ this part yields

$$
\begin{aligned}
\mathrm{Tr}\{ \breve{\mu}_{n,m}^\dagger \mathcal{L}_2 \rho_\mathrm{st} \hat{\mu}_{n,m} \} =& \frac{1}{i\hbar} \mathrm{Tr}\{ W_1 \rho_\mathrm{st} \} \big[\langle n|x^2|n\rangle - \langle m|x^2|m\rangle \big] \\
& + \frac{D}{2} \big[2\langle n|x|n\rangle \langle m|x|m\rangle - \langle n|x^2|n\rangle - \langle m|x^2|m\rangle \big] \, .
\end{aligned}
\tag{D.11}
$$

The second term in Eq. (D.11) can be brought in the form

$$\text{Tr}\big\{\breve{\mu}_{n,m}^{\dagger}\mathcal{L}_1\frac{1}{\lambda_{n,m}-\mathcal{L}_0}\mathcal{Q}_\lambda\mathcal{L}_1\rho_{\text{st}}\hat{\mu}_{n,m}\big\} = -\sum_j\big[s^*(\omega_{j,n})|\langle m|x|j\rangle|^2 + s(\omega_{j,m})|\langle n|x|j\rangle|^2\big]$$

(D.12)

and after recombining these two results using $\langle n|x^2|n\rangle = \Sigma_j|\langle n|x|j\rangle|^2$ we obtain

$$\lambda_{n,m}^{(2)} = \frac{i\Delta\Omega^2 k^2\cos^2\phi}{4N}\big(\langle n|x^2|n\rangle - \langle m|x^2|m\rangle\big) + D\langle n|x|n\rangle\langle m|x|m\rangle$$
$$-\frac{1}{2}\sum_j\left[2s(\omega_{j,n}) + D\right]|\langle j|x|n\rangle| - \frac{1}{2}\sum_j\left[2s^*(\omega_{j,m}) + D\right]|\langle j|x|m\rangle|^2. \quad \text{(D.13)}$$

With the definition of the transition rates $A_{n,m}$ given by Eq. (8.47) this corresponds to Eqs. (8.43)-(8.45).

We transform the reduced motional dynamics Eq. (8.49) into a linear system $\mathcal{A}\mathbf{p} = 0$ with $\mathbf{p} = (p_0, p_1, ...)^T$. The trace over the internal degrees of freedom in Eq. (8.49) yields

$$\text{Tr}_{\text{I}}\big\{\mathcal{P}_0\left(\mathcal{L}_1\mathcal{L}_0^{-1}\mathcal{Q}_0\mathcal{L}_1 - \mathcal{L}_2\right)\mathcal{P}_0\rho_{\text{st}}\mu_{\text{st}}\big\} = 0. \qquad (D.14)$$

The action of the projector $\mathcal{P}_0$ is given by

$$\mathcal{P}_0\rho\mu = \rho_{\text{st}}\sum_n\langle n|\mu|n\rangle|n\rangle\langle n| \qquad (D.15)$$

with internal and external density operators ρ and μ, respectively. For the second term in Eq. (D.14) we obtain

$$\langle n|\text{Tr}_{\text{I}}\{\mathcal{L}_2\rho_{\text{st}}\mu_{\text{st}}\}|n\rangle = D\sum_m(p_m - p_n)|\langle n|x|m\rangle|^2 \qquad (D.16)$$

with the diffusion coefficient D defined in Eq. (8.46). The evaluation of the first term in Eq. (D.14) is somewhat more involved and reads

$$\langle n|\text{Tr}_{\text{I}}\{\mathcal{L}_1\mathcal{L}_0^{-1}\mathcal{Q}_0\mathcal{L}_1\rho_{\text{st}}\mu_{\text{st}}\}|n\rangle = \int_0^\infty dt\,\langle n|\text{Tr}_{\text{I}}\{\mathcal{L}_1 e^{\mathcal{L}_0 t}\mathcal{Q}_0\mathcal{L}_1\rho_{\text{st}}\mu_{\text{st}}\}|n\rangle$$
$$= 2\,\text{Re}\sum_m\big[p_m s(\omega_{n,m}) - p_n s(\omega_{m,n})\big]|\langle n|x|m\rangle|^2, \quad \text{(D.17)}$$

where we separated the internal and external expressions and used $s(\omega)$ defined in Eq. (8.48). Recombining the two terms leads to

$$\sum_m A_{n,m} p_m - \sum_m A_{m,n} p_n = 0\,. \tag{D.18}$$

This is the set of equations that determines $\mathbf{p}$ which can be expressed in the matrix notation $\mathcal{A}\mathbf{p} = 0$ with

$$\mathcal{A} = \begin{bmatrix} -\sum\limits_{m\neq 0} A_{m0} & A_{01} & A_{02} & \cdots \\ A_{10} & -\sum\limits_{m\neq 1} A_{m1} & A_{12} & \\ A_{20} & A_{21} & -\sum\limits_{m\neq 2} A_{m2} & \\ \vdots & & & \ddots \end{bmatrix}\,. \tag{D.19}$$

Bibliography

[Abr65] M. ABRAMOWITZ and I. A. STEGUN, *Handbook of Mathematical Functions*, (Dover Publications, New York, 1965).

[Alb13] R. ALBRECHT, A. BOMMER, C. DEUTSCH, J. REICHEL, and C. BECHER, "Coupling of a Single Nitrogen-Vacancy Center in Diamond to a Fiber-Based Microcavity", *Phys. Rev. Lett.* **110**, 243602 (2013).

[Alb14] R. ALBRECHT, A. BOMMER, C. PAULY, F. MÜCKLICH, A. W. SCHELL, P. ENGEL, T. SCHRÖDER, O. BENSON, J. REICHEL, and C. BECHER, "Narrow-band single photon emission at room temperature based on a single nitrogen-vacancy center coupled to an all-fiber-cavity", *Appl. Phys. Lett.* **105**, 073113 (2014).

[Ash06] A. ASHKIN, *Optical Trapping and Manipulation of Neutral Particles Using Lasers*, (World Scientific, Singapore, 2006).

[Asp14] M. ASPELMEYER, T. J. KIPPENBERG, and F. MARQUARDT, "Cavity optomechanics", *Rev. Mod. Phys.* **86**, 1391 (2014).

[Bal08] G. BALASUBRAMANIAN, I. Y. CHAN, R. KOLESOV, M. AL-HMOUD, J. TISLER, C. SHIN, C. KIM, A. WOJCIK, P. R. HEMMER, A. KRUEGER, T. HANKE, A. LEITENSTORFER, R. BRATSCHITSCH, F. JELEZKO, and J. WRACHTRUP, "Nanoscale imaging magnetometry with diamond spins under ambient conditions", *Nature* **455**, 648 (2008).

[Bar87] S. M. BARNETT and B. J. DALTON, "Liouville space description of thermofields and their generalisations", *J. Phys. A* **20**, 411 (1987).

[Bar00] S. M. BARNETT and S. STENHOLM, "Spectral decomposition of the Lindblad operator", *J. Mod. Opt.* **47**, 2869 (2000).

[Bar01] S. M. BARNETT and S. STENHOLM, "Hazards of reservoir memory", *Phys. Rev. A* **64**, 033808 (2001).

[Bie04] M. BIENERT, W. MERKEL, and G. MORIGI, "Resonance fluorescence of a trapped three-level atom", *Phys. Rev. A* **69**, 013405 (2004).

[Bie06] M. BIENERT, W. MERKEL, and G. MORIGI, "Inelastic scattering of light by a cold trapped atom: Effects of the quantum center-of-mass motion", *Phys. Rev. A* **73**, 033402 (2006).

[Bie07] M. BIENERT, J. M. TORRES, S. ZIPPILLI, and G. MORIGI, "Resonance fluorescence of a cold atom in a high-finesse resonator", *Phys. Rev. A* **76**, 013410 (2007).

[Bla04] A. Blais, R.-S. Huang, A. Wallraff, S. M. Girvin, and R. J. Schoelkopf, "Cavity quantum electrodynamics for superconducting electrical circuits: An architecture for quantum computation", *Phys. Rev. A* **69**, 062320 (2004).

[Blo08] I. Bloch, J. Dalibard, and W. Zwerger, "Many-body physics with ultracold gases", *Rev. Mod. Phys.* **80**, 885 (2008).

[Blo12] I. Bloch, J. Dalibard, and S. Nascimbène, "Quantum simulations with ultracold quantum gases", *Nat. Phys.* **8**, 267 (2012).

[Bos97] S. Bose, K. Jacobs, and P. L. Knight, "Preparation of nonclassical states in cavities with a moving mirror", *Phys. Rev. A* **56**, 4175 (1997).

[Bow15] W. P. Bowen and G. J. Milburn, *Quantum Optomechanics*, (CRC Press, Boca Raton, 2015).

[Bra95] V. B. Braginsky, F. Y. A. Khalili, and K. S. Thorne, *Quantum Measurements*, (Cambridge University Press, Cambridge, 1995).

[Bra05] T. Brandes, "Coherent and collective quantum optical effects in mesoscopic systems", *Phys. Rep.* **408**, 315 (2005).

[Bra11] D. Braak, "Integrability of the Rabi Model", *Phys. Rev. Lett.* **107**, 100401 (2011).

[Bre07] H.-P. Breuer and F. Petruccione, *The Theory of Open Quantum Systems*, (Oxford University Press, Oxford, 2007).

[Bre12] D. Breyer and M. Bienert, "Light scattering in an optomechanical cavity coupled to a single atom", *Phys. Rev. A* **86**, 053819 (2012).

[Bri93] H.-J. Briegel and B.-G. Englert, "Quantum optical master equations: The use of damping bases", *Phys. Rev. A* **47**, 3311 (1993).

[Bul09] I. Buluta and F. Nori, "Quantum Simulators", *Science* **326**, 108 (2009).

[Cah69a] K. E. Cahill and R. J. Glauber, "Density Operators and Quasiprobability Distributions", *Phys. Rev.* **177**, 1882 (1969).

[Cah69b] K. E. Cahill and R. J. Glauber, "Ordered Expansions in Boson Amplitude Operators", *Phys. Rev.* **177**, 1857 (1969).

[Cam11] S. Camerer, M. Korppi, A. Jöckel, D. Hunger, T. W. Hänsch, and P. Treutlein, "Realization of an Optomechanical Interface Between Ultracold Atoms and a Membrane", *Phys. Rev. Lett.* **107**, 223001 (2011).

[Car02] H. J. Carmichael, *Statistical Methods in Quantum Optics 1*, (Springer, Berlin, 2002).

[Car05] T. Carmon, H. Rokhsari, L. Yang, T. J. Kippenberg, and K. J. Vahala, "Temporal Behavior of Radiation-Pressure-Induced Vibrations of an Optical Microcavity Phonon Mode", *Phys. Rev. Lett.* **94**, 223902 (2005).

[Cav80] C. M. Caves, K. S. Thorne, R. W. P. Drever, V. D. Sandberg, and M. Zimmermann, "On the measurement of a weak classical force coupled to a quantum-mechanical oscillator. I. Issues of principle", *Rev. Mod. Phys.* **52**, 341 (1980).

[Cha09] Y. Chang, H. Ian, and C. P. Sun, "Triple coupling and parameter resonance in quantum optomechanics with a single atom", *J. Phys. B* **42**, 215502 (2009).

[Cha11] J. Chan, T. P. Mayer Alegre, A. H. Safavi-Naeini, J. T. Hill, A. Krause, S. Gröblacher, M. Aspelmeyer, and O. Painter, "Laser cooling of a nanomechanical oscillator into its quantum ground state", *Nature* **478**, 89 (2011).

[Chu98] S. Chu, "Nobel Lecture: The manipulation of neutral particles", *Rev. Mod. Phys.* **70**, 685 (1998).

[Cir92] J. I. Cirac, R. Blatt, P. Zoller, and W. D. Phillips, "Laser cooling of trapped ions in a standing wave", *Phys. Rev. A* **46**, 2668 (1992).

[Cir93] J. I. Cirac, R. Blatt, A. S. Parkins, and P. Zoller, "Spectrum of resonance fluorescence from a single trapped ion", *Phys. Rev. A* **48**, 2169 (1993).

[Cle03] A. N. Cleland, *Foundations of Nanomechanics*, (Springer, Berlin, 2003).

[Coh15] J. D. Cohen, S. M. Meenehan, G. S. MacCabe, S. Gröblacher, A. H. Safavi-Naeini, F. Marsili, M. D. Shaw, and O. Painter, "Phonon counting and intensity interferometry of a nanomechanical resonator", *Nature* **520**, 522 (2015).

[Con26] E. Condon, "A Theory of Intensity Distribution in Band Systems", *Phys. Rev.* **28**, 1182 (1926).

[Cru05] L. Cruzeiro, "Why are proteins with glutamine- and asparagine-rich regions associated with protein misfolding diseases?", *J. Phys. Condens. Matter* **17**, 7833 (2005).

[CT77] C. Cohen-Tannoudji and S. Reynaud, "Dressed-atom description of resonance fluorescence and absorption spectra of a multi-level atom in an intense laser beam", *J. Phys. B* **10**, 345 (1977).

[CT98] C. N. Cohen-Tannoudji, "Nobel Lecture: Manipulating atoms with photons", *Rev. Mod. Phys.* **70**, 707 (1998).

[Dah88] J. P. Dahl and M. Springborg, "The Morse oscillator in position space, momentum space, and phase space", *J. Chem. Phys.* **88**, 4535 (1988).

[Dal85] J. Dalibard and C. Cohen-Tannoudji, "Atomic motion in laser light: connection between semiclassical and quantum descriptions", *J. Phys. B* **18**, 1661 (1985).

[Dal01] B. J. DALTON, S. M. BARNETT, and B. M. GARRAWAY, "Theory of pseudomodes in quantum optical processes", *Phys. Rev. A* **64**, 053813 (2001).

[Dav74] G. DAVIES, "Vibronic spectra in diamond", *J. Phys. C* **7**, 3797 (1974).

[Dav81] G. DAVIES, "The Jahn-Teller effect and vibronic coupling at deep levels in diamond", *Rep. Prog. Phys.* **44**, 787 (1981).

[Deg08] C. L. DEGEN, "Scanning magnetic field microscope with a diamond single-spin sensor", *Appl. Phys. Lett.* **92**, 243111 (2008).

[Dic53] R. H. DICKE, "The Effect of Collisions upon the Doppler Width of Spectral Lines", *Phys. Rev.* **89**, 472 (1953).

[Die87] F. DIEDRICH and H. WALTHER, "Nonclassical radiation of a single stored ion", *Phys. Rev. Lett.* **58**, 203 (1987).

[Doh11] M. W. DOHERTY, N. B. MANSON, P. DELANEY, and L. C. L. HOLLENBERG, "The negatively charged nitrogen-vacancy centre in diamond: the electronic solution", *New J. Phys.* **13**, 025019 (2011).

[Doh13] M. W. DOHERTY, N. B. MANSON, P. DELANEY, F. JELEZKO, J. WRACHTRUP, and L. C. L. HOLLENBERG, "The nitrogen-vacancy colour centre in diamond", *Phys. Rep.* **528**, 1 (2013).

[Dut07] M. V. G. DUTT, L. CHILDRESS, L. JIANG, E. TOGAN, J. MAZE, F. JELEZKO, A. S. ZIBROV, P. R. HEMMER, and M. D. LUKIN, "Quantum Register Based on Individual Electronic and Nuclear Spin Qubits in Diamond", *Science* **316**, 1312 (2007).

[Eic09] M. EICHENFIELD, J. CHAN, R. M. CAMACHO, K. J. VAHALA, and O. PAINTER, "Optomechanical crystals", *Nature* **462**, 78 (2009).

[Eis11] M. D. EISAMAN, J. FAN, A. MIGDALL, and S. V. POLYAKOV, "Invited Review Article: Single-photon sources and detectors", *Rev. Sci. Instrum.* **82**, 071101 (2011).

[Eke00] A. EKERT, N. GISIN, B. HUTTNER, H. INAMORI, and H. WEINFURTER, "Quantum Cryptography", in "The Physics of Quantum Information", p. 15, (Springer, Berlin, 2000).

[Eng02] B.-G. ENGLERT and G. MORIGI, "Five Lectures on Dissipative Master Equations", in "Coherent Evolution in Noisy Environments", p. 55, (Springer, Berlin, 2002).

[Fav07] I. FAVERO, C. METZGER, S. CAMERER, D. KÖNIG, H. LORENZ, J. P. KOTTHAUS, and K. KARRAI, "Optical cooling of a micromirror of wavelength size", *Appl. Phys. Lett.* **90**, 104101 (2007).

[Fra26] J. FRANCK and E. G. DYMOND, "Elementary processes of photochemical reactions", *Trans. Faraday Soc.* **21**, 536 (1926).

[Fre95] E. S. FREIDKIN, G. K. HORTON, and E. R. COWLEY, "Evaluation of the displacement-displacement correlation function of a one-dimensional crystal:

A comparison of the results of perturbation theory with the Mori-Dupuis method", *Phys. Rev. B* **52**, 3322 (1995).

[Fu09] K.-M. C. Fu, C. Santori, P. E. Barclay, L. J. Rogers, N. B. Manson, and R. G. Beausoleil, "Observation of the Dynamic Jahn-Teller Effect in the Excited States of Nitrogen-Vacancy Centers in Diamond", *Phys. Rev. Lett.* **103**, 256404 (2009).

[Gal80] J. A. C. Gallas, "Some matrix elements for Morse oscillators", *Phys. Rev. A* **21**, 1829 (1980).

[Gal11] A. Gali, T. Simon, and J. E. Lowther, "An ab initio study of local vibration modes of the nitrogen-vacancy center in diamond", *New J. Phys.* **13**, 025016 (2011).

[Gar04] C. Gardiner and P. Zoller, *Quantum Noise*, (Springer, Berlin, 2004).

[Gat97] M. Gatzke, G. Birkl, P. S. Jessen, A. Kastberg, S. L. Rolston, and W. D. Phillips, "Temperature and localization of atoms in three-dimensional optical lattices", *Phys. Rev. A* **55**, R3987 (1997).

[Gav12] E. Gavartin, P. Verlot, and T. J. Kippenberg, "A hybrid on-chip optomechanical transducer for ultrasensitive force measurements", *Nat. Nanotechnol.* **7**, 509 (2012).

[Geo14] I. M. Georgescu, S. Ashhab, and F. Nori, "Quantum simulation", *Rev. Mod. Phys.* **86**, 153 (2014).

[Gig06] S. Gigan, H. R. Böhm, M. Paternostro, F. Blaser, G. Langer, J. B. Hertzberg, K. C. Schwab, D. Bäuerle, M. Aspelmeyer, and A. Zeilinger, "Self-cooling of a micromirror by radiation pressure", *Nature* **444**, 67 (2006).

[Gio11] V. Giovannetti, S. Lloyd, and L. Maccone, "Advances in quantum metrology", *Nature Photon.* **5**, 222 (2011).

[Gis02] N. Gisin, G. Ribordy, W. Tittel, and H. Zbinden, "Quantum cryptography", *Rev. Mod. Phys.* **74**, 145 (2002).

[Gla63] R. J. Glauber, "The Quantum Theory of Optical Coherence", *Phys. Rev.* **130**, 2529 (1963).

[Gla07] R. J. Glauber, *Quantum Theory of Optical Coherence*, (Wiley-VCH, Weinheim, 2007).

[Haa73] F. Haake, "Statistical Treatment of Open Systems by Generalized Master Equations", in "Springer Tracts in Modern Physics, Volume 66", p. 98, (Springer, Berlin, 1973).

[Ham98] S. E. Hamann, D. L. Haycock, G. Klose, P. H. Pax, I. H. Deutsch, and P. S. Jessen, "Resolved-Sideband Raman Cooling to the Ground State of an Optical Lattice", *Phys. Rev. Lett.* **80**, 4149 (1998).

[Ham15] M. HAMAMDA, P. PILLET, H. LIGNIER, and D. COMPARAT, "Rovibrational cooling of molecules and prospects", *J. Phys. B* **48**, 182001 (2015).

[Har06] S. HAROCHE and J.-M. RAIMOND, *Exploring the Quantum: Atoms, Cavities, and Photons*, (Oxford University Press, Oxford, 2006).

[Har13] S. HAROCHE, "Nobel Lecture: Controlling photons in a box and exploring the quantum to classical boundary", *Rev. Mod. Phys.* **85**, 1083 (2013).

[HM04] C. HÖHBERGER METZGER and K. KARRAI, "Cavity cooling of a microlever", *Nature* **432**, 1002 (2004).

[Hoa16] B. T. HOANG, G. M. AKSELROD, and M. H. MIKKELSEN, "Ultrafast Room-Temperature Single Photon Emission from Quantum Dots Coupled to Plasmonic Nanocavities", *Nano Lett.* **16**, 270 (2016).

[Hor97] P. HORAK, G. HECHENBLAIKNER, K. M. GHERI, H. STECHER, and H. RITSCH, "Cavity-Induced Atom Cooling in the Strong Coupling Regime", *Phys. Rev. Lett.* **79**, 4974 (1997).

[Hu15] D. HU, S.-Y. HUANG, J.-Q. LIAO, L. TIAN, and H.-S. GOAN, "Quantum coherence in ultrastrong optomechanics", *Phys. Rev. A* **91**, 013812 (2015).

[Hua50] K. HUANG and A. RHYS, "Theory of Light Absorption and Non-Radiative Transitions in F-Centres", *Proc. R. Soc. A* **204**, 406 (1950).

[Hus40] K. HUSIMI, "Some Formal Properties of the Density Matrix", *J. Phys. Soc. Jpn.* **22**, 264 (1940).

[Jac07] V. JACQUES, E. WU, F. GROSSHANS, F. TREUSSART, P. GRANGIER, A. ASPECT, and J.-F. ROCH, "Experimental Realization of Wheeler's Delayed-Choice Gedanken Experiment", *Science* **315**, 966 (2007).

[Jak03] M. JAKOB and S. STENHOLM, "Variational functions in driven open quantum systems", *Phys. Rev. A* **67**, 032111 (2003).

[Jav81] J. JAVANAINEN and S. STENHOLM, "Laser cooling of trapped particles III: The Lamb-Dicke limit", *Appl. Phys.* **24**, 151 (1981).

[Jav84] J. JAVANAINEN, M. LINDBERG, and S. STENHOLM, "Laser cooling of trapped ions: dynamics of the final stages", *J. Opt. Soc. Am. B* **1**, 111 (1984).

[Jay63] E. T. JAYNES and F. W. CUMMINGS, "Comparison of quantum and semiclassical radiation theories with application to the beam maser", *Proc. IEEE* **51**, 89 (1963).

[Jel06] F. JELEZKO and J. WRACHTRUP, "Single defect centres in diamond: A review", *Phys. Status Solidi A* **203**, 3207 (2006).

[Kip14] L. KIPFSTUHL, F. GULDNER, J. RIEDRICH-MÖLLER, and C. BECHER, "Modeling of optomechanical coupling in a phoxonic crystal cavity in diamond", *Opt. Express* **22**, 12410 (2014).

[Kir04] A. Kiraz, M. Atatüre, and A. Imamoğlu, "Quantum-dot single-photon sources: Prospects for applications in linear optics quantum-information processing", *Phys. Rev. A* **69**, 032305 (2004).

[Kit04] C. Kittel and D. F. Holcomb, *Introduction to Solid State Physics*, (Wiley-VCH, New York, 2004).

[Kok07] P. Kok, W. J. Munro, K. Nemoto, T. C. Ralph, J. P. Dowling, and G. J. Milburn, "Linear optical quantum computing with photonic qubits", *Rev. Mod. Phys.* **79**, 135 (2007).

[Kub10] Y. Kubo, F. R. Ong, P. Bertet, D. Vion, V. Jacques, D. Zheng, A. Dréau, J.-F. Roch, A. Auffeves, F. Jelezko, J. Wrachtrup, M. F. Barthe, P. Bergonzo, and D. Esteve, "Strong Coupling of a Spin Ensemble to a Superconducting Resonator", *Phys. Rev. Lett.* **105**, 140502 (2010).

[Kur00] C. Kurtsiefer, S. Mayer, P. Zarda, and H. Weinfurter, "Stable Solid-State Source of Single Photons", *Phys. Rev. Lett.* **85**, 290 (2000).

[Kur14] G. Kurizki, P. Bertet, Y. Kubo, K. Mølmer, D. Petrosyan, P. Rabl, and J. Schmiedmayer, "Quantum technologies with hybrid systems", *Proc. Natl. Acad. Sci. USA* **112**, 3866 (2014).

[LaH09] M. LaHaye, J. Suh, P. Echternach, K. Schwab, and M. Roukes, "Nanomechanical measurements of a superconducting qubit", *Nature* **459**, 960 (2009).

[Law95] C. Law, "Interaction between a moving mirror and radiation pressure: A Hamiltonian formulation", *Phys. Rev. A* **51**, 2537 (1995).

[Lax52] M. Lax, "The Franck-Condon Principle and Its Application to Crystals", *J. Chem. Phys.* **20**, 1752 (1952).

[Lax63] M. Lax, "Formal Theory of Quantum Fluctuations from a Driven State", *Phys. Rev.* **129**, 2342 (1963).

[Lax67] M. Lax, "Quantum Noise. X. Density-Matrix Treatment of Field and Population-Difference Fluctuations", *Phys. Rev.* **157**, 213 (1967).

[Leb01] P. Lebedew, "Untersuchungen über die Druckkräfte des Lichtes", *Ann. Phys.* **311**, 433 (1901).

[Lec15] F. Lecocq, J. D. Teufel, J. Aumentado, and R. W. Simmonds, "Resolving the vacuum fluctuations of an optomechanical system using an artificial atom", *Nat. Phys.* **11**, 635 (2015).

[Lei03] D. Leibfried, R. Blatt, C. Monroe, and D. Wineland, "Quantum dynamics of single trapped ions", *Rev. Mod. Phys.* **75**, 281 (2003).

[Li15] L. Li, T. Schröder, E. H. Chen, M. Walsh, I. Bayn, J. Goldstein, O. Gaathon, M. E. Trusheim, M. Lu, J. Mower, M. Cotlet, M. L. Markham, D. J. Twitchen, and D. Englund, "Coherent spin control of a nanocavity-enhanced qubit in diamond", *Nat. Commun.* **6**, 6173 (2015).

[Lin76] G. Lindblad, "On the generators of quantum dynamical semigroups", *Commun. Math. Phys.* **48**, 119 (1976).

[Lin84a] M. Lindberg, "Steady state of a laser-cooled trapped ion in the Lamb-Dicke limit", *J. Phys. B* **17**, 2129 (1984).

[Lin84b] M. Lindberg and S. Stenholm, "The master equation for laser cooling of trapped particles", *J. Phys. B* **17**, 3375 (1984).

[Lin86] M. Lindberg, "Resonance fluorescence of a laser-cooled trapped ion in the Lamb-Dicke limit", *Phys. Rev. A* **34**, 3178 (1986).

[Lou90] W. H. Louisell, *Quantum Statistical Properties of Radiation*, (Wiley-VCH, New York, 1990).

[Mag67] W. Magnus, F. Oberhettinger, and R. P. Soni, *Formulas and Theorems for the Special Functions of Mathematical Physics*, (Wiley-VCH, New York, 1967).

[Mah00] G. D. Mahan, *Many-Particle Physics*, (Springer, Berlin, 2000).

[Man13] I. Manai, R. Horchani, M. Hamamda, A. Fioretti, M. Allegrini, H. Lignier, P. Pillet, and D. Comparat, "Laser cooling of rotation and vibration by optical pumping", *Mol. Phys.* **111**, 1844 (2013).

[Mar62] A. A. Maradudin and A. E. Fein, "Scattering of Neutrons by an Anharmonic Crystal", *Phys. Rev.* **128**, 2589 (1962).

[Mar66] A. A. Maradudin, "Theoretical and Experimental Aspects of the Effects of Point Defects and Disorder on the Vibrations of Crystals 1", *Solid State Phys.* **18**, 273 (1966).

[Mar67] A. A. Maradudin, "Theoretical and Experimental Aspects of the Effects of Point Defects and Disorder on the Vibrations of Crystals 2", *Solid State Phys.* **19**, 1 (1967).

[Mau04] P. Maunz, T. Puppe, I. Schuster, N. Syassen, P. W. Pinkse, and G. Rempe, "Cavity cooling of a single atom", *Nature* **428**, 50 (2004).

[Maz08] J. R. Maze, P. L. Stanwix, J. S. Hodges, S. Hong, J. M. Taylor, P. Cappellaro, L. Jiang, M. V. G. Dutt, E. Togan, A. S. Zibrov, A. Yacoby, R. L. Walsworth, and M. D. Lukin, "Nanoscale magnetic sensing with an individual electronic spin in diamond", *Nature* **455**, 644 (2008).

[Maz09] L. Mazzola, S. Maniscalco, J. Piilo, K.-A. Suominen, and B. M. Garraway, "Pseudomodes as an effective description of memory: Non-Markovian dynamics of two-state systems in structured reservoirs", *Phys. Rev. A* **80**, 012104 (2009).

[Meh65] C. L. Mehta and E. C. G. Sudarshan, "Relation between Quantum and Semiclassical Description of Optical Coherence", *Phys. Rev.* **138**, B274 (1965).

[Mes06] D. Meschede and A. Rauschenbeutel, "Manipulating Single Atoms", in "Advances in Atomic, Molecular, and Optical Physics", p. 75, (Elsevier, Amsterdam, 2006).

[Met01] H. J. Metcalf and P. van der Straten, *Laser Cooling and Trapping*, (Springer, Berlin, 2001).

[Mey13] P. Meystre, "A short walk through quantum optomechanics", *Ann. Phys.* **525**, 215 (2013).

[Mir15] I. M. Mirza, "Real-time emission spectrum of a hybrid atom-optomechanical cavity", *J. Opt. Soc. Am. B* **32**, 1604 (2015).

[Miz12] N. Mizuochi, T. Makino, H. Kato, D. Takeuchi, M. Ogura, H. Okushi, M. Nothaft, P. Neumann, A. Gali, F. Jelezko, J. Wrachtrup, and S. Yamasaki, "Electrically driven single-photon source at room temperature in diamond", *Nature Photon.* **6**, 299 (2012).

[Mol69] B. R. Mollow, "Power Spectrum of Light Scattered by Two-Level Systems", *Phys. Rev.* **188**, 1969 (1969).

[Mol72] B. R. Mollow, "Absorption and Emission Line-Shape Functions for Driven Atoms", *Phys. Rev. A* **5**, 1522 (1972).

[Mor29a] P. M. Morse, "Diatomic Molecules According to the Wave Mechanics. II. Vibrational Levels", *Phys. Rev.* **34**, 57 (1929).

[Mor29b] P. M. Morse and E. C. G. Stueckelberg, "Diatomic Molecules According to the Wave Mechanics I: Electronic Levels of the Hydrogen Molecular Ion", *Phys. Rev.* **33**, 932 (1929).

[Mor03] G. Morigi, "Cooling atomic motion with quantum interference", *Phys. Rev. A* **67**, 033402 (2003).

[Mor07] G. Morigi, P. W. H. Pinkse, M. Kowalewski, and R. de Vivie-Riedle, "Cavity Cooling of Internal Molecular Motion", *Phys. Rev. Lett.* **99**, 073001 (2007).

[Nak58] S. Nakajima, "On Quantum Theory of Transport Phenomena", *Prog. Theor. Phys.* **20**, 948 (1958).

[Neu78] W. Neuhauser, M. Hohenstatt, P. Toschek, and H. Dehmelt, "Optical-Sideband Cooling of Visible Atom Cloud Confined in Parabolic Well", *Phys. Rev. Lett.* **41**, 233 (1978).

[Ngu11] J. H. V. Nguyen, C. R. Viteri, E. G. Hohenstein, C. D. Sherrill, K. R. Brown, and B. Odom, "Challenges of laser-cooling molecular ions", *New J. Phys.* **13**, 063023 (2011).

[Nic01] E. F. Nichols and G. F. Hull, "A Preliminary Communication on the Pressure of Heat and Light Radiation", *Phys. Rev. (Series I)* **13**, 307 (1901).

[Nie03] M. A. Nielsen and I. L. Chuang, *Quantum Computation and Quantum Information*, (Cambridge University Press, Cambridge, 2003).

[Nun11] A. Nunnenkamp, K. Børkje, and S. Girvin, "Single-Photon Optome-
chanics", *Phys. Rev. Lett.* **107**, 063602 (2011).

[Pek34] C. L. Pekeris, "The Rotation-Vibration Coupling in Diatomic Molecules",
Phys. Rev. **45**, 98 (1934).

[Phi98] W. D. Phillips, "Nobel Lecture: Laser cooling and trapping of neutral
atoms", *Rev. Mod. Phys.* **70**, 721 (1998).

[Pin00] P. W. H. Pinkse, T. Fischer, P. Maunz, and G. Rempe, "Trapping an
atom with single photons", *Nature* **404**, 365 (2000).

[Pir13] J.-M. Pirkkalainen, S. U. Cho, J. Li, G. S. Paraoanu, P. J. Hakonen,
and M. A. Sillanpää, "Hybrid circuit cavity quantum electrodynamics with
a micromechanical resonator", *Nature* **494**, 211 (2013).

[Pir15] J.-M. Pirkkalainen, S. U. Cho, F. Massel, J. Tuorila, T. T.
Heikkilä, P. J. Hakonen, and M. A. Sillanpää, "Cavity optomechan-
ics mediated by a quantum two-level system", *Nat. Commun.* **6**, 6981 (2015).

[Pla13] J. J. Pla, K. Y. Tan, J. P. Dehollain, W. H. Lim, J. J. L. Morton,
F. A. Zwanenburg, D. N. Jamieson, A. S. Dzurak, and A. Morello,
"High-fidelity readout and control of a nuclear spin qubit in silicon", *Nature*
496, 334 (2013).

[Ple98] M. B. Plenio and P. L. Knight, "The quantum-jump approach to dissipa-
tive dynamics in quantum optics", *Rev. Mod. Phys.* **70**, 101 (1998).

[Poh37] R. W. Pohl, "Electron conductivity and photochemical processes in alkali-
halide crystals", *Proc. Phys. Soc.* **49**, 3 (1937).

[Pon04] M. A. de Ponte, M. C. de Oliveira, and M. H. Y. Moussa, "Deco-
herence in a system of strongly coupled quantum oscillators. I. Symmetric
network", *Phys. Rev. A* **70**, 022324 (2004).

[Poo12] M. Poot and H. S. J. van der Zant, "Mechanical systems in the quantum
regime", *Phys. Rep.* **511**, 273 (2012).

[Pou08] V. Pouthier, "Energy relaxation of the amide-I mode in hydrogen-bonded
peptide units: A route to conformational change", *J. Chem. Phys.* **128**,
065101 (2008).

[Pou10] V. Pouthier, "Phonon anharmonicity-induced decoherence slowing down in
exciton-phonon systems", *J. Phys.: Condens. Matter* **22**, 255601 (2010).

[Poy96] J. F. Poyatos, J. I. Cirac, R. Blatt, and P. Zoller, "Trapped ions
in the strong-excitation regime: Ion interferometry and nonclassical states",
Phys. Rev. A **54**, 1532 (1996).

[Raa00] C. Raab, J. Eschner, J. Bolle, H. Oberst, F. Schmidt-Kaler, and
R. Blatt, "Motional Sidebands and Direct Measurement of the Cooling Rate
in the Resonance Fluorescence of a Single Trapped Ion", *Phys. Rev. Lett.* **85**,
538 (2000).

[Rab36] I. I. RABI, "On the Process of Space Quantization", *Phys. Rev.* **49**, 324 (1936).

[Rab10] P. RABL, S. J. KOLKOWITZ, F. H. L. KOPPENS, J. G. E. HARRIS, P. ZOLLER, and M. D. LUKIN, "A quantum spin transducer based on nano-electromechanical resonator arrays", *Nat. Phys.* **6**, 602 (2010).

[Rab11] P. RABL, "Photon Blockade Effect in Optomechanical Systems", *Phys. Rev. Lett.* **107**, 063601 (2011).

[Ram13] T. RAMOS, V. SUDHIR, K. STANNIGEL, P. ZOLLER, and T. J. KIPPEN-BERG, "Nonlinear Quantum Optomechanics via Individual Intrinsic Two-Level Defects", *Phys. Rev. Lett.* **110**, 193602 (2013).

[Res14] J. RESTREPO, C. CIUTI, and I. FAVERO, "Single-Polariton Optomechanics", *Phys. Rev. Lett.* **112**, 013601 (2014).

[Ris96] H. RISKEN, *The Fokker-Planck Equation*, (Springer, Berlin, 1996).

[Rit04] H. RITSCH, G. J. MILBURN, and T. C. RALPH, "Deterministic generation of tailored-optical-coherent-state superpositions", *Phys. Rev. A* **70**, 033804 (2004).

[Rit13] H. RITSCH, P. DOMOKOS, F. BRENNECKE, and T. ESSLINGER, "Cold atoms in cavity-generated dynamical optical potentials", *Rev. Mod. Phys.* **85**, 553 (2013).

[Riv12] A. RIVAS and S. F. HUELGA, *Open Quantum Systems: An Introduction*, (Springer, Heidelberg, 2012).

[RM12] J. RIEDRICH-MÖLLER, L. KIPFSTUHL, H. HEPP, E. NEU, C. PAULY, F. MÜCKLICH, A. BAUR, M. WANDT, S. WOLFF, M. FISCHER, S. GSELL, M. SCHRECK, and C. BECHER, "One- and two-dimensional photonic crystal microcavities in single crystal diamond", *Nat. Nanotechnol.* **7**, 69 (2012).

[RM14] J. RIEDRICH-MÖLLER, C. AREND, C. PAULY, F. MÜCKLICH, M. FISCHER, S. GSELL, M. SCHRECK, and C. BECHER, "Deterministic Coupling of a Single Silicon-Vacancy Color Center to a Photonic Crystal Cavity in Diamond", *Nano Lett.* **14**, 5281 (2014).

[RM15] J. RIEDRICH-MÖLLER, S. PEZZAGNA, J. MEIJER, C. PAULY, F. MÜCKLICH, M. MARKHAM, A. M. EDMONDS, and C. BECHER, "Nanoimplantation and Purcell enhancement of single nitrogen-vacancy centers in photonic crystal cavities in diamond", *Appl. Phys. Lett.* **106**, 221103 (2015).

[Roc10] T. ROCHELEAU, T. NDUKUM, C. MACKLIN, J. B. HERTZBERG, A. A. CLERK, and K. C. SCHWAB, "Preparation and detection of a mechanical resonator near the ground state of motion", *Nature* **463**, 72 (2010).

[Rog14] B. ROGERS, N. LO GULLO, G. DE CHIARA, G. M. PALMA, and M. PATERNOSTRO, "Hybrid optomechanics for Quantum Technologies", *Quantum Meas. Quantum Metrol.* **2**, 11 (2014).

[Roy13] A. K. Roy, "Accurate ro-vibrational spectroscopy of diatomic molecules in a Morse oscillator potential", *Results Phys.* **3**, 103 (2013).

[San90] L. Sandoval and A. Palma, "One-Center matrix elements for the morse oscillator", *Int. J. Quant. Chem.* **38**, 481 (1990).

[San10] C. Santori, D. Fattal, and Y. Yamamoto, *Single-photon Devices and Applications*, (Wiley-VCH, New York, 2010).

[Sar74] M. Sargent, M. O. Scully, and W. E. Lamb Jr., *Quantum Statistical Properties of Radiation*, (Addison-Wesley, London, 1974).

[Sch32] K. Scholz, "Zur quantenmechanischen Berechnung von Intensitäten ultraroter Banden", *Z. Phys.* **78**, 751 (1932).

[Sch62] J. H. Schulman and W. D. Compton, *Color Centers in Solids*, (Pergamon Press, New York, 1962).

[Sch01] W. P. Schleich, *Quantum Optics in Phase Space*, (Wiley-VCH, Weinheim, 2001).

[Sch06] A. Schliesser, P. Del'Haye, N. Nooshi, K. J. Vahala, and T. J. Kippenberg, "Radiation Pressure Cooling of a Micromechanical Oscillator Using Dynamical Backaction", *Phys. Rev. Lett.* **97**, 243905 (2006).

[Sch08] A. Schliesser, R. Rivière, G. Anetsberger, O. Arcizet, and T. J. Kippenberg, "Resolved-sideband cooling of a micromechanical oscillator", *Nat. Phys.* **4**, 415 (2008).

[Sch12] G. Schaller, *Open Quantum Systems Far from Equilibrium (Lecture Notes in Physics)*, (Springer, Berlin, 2012).

[Sch16] T. Schröder, S. L. Mouradian, J. Zheng, M. E. Trusheim, M. Walsh, E. H. Chen, L. Li, I. Bayn, and D. Englund, "Quantum nanophotonics in diamond", *J. Opt. Soc. Am. B* **33**, B65 (2016).

[Scu97] M. O. Scully and M. S. Zubairy, *Quantum Optics*, (Cambridge University Press, Cambridge, 1997).

[Sil06] P. A. S. Silva and L. Cruzeiro, "Dynamics of a nonconserving Davydov monomer", *Phys. Rev. E* **74**, 021920 (2006).

[Ste86] S. Stenholm, "The semiclassical theory of laser cooling", *Rev. Mod. Phys.* **58**, 699 (1986).

[Su08] C.-H. Su, A. D. Greentree, and L. C. L. Hollenberg, "Towards a picosecond transform-limited nitrogen-vacancy based single photon source", *Opt. Express* **16**, 6240 (2008).

[Sud63] E. C. G. Sudarshan, "Equivalence of Semiclassical and Quantum Mechanical Descriptions of Statistical Light Beams", *Phys. Rev. Lett.* **10**, 277 (1963).

[Tar08] V. E. Tarasov, *Quantum Mechanics of Non-Hamiltonian and Dissipative Systems*, (Elsevier, Amsterdam, 2008).

[Tei14] J. TEISSIER, A. BARFUSS, P. APPEL, E. NEU, and P. MALETINSKY, "Strain Coupling of a Nitrogen-Vacancy Center Spin to a Diamond Mechanical Oscillator", *Phys. Rev. Lett.* **113**, 020503 (2014).

[Teu11] J. D. TEUFEL, T. DONNER, D. LI, J. W. HARLOW, M. S. ALLMAN, K. CICAK, A. J. SIROIS, J. D. WHITTAKER, K. W. LEHNERT, and R. W. SIMMONDS, "Sideband cooling of micromechanical motion to the quantum ground state", *Nature* **475**, 359 (2011).

[Tog10] E. TOGAN, Y. CHU, A. S. TRIFONOV, L. JIANG, J. MAZE, L. CHILDRESS, M. V. G. DUTT, A. S. SØRENSEN, P. R. HEMMER, A. S. ZIBROV, and M. D. LUKIN, "Quantum entanglement between an optical photon and a solid-state spin qubit", *Nature* **466**, 730 (2010).

[Tor11] J. M. TORRES, M. BIENERT, S. ZIPPILLI, and G. MORIGI, "Quantum jumps induced by the center-of-mass motion of a trapped atom", *Eur. Phys. J. D* **61**, 21 (2011).

[Tri16] L. TRIFUNOVIC, F. L. PEDROCCHI, S. HOFFMAN, P. MALETINSKY, A. YACOBY, and D. LOSS, "High-efficiency resonant amplification of weak magnetic fields for single spin magnetometry at room temperature"", *Nat. Nanotechnol.* **10**, 541 (2016).

[Wal14] G. WALDHERR, Y. WANG, S. ZAISER, M. JAMALI, T. SCHULTE-HERBRÜGGEN, H. ABE, T. OHSHIMA, J. ISOYA, J. F. DU, P. NEUMANN, and J. WRACHTRUP, "Quantum error correction in a solid-state hybrid spin register", *Nature* **506**, 204 (2014).

[Wan08] C. WANG, L. C. WANG, and H. Y. SUN, "Dynamics of a Coupled Atom and Optomechanical Cavity", *J. Korean Phys. Soc.* **57**, 704 (2008).

[Wei12] U. WEISS, *Quantum Dissipative Systems*, (World Scientific, Singapore, 2012).

[Wig32] E. WIGNER, "On the Quantum Correction For Thermodynamic Equilibrium", *Phys. Rev.* **40**, 749 (1932).

[Wil15] D. J. WILSON, V. SUDHIR, N. PIRO, R. SCHILLING, A. GHADIMI, and T. J. KIPPENBERG, "Measurement and control of a mechanical oscillator at its thermal decoherence rate", *Nature* **524**, 325 (2015).

[Win79] D. J. WINELAND and W. M. ITANO, "Laser cooling of atoms", *Phys. Rev. A* **20**, 1521 (1979).

[Woo14] M. P. WOODS, R. GROUX, A. W. CHIN, S. F. HUELGA, and M. B. PLENIO, "Mappings of open quantum systems onto chain representations and Markovian embeddings", *J. Math. Phys.* **55**, 032101 (2014).

[WR02] I. WILSON-RAE and A. IMAMOǦLU, "Quantum dot cavity-QED in the presence of strong electron-phonon interactions", *Phys. Rev. B* **65**, 235311 (2002).

[WR04] I. WILSON-RAE, P. ZOLLER, and A. IMAMOǦLU, "Laser Cooling of a Nanomechanical Resonator Mode to its Quantum Ground State", *Phys. Rev. Lett.* **92**, 075507 (2004).

[WR08a] I. WILSON-RAE, "Intrinsic dissipation in nanomechanical resonators due to phonon tunneling", *Phys. Rev. B* **77**, 245418 (2008).

[WR08b] I. WILSON-RAE, N. NOOSHI, J. DOBRINDT, T. J. KIPPENBERG, and W. ZWERGER, "Cavity-assisted backaction cooling of mechanical resonators", *New J. Phys.* **10**, 095007 (2008).

[Xia13] Z.-L. XIANG, S. ASHHAB, J. Q. YOU, and F. NORI, "Hybrid quantum circuits: Superconducting circuits interacting with other quantum systems", *Rev. Mod. Phys.* **85**, 623 (2013).

[Zho13] H. ZHONG, Q. XIE, M. T. BATCHELOR, and C. LEE, "Analytical eigenstates for the quantum Rabi model", *J. Phys. A* **46**, 415302 (2013).

[Zim60] J. M. ZIMAN, *Electrons and Phonons: The Theory of Transport Phenomena in Solids*, (Oxford University Press, Oxford, 1960).

[Zwa60] R. ZWANZIG, "Ensemble Method in the Theory of Irreversibility", *J. Chem. Phys.* **33**, 1338 (1960).

Danksagung

Es ist mir eine große Freude auf dieser letzten Seite die Gelegenheit zu nutzen mich bei denjenigen zu bedanken, die zur Fertigstellung dieser Arbeit beigetragen haben. An oberster Stelle stehen hierbei natürlich zwei Personen: *Giovanna Morigi* und *Marc Bienert*. Danke, dass ihr mir (aus mir immernoch unerfindlichen Gründen) die Chance gegeben habt diesen Weg vom Anfang bis zum Ende zugehen. Ich weiß, ich habe vor allem Marc viele Nerven gekostet, aber so ein Doktorand wie ich war wahrscheinlich die beste Vorbereitung auf die Schule. An zweiter Stelle möchte ich mich herzlich bei der *Graduiertenförderung* der Universität des Saarlandes bedanken, ohne die ich mein Vorhaben nicht hätte durchführen können. Dabei bedanke ich mich besonders bei der Vergabekommission für ihr Vertrauen in meine Förderwürdigkeit und bei Herrn *Dr. Theo Jäger* für seine Hilfe bei jeglichen Formalitäten. An nächster Stelle geht mein Dank an die gesamte *AG Morigi* für die stets angenehme Arbeitsatmosphäre. Wegen seiner unvergleichbaren Hilfsbereitschaft möchte ich dabei *Mauricio Torres* erwähnen, der immer ein offenes Ohr für Fragen hatte. Außerdem bedanke ich mich bei allen meinen Büronachbarn, neben denen ich die Ehre hatte zu arbeiten: *Florian, Christian, Tristan, Katharina, Oxana* und *Rebecca*. Ihr habt die Arbeit um einiges erträglicher gemacht. Besonders bedanke ich mich dabei bei *Simon*, du weißt wofür. Ich bedanke mich auch bei *Bruno* für die langen und stets interessanten Diskussionen. Außerdem seien *Cecilia, Endre, Jens, Hessam, Andreas, Tim, Thomás, Sascha* und *Rick* erwähnt. Bei *Timo* bedanke ich mich für die optomechanische Zusammenarbeit. Besonders bedanke ich mich bei meinen Mitdoktoranden *Luigi, Susanne, Florian* und *Stefan*, ohne die die Zeit mit Sicherheit härter gewesen wäre. Auch den Kollegen aus der Experimentalphysik sei (nicht nur für ihre Expertise) gedankt, *Roland* und *Alexander*. Aber natürlich besteht das Leben nicht nur aus Arbeit, deshalb möchte ich auch den Leuten danken, die mich von außerhalb begleitet haben. Eine Liste aller Freunde, die mir in der ein oder anderen Weise geholfen haben wäre sicherlich zu lang. Deshalb seien hier nur einige wenige namentlich erwähnt, die mir besonders zur Seite standen: *Lars, Sven* und *Michael*. Danke! Alle, die hier nicht explizit erwähnt werden: Ihr wisst wer ihr seid! Die Person aber, die am meisten für mich da war in der Zeit, als diese Arbeit entstanden ist, ist *Jang Mi*. Ich hoffe, dass ich dir nur in annähernder Weise soviel Kraft gegeben habe wie du mir. 고마워! Nicht nur während der Entstehung dieser Arbeit, sondern seit jeher, erfahre ich von meiner Familie eine unglaubliche, bedingungslose Unterstützung, die hier erwähnt werden muss. *Mama, Papa, Bernd* und *Elias*, ich wüsste nicht wo ich ohne euch wäre, mit Sicherheit nicht hier. Die größte Motivation aber gab mir meine Tochter *Sonya*. Wenn auch in der Ferne, du warst immer bei mir!